

UC Berkeley

UC Berkeley Electronic Theses and Dissertations

Title

The Good, the Bad, the Algae: Using High Resolution Imagery to Detect Freshwater Algal Blooms in California

Permalink

<https://escholarship.org/uc/item/2m57482f>

Author

Kislik, Emily Anne

Publication Date

2022

Peer reviewed|Thesis/dissertation

The Good, the Bad, the Algae:
Using High Resolution Imagery to Detect Freshwater Algal Blooms in California

By

Emily Anne Kislik

A dissertation submitted in partial satisfaction of the

requirements for the degree of

Doctor of Philosophy

in

Environmental Science, Policy, and Management

in the

Graduate Division

of the

University of California, Berkeley

Committee in charge:

Professor Maggi Kelly, Chair

Professor Iryna Dronova

Professor Theodore Grantham

Spring 2022

Abstract

The Good, the Bad, the Algae:

Using High Resolution Imagery to Detect Freshwater Algal Blooms in California

by

Emily Anne Kislik

Doctor of Philosophy in Environmental Science, Policy, and Management

University of California, Berkeley

Professor Maggi Kelly, Chair

Algae are an essential component of aquatic ecosystems. They provide food, habitat, structural support, and oxygen to marine, freshwater, and brackishwater environments alike. However, algae in excess can be problematic. Harmful algal blooms (HABs) are proliferations of both toxic and non-toxic algal species that can cause ecological and environmental damage in lakes, reservoirs, and rivers. As global temperatures rise, coupled with increasing nutrient inputs from eutrophication and atmospheric deposition, many predict HABs will also increase in frequency and intensity. There is a need to advance methods in algal bloom monitoring to keep pace with these global trends. As in situ techniques such as water quality samples, swimming, and laboratory assessments can be time-consuming and expensive, remote sensing may offer a faster, more cost-effective method to investigate blooms at greater spatial and temporal extents in freshwater ecosystems. Rivers, reservoirs, and lakes are particularly important because of their environmental, economic, cultural, and recreational roles in nature and society, and advancing remote sensing methods could improve our ability to monitor and mitigate blooms in these settings across the world. This dissertation explores the spatial and temporal dynamics of algal blooms, both “good” (non-toxic filamentous algae) and “bad” (toxic cyanobacteria), throughout freshwater environments of California. In Chapter 1, I introduce the importance and risks of algae, as well as a background of in situ and remote sensing methods to monitor algae. Chapter 2 examines the use of unoccupied aerial vehicle (UAV) imagery over the Klamath River to understand the distribution of aquatic plants and filamentous algae prior to the largest dam removal in history. Chapter 3 moves upstream in the Klamath River to two reservoirs, Iron Gate and Copco, and uses high-resolution Sentinel-2 satellite imagery to detect the spatial distribution and timing of potentially toxic blooms in a five-year time series. Chapter 4 integrates two statewide harmful algal bloom datasets (one of crowdsourced reports and another of 300-meter Sentinel-3 satellite imagery) with higher-resolution Sentinel-2 imagery in order to monitor a greater number of lakes and reservoirs in California with higher resolution data. Finally, in Chapter 5, I review the major findings, lessons learned, and challenges of this research and posit new directions of future research to improve remote sensing techniques of algal bloom detection in freshwater environments.

Table of Contents

Acknowledgements	ii
Chapter 1: An Introduction to High-Resolution Remote Sensing of Algal Blooms	1
Chapter 2: Application of UAV Imagery to Detect and Quantify Submerged Filamentous Algae and Rooted Macrophytes in a Non-Wadeable River	6
Chapter 3: Mapping Algal Bloom Dynamics in Small Reservoirs using Sentinel-2 Imagery in Google Earth Engine	26
Chapter 4: Integrating Crowdsourced Incident Reports with Satellite Imagery to Understand Algal Blooms in California Lakes and Reservoirs	44
Chapter 5: Lessons Learned and Future Directions of High-Resolution Remote Sensing of Algal Blooms	60
References	64

Acknowledgements

First and foremost, I'd like to thank my advisor, Dr. Maggi Kelly. She has been a rock in my life for the past decade, inspiring me to dive deeper into geographic information systems (GIS) when I was an undergraduate student at UC Berkeley, and motivating me to apply to graduate school and join her lab. She is an incredible storyteller and always helps me see the big picture. Also, some of my favorite parts of grad school were teaching the GIS & Environmental Science course with her for 3 semesters. She is fun to work with, she prioritizes her students, and she brings so much enthusiasm to the classroom. Maggi is incredibly caring, and she carried our lab through difficult times including during the pandemic. She is also one of the most hilarious professors I have ever met. I have grown immensely as a science communicator, researcher, and mentor from working with Maggi, and I am so grateful to have been her student in the Kelly Lab.

I couldn't have made it this far without the support of my dissertation committee. Maggi, Iryna Dronova, and Ted Grantham have been so considerate, thoughtful, and responsive throughout my time in grad school. Iryna has been instrumental in my growth as a remote sensing scientist, and her Remote Sensing course changed my life. She is a very kind person with an immense amount of knowledge, and she is always a pleasure to work with. Ted has been very influential in my development as an environmental scientist in the field of water resources. From meetings in the Freshwater lab, collaborations with the Berkeley Water Group, and through his detailed advice on my dissertation research, Ted is always willing to help. He is also very kind, intelligent, and an excellent writer. I am so proud of both Iryna and Ted for being awarded tenure and advancing their careers while I've been in grad school. They certainly deserve these big achievements!

I want to thank my labmates and collaborators who helped me along my academic journey and were vital assets in this process. Annie Taylor has been one of the most influential people throughout my time in grad school, being not only my anchor, but also a collaborator and coding genius. I want to thank her for all of her support, especially on my last chapter. The Kelly Lab is such a special group, and I sincerely thank Roxy Cruz, Christine Wilkinson, Kelly Easterday, Erin Beller, and Jenny Palomino for being amazing women in my life and for supporting me through all phases of grad school. Members of the Klamath community, such as Laurel Genzoli, Randy Turner, Eli Asarian, Jake Kann, and water quality researchers such as Keith Bouma-Gregson, were paramount to my success and I sincerely appreciate their contributions.

Finally, I couldn't have done it without my friends and family. My sister, Liz, is an angel and has spent hours with me practicing presentations and helping me navigate big chapters in life. My mom, dad, brother, stepparents, and family friends have also been incredibly supportive cheerleaders throughout my life. HiP House Cooperative has been a saving grace throughout grad school and I have loved living with other HiPpos for the past 5 years. My best friends and partner always have my back and they mean the world to me. Excited for more camping adventures, bike parties, and hot spring soaks in the future. Thank you all so, so much!

Chapter 1: An Introduction to High-Resolution Remote Sensing of Algal Blooms

Part of this chapter has been previously published and is reproduced here with kind permission of the co-authors.

Kislik, C., Dronova, I., Kelly, M. (2018). UAVs in Support of Algal Bloom Research: A Review of Current Applications and Future Opportunities. *Drones*, 2(4), 35; doi:10.3390/drones2040035

Algae are among the most important living beings on Earth. They are a complex group of organisms that thrive in freshwater, frozen, marine, and brackish ecosystems across the globe (Peacock et al. 2018; Vincent and Howard-Williams 1986), and there are an estimated 30,000 to 1 million different species of algae (Guiry 2012). Unlike plants, algae do not have roots, stems, leaves, or a vascular system to transport nutrients and water. However, algae photosynthesize as plants do and produce oxygen (Weiss 1952). Algae range in size, from microscopic unicellular organisms such as the *Chlamydomonas* genus (<20 micrometers long) (Makino et al. 2019) to giant kelp, such as *M. pyrifera* (up to 50 meters long) (Macaya and Zuccarello 2010). They are diverse in that they can be single-celled, filamentous, or more plant-like and they vary in color, ranging from green (Chlorophyta) to red (Rhodophyta) to brown (Phaeophyta) (Chan, Ho, and Phang 2006). Blue-green algae, also known as cyanobacteria, have been on this planet for about 3.5 billion years (Schopf and Packer 1987), and their ability to photosynthesize is linked to the initial oxygenation of Earth's atmosphere. Algae currently provide about 30-50% of the oxygen available to humans, other animals, and plants on the planet (Chapman 2013), sustaining life as we know it.

In addition to oxygen production, algae provide vital environmental and economic benefits. As primary producers, algae create the foundation for aquatic food webs and are essential to the health of many freshwater and marine ecosystems (Klemas 2012; Lee et al. 2015; Blondeau-Patissier et al. 2014). They also sequester large volumes of carbon and can be used to produce food and fuel (Chapman 2013; Okada and Watanabe 2007). For example, the blue-green alga *Spirulina* is harvested commercially across the globe for its high vitamin A content (Tang and Suter 2011) and the green alga *Chlorella* is consumed globally, and especially in several Asian countries, for its high protein content (Ramazanov and Ramazanov 2006). Algae have also been cultivated for biofuel; a green alga called *Botryococcus braunii* is harvested for its oil and rivals the efficiency of other alternative fossil fuel crops, including those grown for feedstock purposes (Ramaraj, Kawaree, and Unpaprom 2016). There are many other types of "good algae," such as microalgal phytoplankton to macroalgal kelp fields, that benefit the environment and economy. However, the same species that provide benefits can also cause economic, environmental, and health problems when they proliferate to an extraordinary extent or produce dangerous toxins.

Algae can become perilous when large patches grow in response to excess nutrients and environmental changes in light availability, water pH, wind intensity, and water temperature (Van der Merwe and Price 2015). Some algae also produce toxins, including dinoflagellates, diatoms, and cyanobacteria (Smayda 1997; Moore et al. 2008; Van der Merwe and Price 2015). For

example, toxic phytoplankton species can cause paralytic, diarrhetic, amnesic, ciguatera, and neurotoxic shellfish poisoning in shellfish consumers, and can materialize as aerosols that drift from estuarine or coastal regions and trigger asthma symptoms (Moore et al. 2008). It is uncertain what causes specific algal species to express toxins at certain times, although some believe it is in response to the availability of limited nutrients, the presence of certain bacteria, or to protect against grazing from zooplankton (S. S. Bates et al. 1995; Mos 2001; Stephen S. Bates et al. 2004; W. W. Carmichael 1992). Both toxic and non-toxic algal species can have deleterious effects on aquatic life by clogging fish gills, depleting the water's oxygen levels, and killing fish and other organisms (G. M. Hallegraeff 2003; Kirkpatrick et al. 2004). The proliferation of these "bad algae" in aquatic ecosystems are commonly referred to as harmful algal blooms, or HABs.

Harmful algal blooms have existed for centuries. The first written record of algal blooms is believed to be from the Bible around 1000 B.C.: ". . . all the waters that were in the river were turned to blood. And the fish that was in the river died; and the river stank, and the Egyptians could not drink of the water of the river' (Exodus 7: 20–1)." (G. M. Hallegraeff 1993). The first recorded instance of the most common and severe type of shellfish poisoning produced by algal toxins, paralytic shellfish poisoning, was in 1793 from Captain George Vancouver's *A Voyage of Discovery to the North Pacific Ocean and Round the World*. Captain Vancouver's crew landed in British Columbia (in what is now known as Poison Cove) where it was then taboo for local Tribes to eat shellfish if the ocean was a specific color (G. M. Hallegraeff 1993). One of the 5 crew members who ate the poisoned mussels died within 6 hours of consumption (Ansdell 2019). Paralytic shellfish toxins were not considered a serious public health concern until 1927 when over 100 people near San Francisco became ill and several died after consuming poisoned shellfish (Price, Kizer, and Hansgen 1991). A paralytic shellfish toxic monitoring program was then established, becoming the first of its kind in the United States (D. M. Anderson et al. 2021). Harmful algae remain a significant health risk. From 2017 to 2019, there were 321 emergency room visits associated with toxic algal blooms across the country (Lavery et al. 2021). Harmful algae have plagued human civilization for thousands of years and they continue to increase (D. M. Anderson 2009). However, only within the past 200 years have we been able to mitigate these harmful outbreaks.

While most HABs are related to toxin exposure in marine ecosystems, these events can exist in any type of aquatic environment. They have become notorious in locations such as Toledo, Ohio, for poisoning the city's drinking water (J. C. Ho and Michalak 2015), as well as Lake Champlain, Vermont, for dog mortalities (Boyer et al. 2004). It is important to understand the dynamics of HABs that flourish in freshwater bodies because these are the resources we depend on for drinking, farming, boating, cultural practices, and recreation (Pitois, Jackson, and Wood 2000). Furthermore, freshwater blooms are estimated to cost the United States about \$4 billion in economic losses each year (J. C. Ho, Michalak, and Pahlevan 2019), and mitigating these events would save money and diminish the risk of severe illness and death.

Cyanobacteria (blue-green algae) are one of the most prevalent groups of HABs in freshwater ecosystems (D. M. Anderson, Glibert, and Burkholder 2002; Coffey et al. 2020), and they have been linked to toxic events in small freshwater environments (Backer 2002; A. de la Cruz et al. 2017; Dalu and Wasserman 2018; Quesada et al. 2006; J. Yang et al. 2016; Mwaura, Koyo, and Zech 2004) in over 100 countries (Harke et al. 2016). Cyanobacteria HABs are common in small lakes and reservoirs across the globe, likely due to high concentrations of nutrients such as phosphorus that can quickly accumulate in these environments (Lobo et al. 2021). These blooms are typically seasonal, often reaching highest values from August to

September in temperate-region reservoirs (Jacoby and Kann 2007; Oliver, Dahlgren, and Deas 2014), although cyanobacteria HABs have also been detected in freshwater ecosystems year round (Filatova et al. 2020; Coffey et al. 2020). Due to the increasing number of cyanobacteria HABs in the United States, the Environmental Protection Agency has created advisories to better monitor and understand public health risks associated with these events (United States Environmental Protection Agency 2021).

As global water temperatures warm (Gobler et al. 2017; Jochens et al. 2010) and urban and agricultural runoff continues to supply water systems with nutrients (Klemas 2012), the frequency of algal bloom events, including HABs, will likely continue to climb (Hans W. Paerl and Huisman 2008; Hudnell 2010). These events pose threats to aquatic ecosystems and human health and call for new management strategies with tools at scales appropriate to the events in question. Ho et al. (2019) determined that phytoplankton blooms in lakes across the globe have been increasing intensely since the 1980s, pointing to increased fertilizer use as a potential culprit (J. C. Ho, Michalak, and Pahlevan 2019). However, Hallegraff et al. (2021) believe that increased monitoring, rather than climate change or nutrient inputs, is the real reason for this perceived increase in HABs across the globe (Gustaaf M. Hallegraeff et al. 2021). In any case, the potential for an increase in global algal blooms is alarming because of the threat of deleterious health effects within humans and other organisms. It also underscores the need to improve and standardize the way in which HABs are monitored in order to better understand and ultimately mitigate the risks of algae blooms in freshwater ecosystems across the world.

The first methods used to detect and quantify algal blooms date back to the 1700s when sea navigators and botanists recorded visual and microscopic observations of various marine algae in their notebooks (Papenfuss 1992). By the early 20th century, algae sampling methods had developed to include in situ measurements of chlorophyll-a, turbidity, total suspended matter, and surface water temperature (C. I. Weber 1986; Goldberg, Kirby, and Licht 2016; Pölönen et al. 2014), as well as field sampling of algal cover and spectroradiometer measurements of algal spectral reflectance (Honkavaara et al. 2013; Jang et al. 2016; Shang et al. 2017; F. Xu et al. 2018). Since the late 19th century and early 20th century, researchers have used microscopy to identify specific algal species present in water bodies, and this method continues today (Bollard-Breen et al. 2015; Van der Merwe and Price 2015; Whipple 1914). Contemporary laboratory analyses for toxins include Enzyme-Linked Immunosorbent Assays (ELISA) and Protein Phosphatase Inhibition Assays (PPIA), which can be time intensive and expensive (Watson et al. 2017). Recently, visual, ground-based methods have been developed that involve snorkeling, swimming, and wading across bodies of water (Kislik et al. 2020). While improving the ability to detect and monitor algal blooms, many of these in situ sampling methods are time-consuming, financially burdensome, and even dangerous. Furthermore, algal sampling programs that involve laboratory analyses are expensive and involve problematic time lags that can delay posting of advisory signs of potentially toxic blooms.

Recent advances in remote sensing technology are creating opportunities to develop faster, safer, and less expensive methods to monitor algal blooms. Remote sensing has proven to be an effective tool to study algae because of optical detection capabilities, and algal blooms are commonly studied water quality topics that incorporate remote sensing methods in current literature. Algae contain a photosynthesizing pigment called chlorophyll-a (chl-a) which can be detected to understand the presence and distribution of algae in an aquatic environment. Generally, water scatters blue light in non-productive portions of water bodies, making them appear blue, while productive regions with high plankton content appear green (Klemas 2012).

This coloration distinction can be used to optically detect algal blooms by measuring chl-a absorption peaks at 500 nm and 675 nm, reflectance peaks at 550 nm and 700 nm, and a fluorescence peak at 683 nm (Shen, Xu, and Guo 2012). Algae also have different accessory pigments to absorb light for photosynthesis, such as phycocyanin in cyanobacteria (Simis, Peters, and Gons 2005). Such pigments have unique spectral signatures, allowing for the identification of algae to the genus level using high resolution imagery. Many methods of optical identification of cyanobacteria involve algorithms that accentuate phycocyanin by observing measurements in the 615-630 nm range. Other methods rely on observing the spectral shape of algae to increase the signal-to-noise ratio (Kudela et al. 2015). These methods have been applied through various technologies, including remote sensing instruments, which have advanced algal research to greater spatial, temporal, and spectral detection capacities.

Common remote sensing approaches used to identify algal blooms include data from satellite and airborne imagery analysis (Shen, Xu, and Guo 2012; Kutser 2009; Hook et al. 2001). Classic remote sensing methods that have been used to observe algal blooms since the late 1970s include multispectral satellite sensors such as the Coastal Zone Color Scanner (CZCS) (which was the first ocean satellite sensor), the Sea-viewing Wide Field-of-view Sensor (SeaWiFS), Moderate Resolution Imaging Spectrometer (MODIS), Medium Resolution Imaging Spectrometer (MERIS), Ocean Color Monitor (OCM) sensors, and the Advanced Very High Resolution Radiometer (AVHRR). However, coarse spatial resolution (> 300 m / pixel) of satellite imagery can only identify massive blooms that encompass tens to hundreds of square kilometers. It is often very difficult to discern a bloom in a relatively small water body, such as a bay, lake, river, or estuary, from satellite imagery (Shen, Xu, and Guo 2012). Aerial monitoring of algal blooms via airplanes has been conducted to identify blooms in smaller water bodies. Sensors that have been flown on aircraft and used for algal bloom studies include the Airborne Visible / Infrared Imaging Spectrometer (AVIRIS), the Compact Airborne Spectrographic Imager (CASI), and the MODIS/ASTER airborne simulator (MASTER) (Hook et al. 2001; Kutser 2009).

Recent developments in unoccupied aerial vehicles (UAVs, also known as drones) technology and a transition from military applications to environmental research purposes (Shang et al. 2017) have also opened the door for high-resolution algal bloom monitoring. Although UAVs currently cannot rival the spatial extent and often spectral capacity captured by satellite or aircraft sensors, they offer the potential benefit of higher temporal revisit times and spatial resolution to the centimeter scale. They can also be flexibly modified with different sensors to perform specific tasks or capture specific spectral properties (Manfreda et al. 2018; DeBell et al. 2015). Since compact sensors for UAVs entered the commercial market in the early 2000s, their use in research has skyrocketed (DeBell et al. 2015; Johnston 2018), including several studies that have tested UAV-based phytoplankton bloom identification methods. As UAV technology and algal bloom detection algorithms continue to advance, small unoccupied platforms are likely to become invaluable tools for algal bloom research.

In this dissertation, I introduce improved monitoring techniques for both benthic (attached to the bottom of the water body) and planktonic (on the water's surface) blooms in California, with particular focus on the Klamath River Basin. While extensive research has been conducted to identify algal blooms using satellite imagery, few studies have used very high resolution drone or satellite images to identify blooms in large, non-wadeable rivers and in small lakes and reservoirs. More specifically, little work has been conducted to examine the spatial and temporal dynamics of potentially toxic freshwater blooms using aerial imagery in the Klamath

Basin and throughout California. This work also establishes new methods for how best to acquire, process, and interpret new and existing water quality datasets to study algal blooms and inform management of rivers, lakes, and reservoirs in California and beyond. There is a plethora of water-related datasets available (Strobl and Robillard 2008), and this dissertation helps make several of these datasets and data processing methodologies more accessible. Here, we describe the “good” (benthic filamentous algae), the “bad” (potentially toxic cyanobacteria), the algae (any other types of algae).

This dissertation is composed of three research chapters and a concluding chapter. The first research chapter (Chapter 2: Application of UAV Imagery to Detect and Quantify Submerged Filamentous Algae and Rooted Macrophytes in a Non-Wadeable River) provides a standardized approach to map submerged filamentous algae and rooted macrophytes along the Klamath River using a pixel-based supervised classification method applied to aerial drone imagery. I quantified the spatial distribution and percent cover of these primary producers throughout 32 transects along the river, and also determined to what depth aerial imagery could perceive filamentous algae and aquatic plants below the water surface. Chapter 3: Mapping Algal Bloom Dynamics in Small Reservoirs using Sentinel-2 Imagery in Google Earth Engine tests the ability of four spectral indices applied to Sentinel-2 satellite imagery to detect algal blooms in two reservoirs of the Klamath River between 2015 to 2020. I analyzed the heterogeneity of bloom events and showed that discrete, single in situ samples cannot capture the dynamics that are present in these small reservoirs. In Chapter 4, I explore how Sentinel-2 imagery can be used to monitor HABs in California lakes and reservoirs. Entitled, “Integrating Crowdsourced Incident Reports with Satellite Imagery to Understand Algal Blooms in California Lakes and Reservoirs,” this chapter compares two distinct California freshwater HAB datasets (one of crowdsourced reports and another of coarse-resolution satellite imagery) with detections of HABs from higher-resolution Sentinel-2 imagery. Data at this spatial resolution has the potential to increase near-real time satellite-based monitoring in California lakes and reservoirs by 55 times, although spectral resolution remains a challenge. In the conclusion of my dissertation (Chapter 5), I summarize the key findings, lessons learned, and challenges encountered in my research, along with proposed future directions in the field of algal bloom remote sensing. In particular, I explore the potential to take advantage of greater spectral resolution imagery, the need for improved understanding of the causes of blooms, and the potential for freshwater algal bloom forecasting. This body of work is intended to help other researchers, water quality managers, recreational water users, dog owners, and the general public leverage new data and tools to better track and understand algal bloom dynamics throughout California and in rivers, lakes, and reservoirs around the globe.

Chapter 2: Application of UAV Imagery to Detect and Quantify Submerged Filamentous Algae and Rooted Macrophytes in a Non-Wadeable River

This chapter has been previously published and is reproduced here with kind permission of the co-authors.

Kislik, C., Genzoli, L., Lyons, A., Kelly, M. (2020). Application of UAV Imagery to Detect and Quantify Submerged Filamentous Algae and Rooted Macrophytes in a Non-Wadeable River. *Remote Sensing*. 12, 3332; doi:10.3390/rs12203332

Abstract

Imagery from unoccupied aerial vehicles (UAVs) is useful for mapping floating and emerged primary producers, as well as single taxa of submerged primary producers in shallow, clear, lakes and streams. However, there is little research on the effectiveness of UAV imagery-based detection and quantification of submerged filamentous algae and rooted macrophytes in deeper rivers using a standard red-green-blue (RGB) camera. This study provides a novel application of UAV imagery analysis for monitoring a non-wadeable river, the Klamath River in northern California, USA. River depth and solar angle during flight were analyzed to understand their effects on benthic primary producer detection. A supervised, pixel-based Random Trees classifier was utilized as a detection mechanism to estimate the percent cover of submerged filamentous algae and rooted macrophytes from aerial photos within 32 sites along the river in June and July 2019. In-situ surveys conducted via wading and snorkeling were used to validate these data. Overall accuracy was 82% for all sites and the highest overall accuracy of classified UAV images was associated with solar angles between 47.5 and 58.72 degrees (10:04 am to 11:21 am). Benthic algae were detected at depths of 1.9 m underwater and submerged macrophytes were detected down to 1.2 m (river depth) via the UAV imagery in this relatively clear river (Secchi depth > 2 m). Percent cover reached a maximum of 31% for rooted macrophytes and 39% for filamentous algae within all sites. Macrophytes dominated the upstream reaches, while filamentous algae dominated the downstream reaches closer to the Pacific Ocean. In upcoming years, four proposed dam removals are expected to alter the species composition and abundance of benthic filamentous algae and rooted macrophytes, and aerial imagery provides an effective method to monitor these changes.

1. Introduction

The extent, distribution, and assemblage of primary producers can indicate the ecological health of a water body (Dennison et al. 1993; Carpenter and Lodge 1986). Like vegetation on land, algae and aquatic plants provide a large portion of the nutritional and structural foundation for aquatic ecosystems (Wetzel 1964). In many rivers and clear lakes, primary producer assemblages are dominated by benthic algae and aquatic plants growing attached to the substrate, where filamentous algae and aquatic plants provide structural support to streambeds, as well as improve water quality by storing and processing nutrients and promoting settlement of suspended particles (Jones et al. 2012; *Algal Ecology: Freshwater Benthic Ecosystem* 1996). Diverse assemblages of primary producers, including thin films of diatoms, filamentous algae,

and rooted aquatic plants also provide food resources and habitat for invertebrates and fish in these ecosystems (Vadeboncoeur and Power 2017; Lusardi, Jeffres, and Moyle 2018).

Macrophytes and benthic algae can become a nuisance to water bodies when dams, changing flows, and excess nutrients stimulate algal proliferations that reduce overall biodiversity and degrade water quality (Duarte 1995; Torn and Martin 2012; Welch et al. 1988; Flinders and Hart 2009; Dodds and Gudder 1992; Rørslett and Johansen 1996). Medium and large rivers are especially vulnerable to nutrients and environmental conditions that promote algal and aquatic plant proliferations due to their position in watersheds and proximity to human habitation (*Algal Ecology: Freshwater Benthic Ecosystem* 1996; B. J. F. Biggs 1996, 2000; Hilton et al. 2006; Smith, Tilman, and Nekola 1999). Despite the importance of primary producers in rivers and their vulnerability to alterations, monitoring the extent, types, and coverage of benthic primary producers in rivers is rarely conducted due to challenges associated with heterogeneity in benthic communities and field conditions. Given the important ecological functions and potential problems of macrophyte and benthic algal proliferations, it is valuable to monitor and understand primary producer assemblages in aquatic ecosystems.

High-resolution imagery can provide fine-scale detection of algae and vegetation (Aguirre-Gómez et al. 2017; Husson, Hagner, and Ecke 2014; C. N. Brooks et al. 2019; Van der Merwe and Price 2015). Unoccupied Aerial Vehicles (UAVs) have been utilized for algal bloom and submerged aquatic vegetation detection for nearly two decades (Kislik, Dronova, and Kelly 2018; Flynn and Chapra 2014; Nowak, Dziób, and Bogawski 2019). This type of high-resolution aerial imagery offers a cost-effective and rapid method to assess primary producer assemblages in aquatic environments and provides greater spatial resolution than current commercially available satellite imagery (B. Yang et al. 2019; Díaz-Delgado et al. 2019; Manfreda et al. 2018). Furthermore, UAV image capture can provide benefits to traditional surveying of submerged filamentous algae and rooted aquatic vegetation in deep rivers, such as wading, swimming, kayaking, boating, and scuba diving (Preskitt, Vroom, and Smith 2004; Priddle 1980; Pennuto, Howell, and Makarewicz 2012; Suplee et al. 2009), because this method is more accessible than physically entering a body of water, and it can accelerate the data acquisition process (Beijbom et al. 2015). For these reasons, this study explored UAV image capture as a method to supplement current detection and quantification techniques.

Several researchers, such as Husson et al. (Husson, Hagner, and Ecke 2014), Flynn & Chapra (Flynn and Chapra 2014), Visser et al. (Visser, Wallis, and Sinnott 2013), and Stanfield (Stanfield 2009), have been successful in identifying species and quantifying percent cover of submerged aquatic vegetation and benthic algae using UAV imagery over freshwater ecosystems. In these studies, Flynn & Chapra (Flynn and Chapra 2014) and Stanfield (Stanfield 2009) used multirotor DJI drones and Visser et al. (Visser, Wallis, and Sinnott 2013) used a Helikite UAV to capture imagery with red-green-blue (RGB) and multispectral cameras in wadeable (< 1 meter) (Flynn and Chapra 2014), and non-turbid (0-10 Formazin Nephelometric Units (FNU)) (Stanfield 2009) rivers. Several researchers flew over aquatic environments at low altitudes, such as Visser et al. (Visser, Wallis, and Sinnott 2013) at 5 m, Husson et al. (Husson, Hagner, and Ecke 2014) at 10 to 25 m, and Stanfield (Stanfield 2009) at 10 to 50 m, while others flew much higher, such as Flynn & Chapra (Flynn and Chapra 2014) at 120 m and Brooks et al. (C. N. Brooks et al. 2019) at 150 m. Flynn & Chapra (Flynn and Chapra 2014) and Stanfield (Stanfield 2009) used pixel-based classification techniques, and Visser et al. (Visser, Wallis, and Sinnott 2013) employed object-based image analysis (OBIA) methods. With the exception of Visser et al. (Visser, Wallis, and Sinnott 2013), which used a near-infrared camera to identify three

macrophyte species, Brooks et al. 2019 (C. N. Brooks et al. 2019), Flynn & Chapra (Flynn and Chapra 2014), and Stanfield (Stanfield 2009) focused on distinguishing one specific taxa from the rest of a submerged aquatic vegetation patch in clear, shallow environments. As green wavelengths are known to penetrate to deeper portions of the water column than other optical wavelengths (Silva et al. 2008; Visser, Wallis, and Sinnott 2013; Legleiter et al. 2004), Flynn & Chapra (Flynn and Chapra 2014), Visser et al. (Visser, Wallis, and Sinnott 2013), and Stanfield (Stanfield 2009) leveraged the green portion of the electromagnetic spectrum to detect submerged filamentous algae and macrophytes. However, a common challenge in this field involves detection interference due to sun glint (Aguirre-Gómez et al. 2017; Flynn and Chapra 2014; Stanfield 2009; Kwon et al. 2020), or the solar reflection of the sun off the water's surface. Several researchers have incorporated techniques such as dark object subtraction (Aguirre-Gómez et al. 2017) or calculations of solar angle (Mount 2005) to mitigate these effects.

Recent submerged algae and macrophyte monitoring via UAVs has expanded the use of high spectral resolution sensors and algorithms, but has yet to implement these techniques for multiple taxa in non-wadeable environments. Current researchers, such as Flynn & Chapra (Flynn Kyle F. and Chapra Steven C. 2020) use acoustic profiling, and others such as Brooks et al. (C. N. Brooks et al. 2019), Taddia et al. (Taddia et al. 2019), and Brinkhoff et al. (Brinkhoff, Hornbuckle, and Barton 2018) use RGB, multispectral, and hyperspectral sensors over shallow (less than 1 meter) aquatic environments. With the exception of Tait et al. (Tait et al. 2019), in which several macroalga species were detected using RGB and multispectral imagery in a shallow coastal environment, and Brinkhoff et al. (Brinkhoff, Hornbuckle, and Barton 2018), in which three aquatic vegetation species were identified using multispectral imagery in irrigation canals, current studies primarily identify a single submerged primary producer taxa (Flynn Kyle F. and Chapra Steven C. 2020; C. N. Brooks et al. 2019; Taddia et al. 2019). In marine environments, researchers such as Slocum et al. (Slocum et al. 2019) leverage RGB sensors on fixed-wing and rotary-wing UAVs to create 3D point clouds of submerged aquatic vegetation or coral reefs from structure from motion photogrammetry. Tait et al. (Tait et al. 2019) flew at 50 m, Taddia et al. (Taddia et al. 2019) flew at 70 m, and Brinkhoff et al. (Brinkhoff, Hornbuckle, and Barton 2018) flew at 75 m altitude. Several researchers used supervised classification techniques, such as Tait et al. (Tait et al. 2019) with support vector machines and Taddia et al. (Taddia et al. 2019) with maximum likelihood classification, and others, such as Brooks et al. (C. N. Brooks et al. 2019) and Brinkhoff et al. (Brinkhoff, Hornbuckle, and Barton 2018), used vegetation indices to identify submerged algae or macrophytes. Notable vegetation indices that have been applied to submerged aquatic vegetation detection in recent years include the Normalized Difference Aquatic Vegetation Index (NDAVI) and the Water Adjusted Vegetation Index (WAVI), both of which combine the near-infrared and blue bands (Brinkhoff, Hornbuckle, and Barton 2018; C. N. Brooks et al. 2019). Furthermore, the red edge band has been incorporated into submerged aquatic vegetation detection, as shown by studies from Taddia et al. (Taddia et al. 2019) and Brinkhoff et al. (Brinkhoff, Hornbuckle, and Barton 2018). Researchers, such as Slocum et al. (Slocum et al. 2019) and Kwon et al. (Kwon et al. 2020), are continuing to address issues of solar glint by flying slightly off-nadir and flying during times when solar angles are between 35 to 40 degrees. As demonstrated in previous studies conducted by Brooks et al. (C. N. Brooks et al. 2019), Flynn & Chapra (Flynn Kyle F. and Chapra Steven C. 2020), and Taddia et al. (Taddia et al. 2019), there is a paucity of research on the effectiveness of UAV-based benthic discrimination and quantification of multiple submerged taxa using RGB imagery in non-wadeable rivers.

This study employed an inexpensive (<\$1,500 USD) UAV with an RGB camera and used a machine learning algorithm to investigate how depth and solar angle influenced benthic primary producer identification and quantification in a non-wadeable river in northern California. The Klamath River is an ideal system to test the effectiveness of high-resolution aerial imagery to quantify benthic primary producer assemblages in a deep river because of its high rates of productivity, high associated algal biomass (Genzoli and Hall 2016; Gillett et al. 2016), and relatively high optical depth at baseflow. Also, because the Klamath River is dominated by swift currents and areas of depth > 1 m, surveying benthic primary producers using traditional transect survey methods designed for wadeable rivers is not possible (B. J. Biggs and Kilroy 2000; Ode, Fetscher, and Busse 2016). Furthermore, monitoring changes in primary producer assemblages is needed to track changes in flow management, restoration activities, climate change, and the planned removal of four large dams along this river (Bellmore et al. 2019; Van Kirk and Naman 2008). This study analyzed aerial images at 32 sites that had variable primary producer assemblages within the Klamath River during June and July of 2019. Research objectives were to: (1) classify submerged filamentous algae and rooted macrophytes using a Random Trees classification algorithm; (2) evaluate the accuracy of this classification scheme based on in-situ river surveys; (3) investigate the maximum depths and optimal solar angles at which submerged filamentous algae and rooted macrophytes can be detected with an RGB camera on board a UAV; and (4) quantify the percent cover of filamentous algae and rooted macrophytes at river locations with variable primary producer assemblages. This paper assesses the efficacy of RGB aerial imagery to identify and quantify multiple taxa of submerged filamentous algae and rooted macrophytes in a non-wadeable river, thereby providing a low-cost and accessible methodology to supplement current in-situ survey methods. Section 2 provides an overview of the study sites, technological components, data acquisition, and data processing methods. Section 3 focuses on the reported classification accuracies and distribution of submerged filamentous algae and rooted macrophytes throughout the study sites. Finally, sections 4 and 5 discuss limitations, recommendations, and applications of this study.

2. Materials and Methods

This section describes the study sites, aerial imagery and in-situ data collection methods, image processing and validation techniques, and percent cover calculation methods used in this study.

2.1. Study Sites

The 40,600-km² Klamath River watershed spans south-central Oregon and northwestern California, USA (Figure 1). The Klamath River starts at the outflow of Upper Klamath Lake in Oregon (42.3996° N, -121.8777° E), and travels approximately 420 km to the Pacific Ocean (41.5430° N, -124.0750° E). Free-flowing tributaries contribute substantial water during rain and snowmelt periods (generally October–May/June), with tributaries increasing in size and frequency with greater proximity to the Pacific Ocean. Summer base flows stabilize in July and August, when the outflow from Iron Gate Dam is the primary source of water to the river (mean August discharge from 2000–2019 = 27 m³/s, USGS Gage 11516530) until the confluence with the Trinity River, 262 km below the outflow of Iron Gate Dam. Flows from the Trinity River greatly increase flows below Iron Gate Dam (mean August discharge from 2000–2019 = 26 m³/s, Trinity River USGS Gage 11530000), which, combined with the contribution of smaller tributaries, result in August base flows of about 81 m³/s near the river mouth (Klamath River

near Klamath, USGS Gage 11530500). The Klamath River is a non-wadeable river due to both excessive depth and velocity, even during summer baseflow periods. This study examined benthic primary producer assemblages (submerged rooted macrophytes and filamentous algae) in June and July of 2019, as this is peak primary productivity season in the Klamath River (Gillett et al. 2016; Genzoli and Hall 2016), a time of lower flows, and when water clarity is sufficient to remotely sense benthic and emergent primary producers (Marcus and Fonstad 2008).

The upper watershed which supplies flows at Iron Gate Dam supports heavy agricultural use, including water withdrawals for irrigation and increased nutrient runoff (Snyder and Morace 1997), resulting in lower peak flows and increased nutrient concentrations to the Klamath River. A series of 4 hydroelectric dams located between 61 and 113 km below the Upper Klamath Lake outflow alters flow within the river and reservoirs and increases hydrologic stability below the dams (Bartholow, Campbell, and Flug 2004). High nutrient concentrations and stable flows support high rates of riverine primary productivity and substantial autotrophic biomass in the Klamath River (Genzoli and Hall 2016), with peak proliferations typically occurring below Iron Gate Dam in early summer. Standing stock of primary producers includes dense beds of filamentous algae and rooted-aquatic plants, such as *Cladophora* spp., *Potamogeton* spp., and *Elodea* spp. Both rooted aquatic plants and filamentous algae create seasonally dense plant and algal patches (Holmquist-Johnson and Milhous 2010) that are visible from river margins. Primary producer dominance changes longitudinally below the hydroelectric dams, shifting from rooted aquatic plant dominance to filamentous algae dominance downstream.

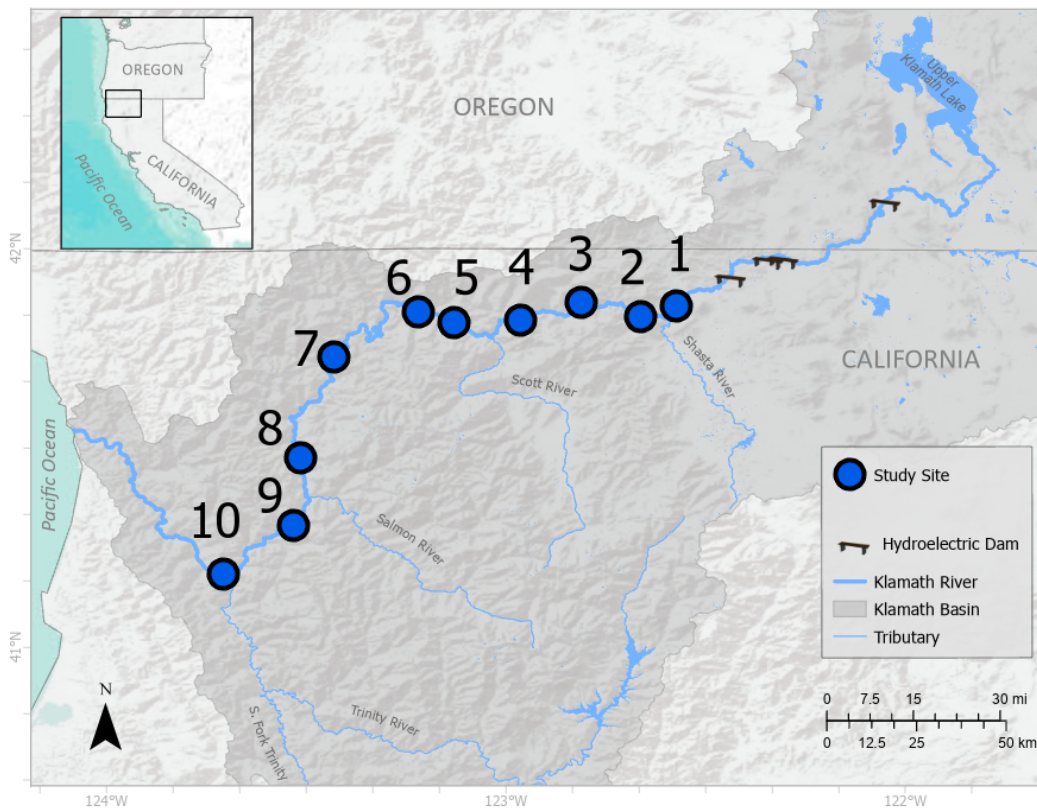


Figure 1. Ten river reach study locations on the Klamath River below Iron Gate Dam. The ten reaches that host 32 total sites are: 1. 15 Bridge (I5), 2. Tree of Heaven (TH), 3.

Above Beaver Creek (**ABC**), 4. Brown Bear (**BB**), 5. Rocky Point (**RP**), 6. Seiad Valley (**SV**), 7. Happy Camp (**HC**), 8. Old Man River (**OMR**), 9. Orleans (**OR**), 10. Weitchpec (**WE**).

2.2. Data Acquisition

2.2.1. UAV Data

Aerial imagery was captured to classify submerged filamentous algae and rooted macrophytes and estimate percent cover of each class from 32 sites within ten reaches of the Klamath River (Figure 1) between Iron Gate Dam and Weitchpec, CA. Imagery was acquired using a DJI Phantom 4 Pro rotorcraft (DJI, Shenzhen, China) (Figure 2), using the native RGB 20 megapixel camera. This camera has an 8.8 mm focal length and a resolution of 5,472 x 3,648 pixels (Peppas et al. 2019). Flights were conducted for 15 to 20 minutes over each of the 32 sites, at flying heights between 19 and 104 m. This resulted in estimated ground sampling distances between 0.52 and 2.85 cm (Table A1). Single images per site that encompassed the width of the channel and included portions of each side of the riverbank in every photo were acquired. Images were captured manually (without an automated mission flight plan) at nadir above each site, avoiding sunglint to minimize the relative angle between the sun and surface ripples. The UAV was flown between 10:04 am and 5:11 pm to correspond with in-situ transect surveys, from June 26 to July 9, 2019. The time of each UAV flight was converted to solar elevation in degrees (now referred to as solar angle) using the University of Oregon Solar Radiation Monitoring Lab's Sun Chart Program (<http://solardat.uoregon.edu/SunChartProgram.html>). Solar angle helps predict the amount of solar glare that is reflected off the water's surface and into the aerial sensor. No calibration panel was used for the RGB image analysis, and no atmospheric correction was applied, as this is often unnecessary for low-flying UAV image collection over a small region (Su and Chou 2015).



Figure 2. Examples of data acquisition using (A) a quadrant for in-situ river surveys and (B) a Phantom 4 Pro UAV for aerial image collection.

2.2.2. In-Situ Surveys

To validate the UAV imagery, in-situ surveys were conducted for rooted aquatic plants and filamentous algae along three to four transects (from one side of the river bank to the other) at each of the 10 reaches (Figure 3) in the Klamath River below Iron Gate Dam between June 26 and July 9, 2019. Reaches were surveyed starting at the reach closest to Iron Gate Dam, and ending near Weitchpec, CA. At each of the 10 reaches, the riverbed was surveyed to assess the coverage of aquatic vegetation. Reaches ranged from 1–8 km in length, based on river access points. Kayaks were used to float the 10 reaches, surveying six transects in each reach, with transects randomly chosen among variable habitats represented in the reach. Three to four out of the six transects per reach were selected for analysis based on corresponding UAV image quality and to reduce computational processing time. Each transect was a minimum of 100 m downstream from the previous transect, and attempts were made to survey transects with more pool-type and riffle-type characteristics. Each transect's general habitat type was estimated based on river velocity and surface tension characteristics and classified as a run, riffle, or pool (Table A1). Areas of rapids and swift current were under-represented in surveys due to safety concerns and the general inability of a surveyor to access these swift sections. Transect selection was balanced with what was possible to survey safely, as well as what was representative of the reach; thus, transects were selected in the field while conducting these surveys. No transects were fully wadeable across the river, confirming that the mixed survey method of wading and snorkeling was necessary. Each in-situ survey was completed in about an hour per site.

Several variables were measured and collected during the in-situ surveys. At each transect, a shore-based field technician recorded longitude and latitude with a handheld GPS (GPSMAP 76CSx, Garmin Inc., Olathe, Kansas) and a GPS-enabled GoPro Hero 5 (GoPro Inc., San Mateo, California), and measured wetted width with laser rangefinders from the river's edge. The technician calculated the width of the channel using the rangefinders, and divided each transect into 11 evenly spaced quadrants, from one side of the riverbank to the other. When possible, the surveyor waded to each of the quadrant locations (Figure 2). However, when the river became too deep for wading ($> 1\text{--}1.4$ m, depending on river velocity), the surveyor transitioned to snorkeling. Individual quadrants were not surveyed along some transects due to especially swift or deep points (N=56). At all transects, a minimum of seven quadrants were surveyed. At each quadrant, the surveyor lowered a 40 x 40 cm weighted PVC square to the riverbed to visually estimate information about filamentous algae and rooted macrophytes. Filamentous algae coverage was recorded when filaments were > 2 cm long. For each species or genera observed in a quadrant (generally identified to species for rooted aquatic plants and genus for algae), the surveyor recorded the species or genus code, percent cover of the specific taxa, the substrate that the vegetation type was growing on, plant condition and color, and the average length of the plant or its filaments within the quadrant. Mat thickness was recorded in species without obvious filaments. Water depth was recorded using a marked depth stick (quadrants < 2 m deep) or sonar depth finder (quadrants > 2 m deep, Vexilar LPS-1, Vexilar, Minneapolis, Minnesota). To test the effect of increasing mean river depth on the detectability and classification accuracy of benthic primary producers, in-situ depth measurements were averaged per site. Discrete points within each site were also evaluated to assess the maximum depth detection of filamentous algae and

rooted macrophytes in the aerial imagery. Turbidity was measured at deep portions (> 1 m) of a river reach by vertically deploying a Secchi disk from a kayak up to five times and taking an average. Secchi disk observations were not available at each reach due to depth limitations. Finally, the technician and UAV pilot recorded observational field notes regarding the composition of benthic filamentous algae and rooted macrophytes 100 m upstream and 100 m downstream of each transect by kayaking and collecting samples from sizeable patches (> 1 m²) to assist in the image classification and validation processes.

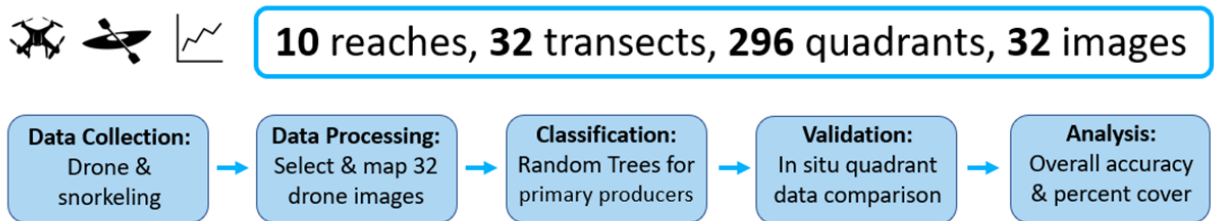


Figure 3. Methodology of field data collection and data processing and analysis for this study.

2.3. Image Classification

A supervised classification scheme was employed to categorize image pixels into several classes after images were chosen. First, all aerial photos were reviewed and 3 to 4 images from each of the 10 river reaches were selected based on image quality and in efforts to reduce computational processing time. A total of 32 images (out of 60 images) were chosen for analysis after visually inspecting all photos and selecting the highest-quality images that had reduced sun reflection and glare, variation of in-situ depth measurements, and were captured at a nadir camera angle. In addition to image quality, these 32 images were subjectively selected to reduce image processing time associated with classifications and percent cover estimates. A single-image analysis approach was used in which only one image per site was analyzed (orthomosaics were not constructed for each site) due to challenges in stitching aerial images over a uniform surface such as water. Image metadata was then extracted using the *uasimg* R package (Andrew Lyons and the R Development Core Team 2020) and incorporated to map centroids and footprints of images, as well as to estimate ground sampling distance and above ground altitude of each image. Yaw was manually corrected using Georeference tools in ArcGIS Pro 2.5 (Esri, Redlands, California).

Known GPS locations and visual observation were used to train and classify the UAV imagery into a six-class schema (1. algae, 2. macrophytes, 3. water, 4. land, 5. shadows, and 6. sunglint) with a machine learning algorithm. To detect these classes within the imagery, in-situ validation locations within each image were identified using GPS coordinates extracted from metadata on the GPS devices. It is important to acknowledge that positioning and alignment errors are introduced from the GPS devices used in the river, as well as from the Phantom 4 Pro internal GPS and subsequent EXIF modeling that depends on x, y, and z coordinate values. These errors were minimized by manually aligning images using high resolution basemaps in ArcGIS Pro and Google Earth, comparing river width measurements using ArcGIS Pro tools and in-situ width measurements from laser rangefinders, overlaying several estimated GPS coordinates (GoPro, Garmin, UAV) within the map, and visually detecting the quadrant and surveyor within the photo. When neither the quadrant nor swimmer was visible in the imagery,

training sample pixels were selected from regions identified in the visual observation notes that were taken during aerial missions.

Algae and macrophyte classes were identified within UAV photos by incorporating information from in-situ quadrant measurements that had 80% cover or more of either class, resulting in 162 quadrants used for filamentous algae classification and 46 quadrants for rooted macrophyte classification. These data were used to justify the ‘pure pixel’ assumption employed when selecting samples for classification. All filamentous algae and macrophytes in this study were submerged, and it was assumed that any algae or macrophyte pixels that were visible from above the water’s surface represented only one class (thus were considered ‘pure pixels’). The algae and macrophyte classes were categorized generally, without classification to the species or genus level, and filamentous algae (no diatoms) composed the algae class. The water class included any portion of the river in which filamentous algae or rooted macrophytes were not visible, including wetted channels and riverbed. The land class included any rocks, grass, trees, sand, or otherwise surrounding environment adjacent to the river. The shadows class included dark shadow pixels throughout an image, while the sunglint class involved highly reflective solar glare pixels on the surface of the water. Not all classes were represented in every image.

After creating the class schema, a Random Trees pixel-based supervised classifier was trained and applied to all image pixels in ArcGIS Pro. Roughly 50-80 training sample polygons were selected per class by visually identifying sample pixels of all classes except algae and macrophytes, which were verified with in-situ quadrant surveys and visual observation notes written concurrently during each aerial mission. To minimize error, ‘pure pixel’ samples (containing only pixels of the class) were created by selecting pixels from the center of a patch and with a minimum number of 3 pixels. Each image was classified using a Random Trees classifier (30 maximum number of trees, 30 maximum tree depth, 1,000 maximum number of samples per class). This algorithm iteratively classifies an image using a random subset of training pixels to form a group of decision trees. Samples are classified based on the majority “vote” of the trained decision tree label outputs (D. Shi and Yang 2016; Gerke 2011). This machine learning algorithm was chosen because it reduces computational load, particularly compared to other ensemble classifiers such as boosting and bootstrap aggregating (Benediktsson, Chanussot, and Fauvel 2007), and it is less prone to overfitting data, as artificial neural networks (Maxwell, Warner, and Fang 2018) and maximum likelihood classification (Gómez-Chova et al. 2011) have been reported to do. Furthermore, Random Trees has low error rates of classification (Crisci, Ghattas, and Perera 2012) in comparison to support vector machines and artificial neural networks (Rodríguez-Puerta et al. 2020), and this method is well suited for studies involving multiple sources of remote sensing imagery (Benediktsson, Chanussot, and Fauvel 2007), as in this study in which each image is analyzed separately. Finally, the Random Trees method was chosen over OBIA because of its ability to detect heterogeneous environments (Ghimire, Rogan, and Miller 2010), such as the fine-scale combinations of filamentous algae and rooted macrophyte patches that are common in the Klamath River (J. E. Asarian et al. 2014).

2.4. Validation

UAV imagery classifications were validated using the in-situ survey data and visual observations recorded in the field. The predicted class was compared against the observed class to validate sampling points, and additional variables such as solar angle were analyzed to help understand the factors affecting classification accuracy. The accuracy was assessed by creating

an error matrix to calculate errors of omission, errors of commission, and the overall accuracy using the in-situ transect measurements as reference data, and visual observations to increase the spatial distribution of validation. In this context, omission error can be described as how often filamentous algae in the river is omitted from the proper class, while commission error is how often pixels identified as filamentous algae in the image are incorrectly classified (Husson, Hagner, and Ecke 2014). Overall accuracy describes the proportion of correctly mapped pixels out of the total number of reference pixels. In this study, the overall accuracy, and not the kappa coefficient, is reported following best practices to omit the latter metric in imagery classification accuracy assessments (Foody 2020; Pontius and Millones 2011). ArcGIS Pro 2.5 was used to calculate omission error, commission error, and overall accuracy by assigning ground reference values to 50-100 stratified random points (randomly distributed based proportionally on the area of each class) per image and computing an error matrix.

2.5. Percent Cover Estimates

The percent cover of filamentous algae and rooted macrophytes was estimated based on UAV image classifications to ascertain the spatial distribution of these groups within the Klamath River between Iron Gate Dam and Weitchpec, CA. All filamentous algal species that were classified in the imagery were pooled into one percent cover class (“algae”), and all rooted macrophyte species classified in the imagery were grouped to form another separate percent cover class (“macrophytes”) (Hughes et al. 2011). To maintain a standardized number of pixels per image, all images were resampled to 0.014m (the average resolution of all 32 images), and then clipped using a bounding box of 48.8 m x 48.8 m to mimic a 40 cm x 40 cm quadrant at 160 feet (48.8 m) flight altitude. Next, rasters were converted to polygons (simplified polygons with multipart features), and summary statistics were performed on the area of each class. ArcGIS Pro 2.5 tools, including Resample, Extract by Mask, Raster to Polygon, and Summary Statistics were used within ArcGIS ModelBuilder. Finally, percent cover was calculated by dividing each class’ area by the total number of pixels in the image. Although each image was initially classified using the six-class schema described above, the land class was excluded from the filamentous algae and rooted macrophyte percent cover estimates to more accurately depict these classes within the river rather than within the entire image. Filamentous algae and macrophyte percent cover estimates within the UAV imagery were then compared to the in-situ quadrant class cover estimates per site using a linear regression (“Lm Function | R Documentation” 2017) with the ggplot2 package (Wickham 2016) in R version 3.6.3 software (Core Team and Others 2013).

3. Results

This section details this study’s findings pertaining to image classification outcomes in relation to depth and solar angle, as well as percent cover estimates of benthic filamentous algae and rooted macrophytes calculated throughout study sites via aerial imagery classifications and in-situ surveys.

3.1. Random Trees Classification Results

Overall accuracy of all classes (algae, macrophytes, water, land, shadows, sunglint) from the Random Trees supervised classification of 32 sites of the Klamath River was 82% (Table 1). Commission error was lowest for the water class (5%) and highest for the macrophyte class (41%), while omission error was lowest for the shadows class (5%) and highest for the land class

(32%). The algae class had lower commission error (27%) but higher omission error (17%) than the macrophyte class (41% commission error and 12% omission error). For individual sites, overall accuracy was highest at Weitchpec site 2 (WE 2) (95%) and lowest at Rocky Point site 4 (RP 4) (66%) (Table A1). Weitchpec site 2 (WE 2) and Happy Camp site 1 (HC 1) had the lowest commission error of all 32 images' algae classes at 0%, while Above Interstate 5 site 5 (I5 5) had the lowest commission error of all images' macrophyte classes at 10%. For groups of sites, Weitchpec (WE) reach sites (N=4) had the highest overall accuracy (89%) of all 32 sites, and Brown Bear (BB) reach sites (N=3) had the lowest (73%) overall accuracy.

Table 1. Error Matrix of the Random Trees classification results from all 32 images in this study.

Error Matrix	Algae	Macro-phytes	Water	Land	Shadows	Sun- glint	Total	Commission Error
Algae	209	4	58	11	1	2	285	27%
Macro-phytes	7	91	47	5	3	0	153	41%
Water	22	4	628	3	0	7	664	5%
Land	9	1	23	89	4	9	135	34%
Shadows	5	3	1	5	171	2	187	9%
Sun- glint	0	0	32	18	1	129	180	28%
Total	252	103	789	131	180	149	1604	
Omission Error	17%	12%	20%	32%	5%	13%		82%

Results demonstrated that depth and solar angle impacted the classification accuracies of the UAV imagery. Generally, overall accuracy increased with average depth per transect up to about 2.75 m (in-situ depth measurements ranged from 0 m to 9 m) (Figure 4). While the adjusted R² value was very low (adj R² = 0.115) between average depth per transect and overall accuracy, these results were statistically significant (p-value ≤ 0.05). To further understand the effects of solar angle and depth on accuracy, images were organized into three overall accuracy groups using Jenks natural breaks categorization: 1 (greater than 84% accuracy, N=14), 2 (greater than 74% and less than or equal to 84% accuracy, N=10), and 3 (less than or equal to 74% accuracy, N=8). The majority of images in group 1 (highest overall accuracy) had solar angles between 47.5 and 58.72 degrees (10:04 am and 11:21 am, N=5) or between 48.5 and 62.69 degrees (2:53 pm and 4:16 pm, N=5), and had an average depth of 1.71 meters. Most images in group 2 (second highest overall accuracy) had solar angles between 71.06 and 62.59 degrees (1:32 pm and 2:54 pm), and had an average depth of 1.45 meters. Finally, the majority of images in group

3 (lowest overall accuracy) had solar angles between 62.72 and 71.2 degrees (11:40 am and 1:17 pm), and had an average depth of 1.19 meters. Throughout this study, solar noon occurred between 1:13 and 1:20pm (at about a 71-degree solar elevation angle). Times either before or after solar noon (particularly in the range of about 45 to 60 degrees in the morning or afternoon) rendered the best imagery with both the most illumination of the substrate and least solar glare on the surface (which is heightened around solar noon).

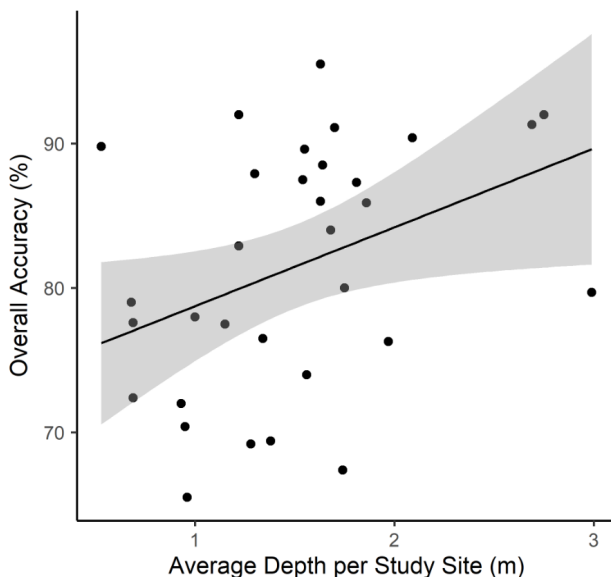


Figure 4. Overall accuracy of the 32 image classifications and average depth per site (adj $R^2 = 0.115$, p -value ≤ 0.05).

The spectral signals of this study’s six classes can be described by the digital numbers captured by the native Phantom 4 Pro UAV RGB camera (Table A2). The algae class had the highest reflectance in the green band and second highest in the blue band, while the macrophyte class had highest values in the green band, followed by the red and then blue bands. The water class had the highest reflectance values in the blue band, and the land class had equal digital number values in the red and green bands. The shadows and sunglint classes each had equal digital numbers in their respective red, green, and blue band values.

3.2. Study Site Characteristics and Percent Cover Estimates

Rooted macrophytes dominated a majority of upstream reaches (I5 through Happy Camp), while filamentous algae dominated downstream reaches closer to the Pacific Ocean (Old Man River through Weitchpec). The I5 site 1 (I5 1) location had the highest macrophyte percent cover (31%), and the Old Man River site 2 (OMR 2) had the highest algae percent cover (39%) (Figure 5). While filamentous algae were present upstream sites (I5 to HC), no macrophytes (0%) were detected in the aerial imagery at Happy Camp site 4 (HC 4) or at any sites downstream of this location.

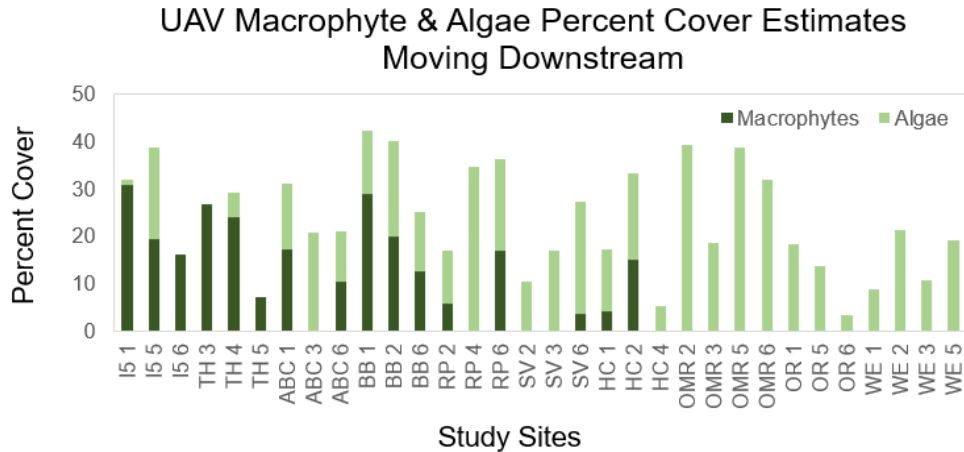


Figure 5. UAV-based percent cover estimates of submerged rooted macrophytes and filamentous algae moving downstream (left to right: I5 to WE) along 32 sites of the Klamath River below Iron Gate Dam.

To illustrate the changes in percent cover of submerged filamentous algae and rooted macrophytes moving downstream along the river, three examples that depicted low, medium, and high percent cover of UAV images were selected and their respective Random Trees classification results were displayed (Figure 6). Tree of Heaven site 5 (TH 5) had low filamentous algae percent cover (0% algae, 7% macrophytes), as was commonly observed in upstream sites within close proximity to Iron Gate Dam. Brown Bear site 6 (BB 6) displayed equal percentages of filamentous algae and macrophytes (13% algae, 13% macrophytes) and represented a medium concentration of percent cover for the 32 sites in this study. Finally, Old Man River site 2 (OMR 2) was selected to display a high amount of primary producer percent cover because aerial imagery over this location detected the highest amount of filamentous algae of all sites (39% algae, 0% macrophytes). This site is representative of downstream sites below Happy Camp site 4, below which no rooted macrophytes were detected. Figure 6 also helps demonstrate the increase in channel width as the Klamath River approaches the Pacific Ocean.

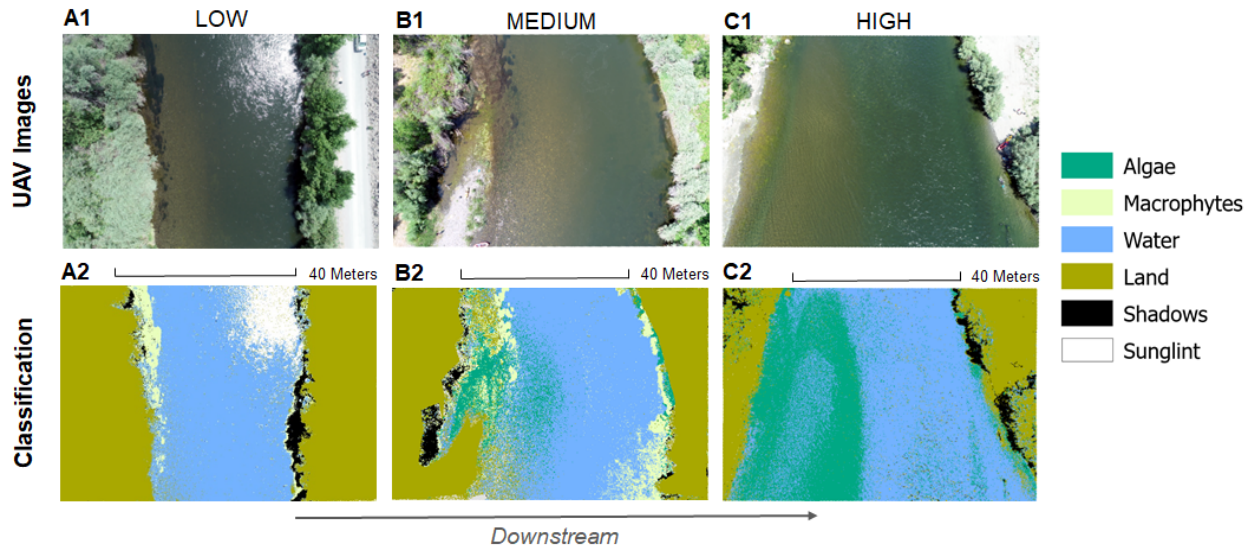


Figure 6. Examples of low, medium, and high filamentous algae and rooted macrophyte percent cover in original UAV images (top row) and Random Trees classification results (bottom row). (A1-A2) Tree of Heaven site 5 (TH 5): low (0% algae, 7% macrophytes); (B1-B2) Brown Bear site 6 (BB 6): medium (13% algae, 13% macrophytes); (C1-C2) Old Man River site 2 (OMR 2): high (39% algae, 0% macrophytes).

The relationship between in-situ and UAV-based percent cover estimates of submerged filamentous algae and rooted macrophytes was assessed within the 32 sites to understand how aerial imagery results compared to river survey results. UAV percent cover estimates were moderately correlated to in-situ quadrant percent cover estimates for both the filamentous algae and macrophyte classes (algae: Pearson's $r = 0.51$, macrophytes: Pearson's $r = 0.72$), indicating a moderately strong linear relationship between each variable per dataset. Although the filamentous algae and macrophyte classes for UAV imagery and in-situ data had low and moderate adjusted R^2 values (algae: $\text{adj } R^2 = 0.23$, macrophytes: $\text{adj } R^2 = 0.50$), this result was statistically significant ($p\text{-value} \leq 0.05$) (Figure 7). Thus, the null hypothesis that there is no relationship between the UAV and in-situ percent cover measurements for both filamentous algae and rooted macrophyte observations was rejected. For algae measurements, the residual standard error, or the average amount the response variable (algae) diverged from the regression line (Jay Kerns 2010) was 9.214 with 30 degrees of freedom. The residual standard error for macrophyte measurements is 7.208 with 30 degrees of freedom. The F-statistic, an indicator of significance between the groups of observations, was relatively low for algae (10.49) and moderate for macrophyte (32.01) measurements.

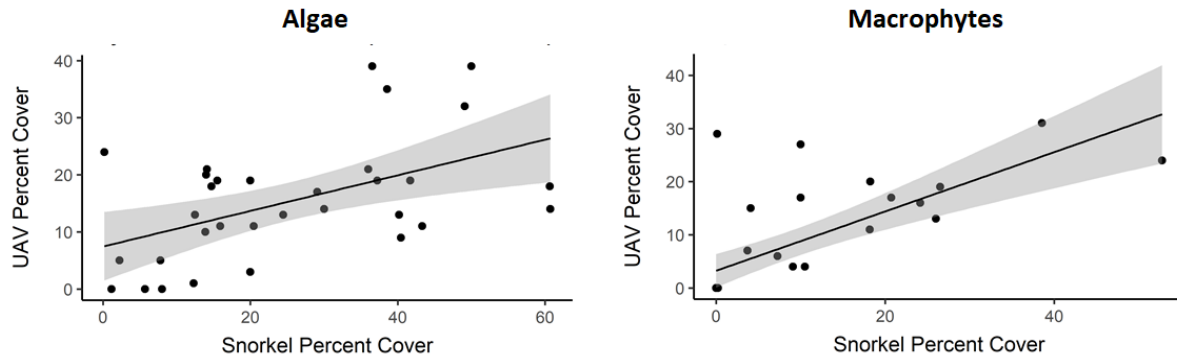


Figure 7. Linear regression of UAV-based percent cover estimates and snorkel-based (in-situ) percent cover estimates of submerged filamentous algae and rooted macrophytes along 32 sites of the Klamath River below Iron Gate Dam.

Results from this study indicated that filamentous algae were more easily detected and quantified in deeper regions and often inhabited areas farther from the riverbanks than did macrophytes below Iron Gate Dam. The filamentous algae class had high overall accuracy (overall accuracy of 80% or more and in-situ percent cover of 80% or greater per quadrant) down to a depth of 1.9 m, while rooted macrophytes (overall accuracy of 80% or more and in-situ percent cover of 80% or greater per quadrant) were accurately classified down to 1.2 m below the water's surface at discrete locations. Within the 32 sites, in-situ quadrant observations revealed that submerged rooted macrophytes generally grew at shallower depths than filamentous algae (0.83 m mean for rooted macrophyte in-situ percent cover > 0% per quadrant, 1.2 m mean for filamentous algae in-situ percent cover > 0% per quadrant). On average, rooted macrophytes grew within 7.7 m from either side of the bank within the 32 sites, and filamentous algae were most commonly found within 8.7 m from either bank. In the 32 sites analyzed, rooted macrophytes and filamentous algae both most frequently inhabited straight-aways with lower river velocity (< 1 m / sec) or in relatively shallow areas along banks.

4. Discussion

This study demonstrates that an inexpensive UAV equipped with an RGB camera is a useful tool for detecting and quantifying multiple types of submerged primary producers in a non-wadeable river. Filamentous algae and rooted macrophyte coverage had > 70% overall accuracy at 28 of 32 sites, and water surface solar reflection was the primary factor limiting the ability to assess submerged vegetation coverage. Along the 32 sites distributed among 10 reaches beginning below a series of large dams, there was greater dominance of rooted macrophytes upstream, transitioning to a greater dominance of filamentous algae at downstream sites. The larger spatial scale documented in UAV image capture can supplement current in-situ survey methods or provide a novel and useful method to assess primary producer coverage in rivers where in-situ surveys are not possible due to excessive depth or velocity.

4.1. UAV Monitoring of Benthic Primary Producers

This study's UAV method resulted in highest classification accuracy in river conditions with high water clarity and homogenous primary producer assemblages. In contrast, other researchers have found that classification accuracy decreased with river depth, particularly in water deeper

than 3 m (Tait et al. 2019; Shintani and Fonstad 2017; Zinke and Flener 2013). Our results were slightly different from these studies in that filamentous algae were more easily detected and quantified in deeper water (up to 2.75 m). In our system, water depth covaried with water clarity (Figure 4), largely as a result of the tributaries entering the Klamath River below Iron Gate Dam which tend to contribute relatively clearer water to the main stem, creating higher water clarity with distance downstream from the dam (PacifiCorp 2020). Deepening river channels created by high winter flows follow a similar longitudinal trend associated with these tributary inputs (Oliver, Dahlgren, and Deas 2014). At the deepest sites with high overall accuracy, (Old Man River site 3: 2.09 m average depth, 90.38% overall accuracy; Orleans site 1: 2.75 m average depth, 92% overall accuracy; Weitchpec site 1: 2.69 m average depth, 91.3% overall average), conditions were optimal for capturing high-quality aerial imagery. At these sites, lower turbidity (Secchi depth between 2.1 and 4.4 m) (Table A1) was measured, and only filamentous algae (no rooted macrophytes) (Figure 5) was detected. Having only one type of submerged primary producer to classify in each of these sites contributed to increased accuracy of the supervised classification (Ahmad and Quegan 2013; I, Pakhriazad, and Shahrin 2009) because it diminished the risk of conflated categorization. The counterintuitive finding that deeper river sites had higher accuracy when these deeper locations co-occur with lower turbidity reinforces previous findings that water clarity is a major predictor for how well imagery can be used to successfully detect and quantify submerged primary producers (Nelson, Cheruvilil, and Soranno 2006; Yadav et al. 2017; Slocum et al. 2019). This demonstrates that UAV methods are not limited to shallow (< 1 m) rivers when turbidity is low and primary producer assemblages are homogenous.

This study was novel in that it attempted to classify both filamentous algae and rooted macrophyte groups using an RGB camera throughout a non-wadeable river (C. N. Brooks et al. 2019; Stanfield 2009). However, there were instances of class confusion between filamentous algae and rooted macrophytes. In some dense areas of aquatic vegetation, algae grew on rooted macrophytes, making class separation challenging. In these cases, spectral unmixing may be a more suitable classification approach (Keshava 2003; Yan et al. 2019). Furthermore, in-situ surveys along a single transect left several unknown or unidentified points of interest in the UAV imagery, making class discrimination challenging. Also, both algae and macrophyte classes had the highest spectral signals in the green band (Table A2), which further exacerbated confusion between these classes (Govender, Chetty, and Bulcock 2007). Some algae genera (*Cladophora*, *Oedogonium*) and macrophyte species (*Zannichellia palustris*, *Potamogeton crispus*) had both light and dark green reflectance values throughout the river, resulting in too much overlap of reflectance values to create a useful spectral library to identify filamentous algae and rooted macrophyte classes across all 32 images. Each image was classified individually and the classifications were reduced to two distinct groups because creating spectral libraries for each image requires in-situ sampling and is time consuming. Due to the individual classification per image and lack of automation in this process, large sample sizes might not be well suited under these specific methods.

While OBIA is commonly used for high-resolution underwater classification of vegetation and wetland species (Dronova 2015; Husson, Ecke, and Reese 2016), this study utilized a pixel-based supervised classification. Pixel-based methods facilitate the identification of large patches of rooted macroalgae or filamentous algae, as well as speckled and interspersed filamentous algae, both of which were common at study sites. Random Forest algorithms have proven successful in previous studies in complex, heterogeneous landscapes (Husson, Hagner, and Ecke 2014; Husson, Ecke, and Reese 2016; Chabot et al. 2017), demonstrating that this

method can effectively reduce speckle and noise within imagery. To build on current work, future image analysis techniques that can be applied to benthic surveys in heterogeneous environments include aquatic vegetation indices, OBIA, structure from motion photogrammetry, and hyperspectral image capture (Becker et al. 2019; Brinkhoff, Hornbuckle, and Barton 2018; C. N. Brooks et al. 2019; Taddia et al. 2019; Chabot et al. 2017; Joyce et al. 2019; Ventura et al. 2018).

One of the most prominent challenges to achieving high classification accuracy in this study involved solar glare, which is affected by solar angle, wind, and ripples or surface tension on the water (Hardin and Jensen 2011; Kutser, Vahtmäe, and Praks 2009; Bandini et al. 2017; Kay, Hedley, and Lavender 2009). In this study, the sun's reflection produced large white spots in photos that were taken close to solar noon (around 71 degrees solar angle in this study), thus making detection below the surface impossible. Several images captured around solar noon had some of the lowest classification accuracy results (between 66% and 72%) due to issues related to solar angle and resulting glare. Wind and higher velocity water (> 1 m / second), such as in areas with ripples, further exacerbated the prominence of solar glare and created distortions within the UAV imagery. These concerns affected how the 32 out of 60 total UAV images were selected for analysis, and several selected photos ($n = 5$) had sizable portions (between 8% and 12% of the image) of solar glare that prohibited visibility below the water's surface. Flying on a uniformly cloudy day would also reduce solar glare, although detection capabilities may suffer as light penetration through the water column would be reduced (Benavides, Fodrie, and Johnston 2020).

Methods from this study can be applied to a variety of environments, including both freshwater and marine (Tamondong et al. 2020; Joyce et al. 2019), and will perform best in clear and relatively shallow (< 2 m) waters. Given that classification accuracy was highest in regions with reduced water surface tension, such as in a pool or a slow-moving river run, techniques from this study would also be well-suited for lake environments (Husson, Hagner, and Ecke 2014). Additionally, the Random Trees classifier most easily identified large, homogenous patches of algae and macrophytes, and would similarly perform well with other large groups of macroalgae and submerged aquatic vegetation, such as kelp or seagrass (Thomsen et al. 2019; Duffy et al. 2018; Mora-Soto et al. 2020). Despite these applications, this method is not optimal for distinguishing multiple aquatic species, as RGB imagery is spectrally sparse. Therefore, aerial hyperspectral sensors would be more effective in these scenarios (Green 2020; Rossiter et al. 2020).

Detection and quantification techniques in future studies might be complicated in water with increasing depth, turbidity, and confounding primary producer types (Gallant 2015; Slocum et al. 2019), and accuracy will likely decrease as these conditions converge. Thus, times of higher river flows that increase water depth and turbidity, including spring snowmelt or autumn rains, are expected to result in lower accuracy of primary producer identification and quantification. Changing water levels associated with water year variation, dam management, and season are expected to influence primary producer assemblages (Abati et al. 2016; Gillett et al. 2016; Power, Parker, and Dietrich 2008) in addition to methodological accuracy, making complementary in-situ surveys important during variable conditions. Examples of expected changes to primary producer assemblages include lower overall coverage of rooted macrophytes during high-flow years, and seasonal progression of rooted macrophyte and filamentous algae coverage, resulting in lower coverage as macrophytes and algae slough in the fall (Wehr 1981; Banish 2017).

4.2. Recommendations

Analysis of UAV photos using a single-image, supervised classification method for 32 sites proved to be time intensive due to the need to create a novel spectral library and separate classification for each high-resolution image. Ways to address this in future studies involve assessing fewer sites and spectrally correcting the imagery in order to apply a uniform spectral library to all photos. While this study represented a static glimpse of conditions on the Klamath River at 32 individual locations, this method can successfully be applied to smaller-scale river studies with greater temporal scale, such as time series or change analyses of benthic communities in small sections of a river. For example, managers can adapt this technique to capture aerial images of the same river location each month to help answer how specific filamentous algal communities in one region of a river change in response to seasonal dam-altered flow regimes. While this small-scale study is best suited for small rotary-wing UAVs, pilots who are designing future projects may consider employing a larger rotary-wing UAV with additional power capacity when surveying larger portions of a river (Rusnák et al. 2018).

For monitoring greater river extents (> 100 m river length per site), it is helpful to consider flight altitudes, platforms, and study site characteristics before conducting a UAV-based benthic primary producer study. A flight plan at high altitudes (above 100 m) is recommended to both avoid obstacles (such as trees, power lines, and bridges) and assist in the image stitching process in order to create orthomosaic maps of large swaths of the river. When generating orthomosaics, researchers should use real-time kinematic GPS, or have ground control points, secured markers or landmarks with known GPS locations, or slivers of land in the images to facilitate image stitching (Nahirnack et al. 2019; Taddia et al. 2019; Hashemi-Beni et al. 2018). When target algal or macrophyte patches are identifiable at large spatial scales, or when higher spectral resolution is required to discern among taxa, high-resolution satellite imagery can be an alternative to UAV imagery (Kutser, Vahtmäe, and Martin 2006). Fixed-wing UAVs may be difficult to fly in meandering river environments unless there are open riverbanks or roads adjacent to the study sites that can be used for take-off and landing (Boon, Drijfhout, and Tesfamichael 2017). As river survey extent increases, UAV data increases, thereby posing additional constraints to computational processing time. The sampling and image capture methods described in this study are broadly applicable to benthic primary producer studies, but caution should be taken when attempting to apply this technique to large spatial extents due to computational and logistical constraints. In summary, this study's methods are best suited for smaller-scale studies across time, rather than across space.

Another recommendation includes changing the order of the in-situ sampling protocol that was employed in this study. Instead of simultaneously conducting an in-situ transect survey and flying a drone overhead, it is more effective to capture aerial imagery first, identify several target sampling areas in the UAV photo, and then collect samples and observations in discrete locations of the river to reflect target areas within the photo. Also, including in-situ biomass calculations of filamentous algae and rooted macrophytes to the sampling protocol would augment percent cover estimates. Finally, incorporating a spectral calibration target and a corrective optical equation (Legleiter et al. 2004) would allow managers to apply a spectral library to the entire UAV image dataset, which would reduce time spent on individual classifications and increase the ability to discriminate among different submerged taxa.

4.3. Management Applications of UAV Monitoring in Non-wadeable Rivers

UAV imagery is useful in detecting and quantifying submerged primary producer assemblages, and can be integrated into monitoring programs where current monitoring is limited or non-existent. Algae and aquatic plants are sensitive to ecosystem change, making them useful indicators of ecosystem health (Bunn et al. 2010; Schneider et al. 2017). The type, distribution, and condition of algae and aquatic plants can drive water quality (pH, dissolved oxygen, suspended sediment, water temperature) and fisheries health (food resources, habitat), making quantification of these taxa useful in identifying mechanisms responsible for ecosystem change (Bunn et al. 2010; Kornijow, Gulati, and Ozimek 1995; Lusardi, Jeffres, and Moyle 2018; Stevenson et al. 2012). In non-wadeable rivers such as the Klamath River, documentation of aquatic plants and algae is generally limited to wadeable areas easily accessible from shore, where the primary producer assemblage may not be representative of the river reach (Gillett et al. 2016). In this study, UAV photos expanded the spatial scale of the surveyed area, and included areas generally ignored in established survey methods, including areas > 1 m deep, areas of swift current, and zones not adjacent to shore-line river access points. Although aerial images cannot capture the taxonomic detail with the same accuracy as in-situ surveys or samples collected for laboratory analysis of species composition, the larger spatial scale can help address other research questions and monitoring goals. Ultimately, combining in-situ and UAV methods will likely provide the most thorough monitoring practice.

UAV images can be used to track ecosystem change associated with management actions and restoration expected to influence primary producer assemblages. The Klamath River and many larger rivers are considered impaired due to high aquatic plant and algae biomass, spurring management actions aimed at reducing these proliferations (J. E. Asarian et al. 2014; Deas and Vaughn 2006). In the case of the Klamath, nutrient criteria are set by water quality management agencies, but challenges with monitoring aquatic plant and algae growth limit the ability to monitor the effectiveness of regulatory nutrient reductions and restoration actions (Poikane, Kelly, and Cantonati 2016; Ebert et al. 2016). In rivers where confounding factors are expected to influence benthic algae growth, including nutrients, flow, and water clarity, alterations including dams and associated flow management can further influence growth patterns of algae and aquatic plants (Blinn et al. 1998; Sabater et al. 2018). Where restoration has the potential to alter algae and aquatic plant assemblages, as is the case in the proposed removal of the four large hydroelectric dams on the Klamath River (Klamath River Renewal Corporation 2018), monitoring these assemblages with UAV-based techniques provides a promising opportunity to learn about the effects of large-scale restoration on non-target taxa that may otherwise be challenging to monitor. In cases in which analytical expertise may not be available, UAV-imagery can still be collected to document conditions before and after management actions, so that data can later be analyzed.

5. Conclusions

Employing a pixel-based Random Trees supervised classification on RGB images from a low-cost UAV is an effective technique to classify and quantify both benthic filamentous algae and rooted macrophytes in a non-wadeable river. Although increases in water-column turbidity, water depth, and complex species assemblages can decrease the accuracy of rooted macrophyte and filamentous algae quantification, overall accuracy was 82% at the 32 assessed sites. This study fits within the level of accuracy of similar studies analyzing submerged aquatic vegetation coverage in clear water at shallow depths (< 1 m) (Husson, Hagner, and Ecke 2014; Husson, Ecke, and Reese 2016; Chabot et al. 2017; Visser et al. 2015), and results verified that these

methods can be applied in deeper bodies of water, both freshwater and marine, that have high water clarity. These findings also expand on existing research by suggesting that classifying vegetation categories and assessing images in mixed vegetation assemblages, in addition to single taxa-dominant ecosystems, is possible with an RGB camera. It is recommended that future studies collect aerial imagery between about 45 to 60 degrees of solar elevation angle in the morning or afternoon to reduce solar glare. Photos taken around solar noon should generally be avoided to diminish the effect of solar reflection. Future analysis involves incorporating in-situ biomass calculations to augment percent cover estimates, and further investigating the utility of multispectral imagery detection at depths deeper than 1 m below the surface. Methods from this study are not suited for a purely white-water river caused by wind and rapids due to visibility issues related to solar glare and water surface tension. Instead, this study's methods are particularly useful in inaccessible study regions that host large, homogenous patches of submerged filamentous algae or macrophytes in relatively shallow (< 2 m) and clear water.

As UAVs become a common tool used by research and monitoring groups, the potential to increase ecosystem monitoring in environments not previously accessible and on larger spatial scales is expanding. Capturing aerial imagery is relatively efficient and can be combined with other sample collection efforts as part of regular water quality monitoring programs. These images can be cataloged for later assessment, which may prove incredibly valuable in the cases of retrospective monitoring of unplanned management actions, natural variation in ecosystem condition, or other changes. The collection of UAV images from established long-term study sites will be comparable through time to assess temporal changes with limited in-situ data, and aerial images collected in conjunction with in-situ samples will be informative in aquatic system management and decision-making.

Chapter 3: Mapping Algal Bloom Dynamics in Small Reservoirs using Sentinel-2 Imagery in Google Earth Engine

Abstract

Freshwater algal blooms have caused ecological damage and public health concerns throughout the world. Monitoring such blooms via in situ sampling is both costly and time-consuming, and satellite imagery provides a rapid and relatively inexpensive way to supplement these techniques. Sentinel-2 MultiSpectral Imager data have effectively detected chlorophyll-a, a proxy for algal biomass, in large bodies of water, but few studies have shown the applicability in small (<10 km²) reservoirs, which are critically important for aquatic species, drinking water, irrigation, cultural activities, and recreation. This study provides a test of the use of Sentinel-2 imagery in Google Earth Engine for algal bloom detection in two small freshwater reservoirs in northern California, USA, from October 2015 to December 2020. Google Earth Engine's cloud computing allows for the analysis of extensive datasets and time series, expanding the capacity to analyze the spatial and temporal heterogeneity of floating algal blooms. Here we analyzed four spectral indices - Normalized Difference Vegetation Index (NDVI), Normalized Difference Chlorophyll Index (NDCI), B8AB4, and B3B2 - to retrieve chlorophyll-a data for algal bloom identification in two highly dynamic freshwater systems. We assessed the relationship between spectral indices and monthly in situ water samples that were collected at three sites within the reservoirs using cubic polynomial regression equations. NDCI, which leverages the red-edge wavelength, most accurately identified chlorophyll-a across all study sites (highest adjusted $R^2 = 0.84$, lowest RMSE = 0.02), followed by NDVI. We demonstrate that Sentinel-2 imagery can capture greater spatial and temporal heterogeneity of algal blooms than typical in situ sampling. This suggests that remote sensing may be an increasingly important tool in monitoring algal bloom dynamics in small reservoirs and other aquatic environments.

1. Introduction

Freshwater harmful algal blooms (HABs), defined as proliferations of toxic or non-toxic algae that negatively affect freshwater ecosystems (Lopez et al. 2008), impact every continent on the planet (Clark et al. 2017). Although algae occur naturally and provide nutritional and structural benefits to aquatic ecosystems, proliferations can become a nuisance or even dangerous to animal and human health (H. W. Paerl et al. 2001). Such health effects include nausea, respiratory illnesses, liver problems, skin damage (Davidson et al. 2014), and mortality of livestock, dogs, and other animals that drink contaminated water (Harke et al. 2016; Backer et al. 2013). In addition to toxigenic events, HABs can cause a variety of ecological and economic problems, such as creating anoxic zones, clogging fish gills, producing strong odors, and impeding waterfront recreation (Weirich and Miller 2014; G. M. Hallegraeff 1993). Furthermore, consuming even small amounts of toxins can be life-threatening (Chorus et al. 2000). HABs are increasing in prevalence in small lakes and reservoirs around the world (Kenneth Hudnell 2008; B. W. Brooks, Lazorchak, and Howard 2016). In fact, lakes and reservoirs often experience the most severe and frequent HABs of all aquatic environments because of high nutrient influx from upstream rivers (Hans W. Paerl, Otten, and Kudela 2018). While much HAB research has been conducted in marine ecosystems and large freshwater ecosystems, few researchers have studied these events in small lakes and reservoirs despite the importance of these water bodies for

irrigation, energy usage, and water supply (Lobo et al. 2021). Evaluating the spatio-temporal trends and variable dynamics of algal blooms in small lakes and reservoirs can provide public health officials and aquatic managers with targeted information to mitigate potentially harmful events around the globe (D. M. Anderson, Cembella, and Hallegraeff 2012).

HABs are typically monitored through in situ methods such as laboratory analysis of water samples that quantify concentrations of algal toxins and chlorophyll-a (chl-a), a proxy for algal biomass (Caballero et al. 2020). However, in situ monitoring techniques are time-consuming and require specialized laboratory equipment (Karlson, Cusack, and Bresnan 2010), reducing the ability to collect data more frequently than once a month per location. Since bloom cycles are heterogeneous and can last from hours to days in various quantities (Cloern 1996), it is important that monitoring techniques capture the rapidly-changing dynamics of bloom events. Remote sensing data from satellites, aircraft, and unoccupied aerial vehicles (Richard P. Stumpf and Tomlinson 2007; Kislik, Dronova, and Kelly 2018) have been used to complement in situ monitoring and improve our ability to observe HABs at broad spatial and temporal scales. Additionally, the growing availability of long-term, high-frequency satellite imagery has enabled robust comparisons of spectral images with in situ data to develop models to forecast blooms (Saberioon et al. 2020; S. Mishra et al. 2021; Ranjbar et al. 2021; S. J. Weber et al. 2020). Chl-a is most commonly used to detect the presence of a variety of algal blooms using both in situ and remote sensing techniques because it is easy to measure visually, although it is only a proxy and cannot determine algae to the species level (Kudela, Stumpf, and Petrov 2017; Richard P. Stumpf and Tomlinson 2007). Therefore, remote sensing techniques combined with in situ water sampling measurements provides a robust mechanism to characterize the spatial and temporal dynamics of HABs.

Satellite remote sensing has been used for decades to identify algal blooms, and advances in sensors have increased the ability to monitor blooms at more local spatial scales. Satellite imagery is particularly useful for HAB detection because algal blooms typically float at the surface and have distinct colorations, making them identifiable from space (Mark William Matthews, Bernard, and Robertson 2012). Previous studies have detected blooms using multispectral imagery from SeaWiFS (1100m spatial resolution), MERIS (300m spatial resolution), MODIS (250m spatial resolution), and Sentinel-3 (300m spatial resolution), leveraging the red-edge and near-infrared (NIR) wavelengths to identify chl-a and general greenness of blooms (Clark et al. 2017; Sebastiá-Frasquet et al. 2020; Shen, Xu, and Guo 2012). The red-edge and NIR wavelengths are advantageous for algal bloom detection because, as with land vegetation reflectance patterns, floating algae have peak reflectance in the NIR and red-edge (Hu 2009) and high absorption in the red wavelengths, especially compared to surrounding water (Alawadi 2010). However, the platforms that have tested red-edge and NIR indices are primarily moderate and low resolution satellite missions that are too coarse to map small lakes and reservoirs. Higher resolution satellite images are needed for this pursuit.

Missions such as Landsat (30m spatial resolution) and Sentinel-2 (10-60m spatial resolution) offer finer-scale spatial data and may allow for more precise quantification of algal biomass in small freshwater lakes and reservoirs (Bresciani et al. 2018). Sentinel-2 MultiSpectral Imager (MSI) has emerged as a new leader in the field of algal bloom remote sensing because of its spectral variety in red-edge and NIR wavelengths, high temporal resolution, and high spatial resolution (Ansper and Alikas 2018; Dogliotti et al. 2018). Although Sentinel-2 sensors were

originally designed for land-use applications (Cillero Castro et al. 2020), this imagery has been applied to several algal bloom studies involving coastal regions (N. Pahlevan et al. 2017) and large inland lakes (Bramich, Bolch, and Fischer 2021; Ha et al. 2017). This satellite has been used in previous algal bloom research, yet few investigations have shown the applicability of Sentinel-2 imagery in small reservoirs. The temporal frequency of Sentinel-2 observations, which is higher than Landsat's 16-day revisit time (Caballero et al. 2020), provides an additional advantage for monitoring HABs in small bodies of water at repeat intervals. It is important to track when and where blooms in small (<10 km²) reservoirs occur to monitor public health concerns in these environments because even small concentrations of toxic algae in small bodies of water can injure animals and humans (Laughrey et al. 2021; Gustaaf M. Hallegraeff et al. 2004). Furthermore, small reservoirs are critical for irrigation, water supply, energy production, recreation, and cultural usage (L. T. Ho and Goethals 2019). Together, in situ measurements paired with remote sensing data offer a unique window into the time and location of algal blooms in small bodies of water, helping public health agencies and water quality managers address these events in a timely and targeted manner.

To test whether Sentinel-2 imagery can monitor HAB occurrences in small water bodies, we compared four spectral indices with in situ water quality data from two small (10km² total) reservoirs in the Klamath River Basin in northern California, USA. Specifically, we used chl-a and cyanobacteria toxin in situ data to validate the satellite imagery and understand water quality data before several large dams are planned for removal in 2023 (Klamath River Renewal Corporation, n.d.). Thus, this study provides an important baseline to later ascertain the effects of dam removal on the presence of HABs in this environment. Objectives for this study include: (1) identifying which satellite-based spectral index best detects chl-a in two reservoirs of the Klamath River from 2015-2020; (2) understanding the spatial and temporal trends of algal blooms in these bodies of water; and (3) quantifying bloom dynamics and anomalies (higher and lower than average values) during this study period. This paper assesses the utility of high-resolution satellite imagery for small algal bloom detection to supplement sampling techniques and enhance HAB identification and monitoring.

2. Materials & Methods

2.1. Study Sites

The study sites for this research are the two most downstream reservoirs of the Klamath River in northern California near the Oregon border: Copco Reservoir (41.97941°, -122.304°) and Iron Gate reservoir (41.93389°, -122.435°) (Figure 1). These reservoirs are small (roughly 4 km² surface area each) and hold about 34,000-59,000 acre-feet of water (Klamath River Renewal Corporation, n.d.). Three dams were built within Copco and Iron Gate reservoirs: Copco I in 1918 (the first blockade to migratory fish species in the Klamath River), Copco II in 1925, and Iron Gate in 1962. The dams were constructed for agricultural water acquisition, hydroelectric production, and flow regulation (U.S. Department of the Interior and U.S. Department of Commerce, National Marine Fisheries Service 2013). Both reservoirs are characterized by elevated nitrogen and phosphorus concentrations, warm water temperatures, and high water residence times (Oliver, Dahlgren, and Deas 2014; Bozarth et al. 2010). Their high nutrient levels are primarily attributed to inflows from the Upper Klamath Lake, a hypertrophic lake surrounded by intensive agriculture (Walker, W.W., J. D. Walker, and J. Kann. 2012), but also to

nitrogen fixation, atmospheric deposition, and nutrient influxes from bottom sediments (Asarian, E., Kann, J. and W. Walker 2009; Moisander, Ochiai, and Lincoff 2009). These conditions support the proliferation of algae, dominated by *Microcystis aeruginosa* and *Aphanizomenon flos-aquae*, particularly in the summer and fall months (Otten et al. 2015). *Microcystis* blooms in these two reservoirs have been documented each year since 2004 (E. Asarian and Kann 2011), producing microcystin toxin levels that often exceed public health standards (Otten et al. 2015). These toxic, recurring events threaten humans and endangered fish species, including chinook salmon (*Oncorhynchus tshawytscha*), coho salmon (*Oncorhynchus kisutch*), and steelhead trout (*Oncorhynchus mykiss*) in the Klamath River (Kann and Corum 2006; {U.S. Department of the Interior and U.S. Department of Commerce, National Marine Fisheries Service} 2013).

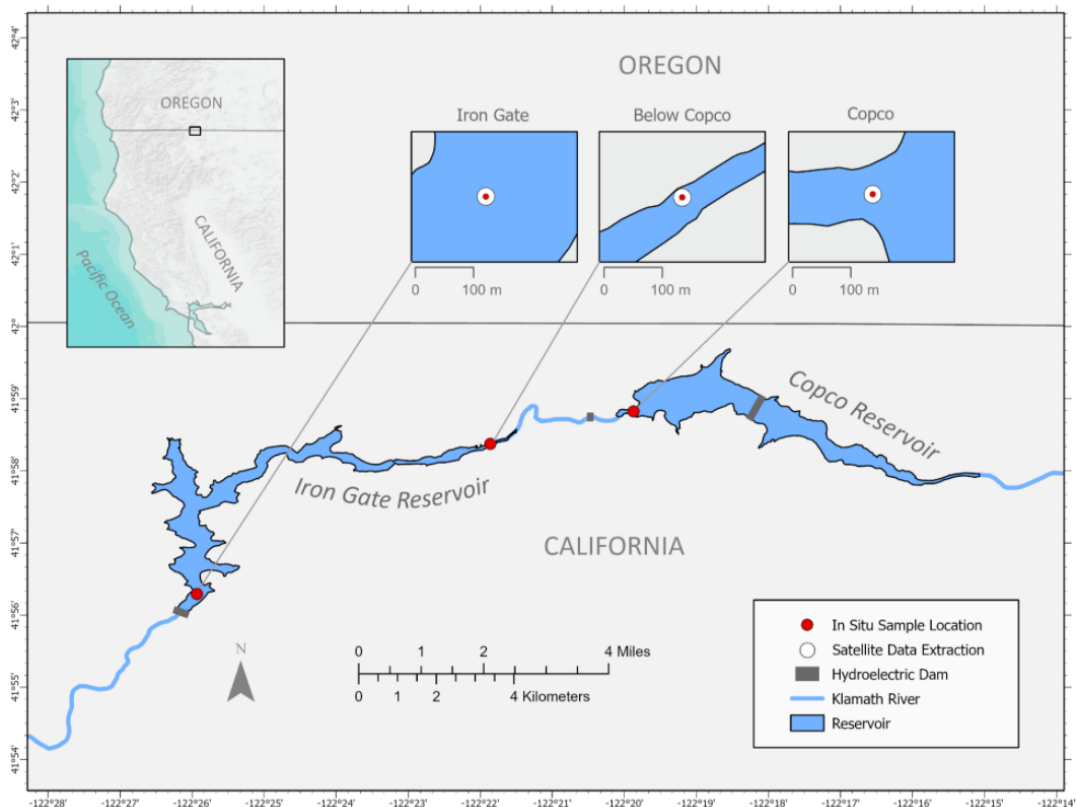


Figure 1. Study sites of Iron Gate Reservoir and Copco Reservoir within the Klamath River Basin in northern California. There are a total of three in situ sample locations (Copco, Below Copco, Iron Gate), each encircled by a 15-meter buffer representing locations of Sentinel-2 satellite data acquisition.

2.2. In Situ Data Collection

PacifiCorp (an electric power company that operates hydroelectric dams in the Pacific Northwest) collects and publishes water quality data pertaining to the Klamath River main stem and reservoirs, including Copco and Iron Gate. We obtained PacifiCorp in situ water quality sampling data at three locations: the outlet of Copco Reservoir (“Copco”) (41.98°, -122.331208998°), the inlet of Iron Gate Dam (“Below Copco”) (41.97°, -122.36438908°), and

the outlet of Iron Gate Dam (“Iron Gate”) (41.94°, -122.432227627°) (Figure 1). These data included chl-a and microcystin toxin concentrations measured in water samples collected at 0.5m depth and subsequently analyzed in a laboratory using Environmental Protection Agency standards (Watercourse Engineering, Inc. 2020). The samples were collected at approximately monthly intervals between March and November from 2015 to 2020 (Figure A.1). Furthermore, there are strong correlations ($\text{adj. } R^2 > 0.85$) between the in situ chlorophyll-a and microcystin toxin data at each of the 3 sites in this study (Figure A.2).

2.3. Sentinel-2 Data Collection & Processing

We obtained multispectral imagery over the study period at the sampling locations from Sentinel-2. These provide high-resolution (10 to 20m) images of the sampling sites at 5-day intervals when combining data from both Sentinel-2A, which began operating in 2015, and Sentinel-2B, in operation since 2017 (Caballero and Stumpf 2020). This temporal resolution can greatly supplement monthly in situ samples. As the Klamath reservoirs are dynamic aquatic systems that have a legacy of nutrient inputs and retention (Oliver, Dahlgren, and Deas 2014), algal bloom proliferations in these bodies of water are very heterogeneous in space and time. To understand this complexity, we first explored all available Sentinel-2 images at each of the three sampling locations and marked coinciding in situ sampling days. Figure 2 shows this heterogeneity in that the Copco and Below Copco sites typically experience their highest chl-a values (as retrieved by Sentinel-2 spectral indices) in the spring and summer, while Iron Gate experiences its highest chl-a measurements in the summer and fall. Winter months, when in situ sampling is halted, are typically a time of low chl-a values (Figure 2).

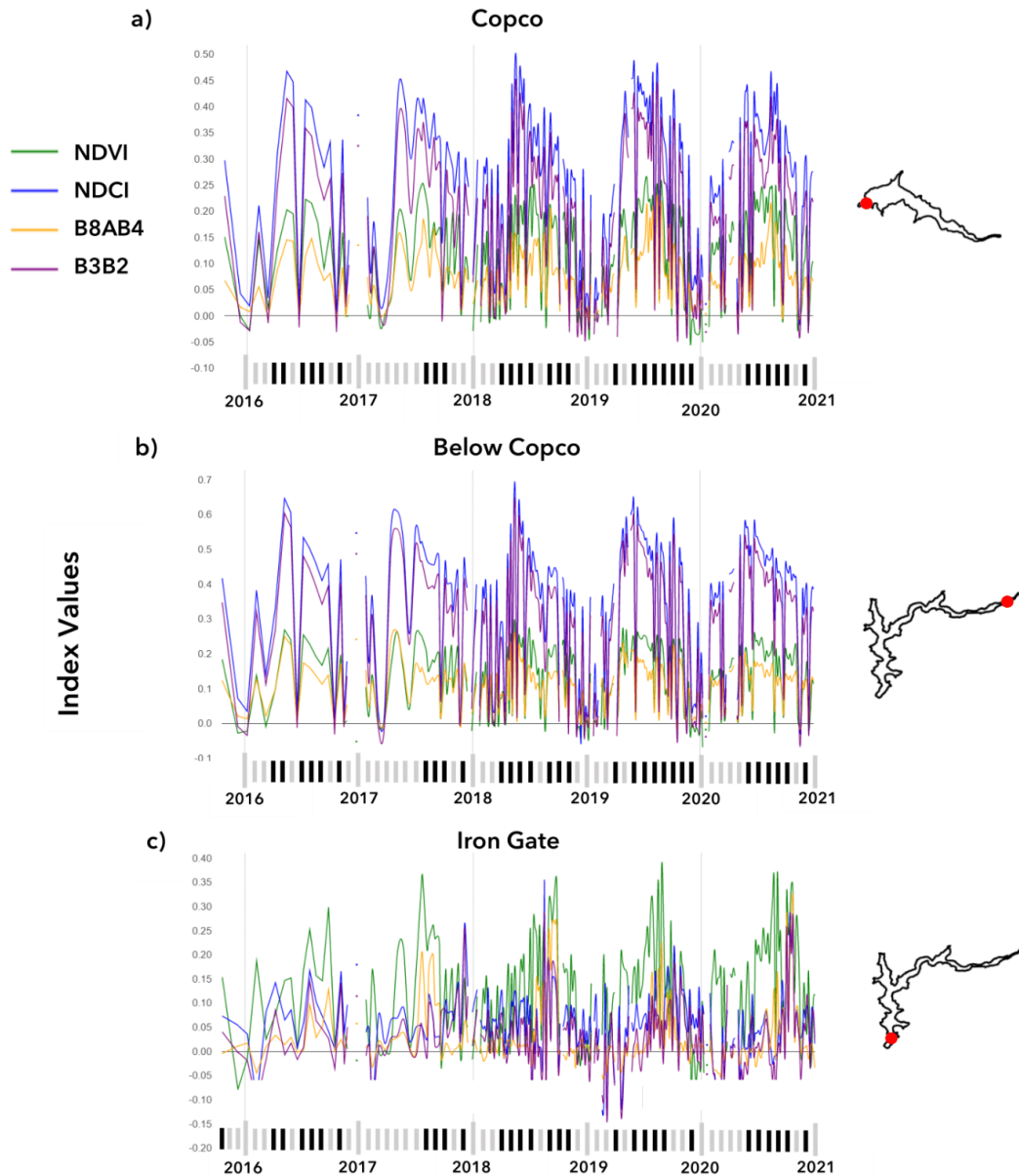


Figure 2. A time series of the four indices used in this study applied to all cloud-free Sentinel-2 images during the study period (October 2015 - December 2020). All values are based on atmospherically-corrected satellite data. *Black lines* on the x-axis indicate sampling dates at each in situ sampling location while *gray lines* on the x-axis indicate months with no in situ sampling.

Sentinel-2 imagery data are comprised of 12 bands, including wavelengths ranging from the blue to the shortwave infrared regions of the electromagnetic spectrum (Toming et al. 2016). To identify chl-a, we used bands 2 (blue), 3 (green), 4 (red), 5 (vegetation red-edge), 8 (near-infrared), and 8A (narrow near-infrared) (Q. Wang et al. 2016). We selected these specific bands because they have been traditionally used for chlorophyll-a identification; blue and green wavelength indices operate well in clear bodies of water while red, red-edge, and near-infrared wavelength indices are successful in turbid waters because they are less affected by surrounding

detritus and organic matter (Gilerson et al. 2010; S. Mishra and Mishra 2012). Due to the variable nature of these reservoirs, we explored both types of indices for this study.

After we acquired in situ water quality data, we processed Sentinel-2 Level 1C imagery in Google Earth Engine (GEE), a satellite imagery analysis application programming interface that enables global-scale processing (Figure 3). Recent studies have proven the applicability of Google Earth Engine for water quality monitoring (L. Wang et al. 2020; Lobo et al. 2021; Vaičiūtė et al. 2021; S. J. Weber et al. 2020; Zong et al. 2019; Maeda et al. 2019; Jia, Zhang, and Dong 2019). We selected images from October 2015 to December 2020 that were captured within 5 days of monthly in situ water quality collection dates. About two-thirds of these images were within 0 to 2 days of an in situ collection date (Copco: 20 out of 30 total, Below Copco: 22 out of 32 total, Iron Gate: 20 out of 30 total). We then implemented a cloud mask to all images using the QA60 (quality assurance) band to remove thick and cirrus clouds from our dataset. We also discarded images in which clouds obscured an in situ sampling location. We then implemented an atmospheric correction algorithm using the Satellite Invariant Atmospheric Correction (SIAC) package to convert imagery from top of atmosphere to surface reflectance values. This package applies linear transformations to estimate surface reflectance, incorporating approximations of aerosol optical thickness and total columnar water vapor using Bayesian statistics and the Copernicus Atmospheric Monitoring Service (Yin et al. 2019). After the initial image selection, image matching within 5 days of in situ collection dates, cloud masking, and atmospheric correction, we were left with a total of 33 Sentinel-2 images that were incorporated into analysis.

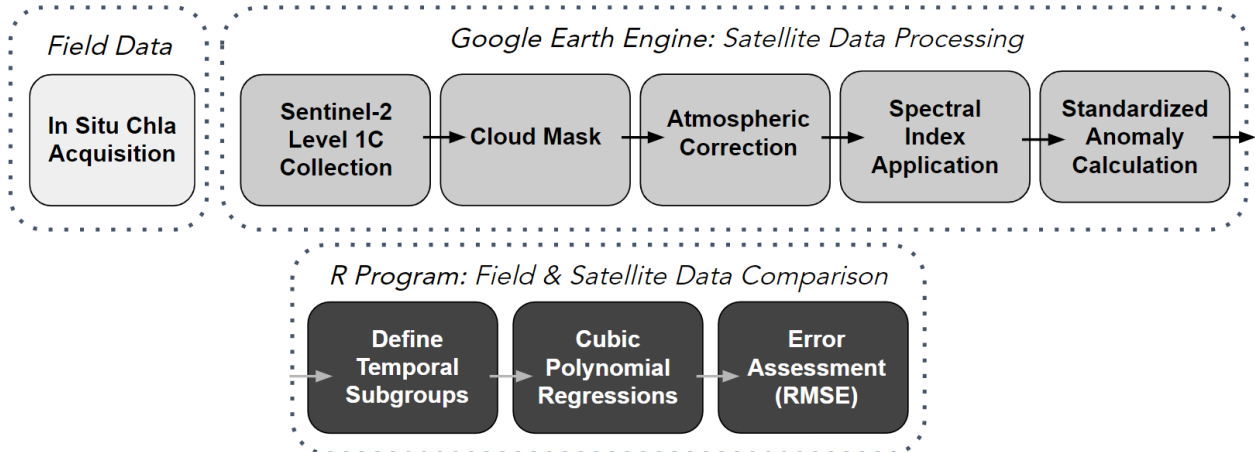


Figure 3. Workflow diagram describing the data acquisition (in situ and satellite imagery), satellite image processing and analysis, and regression and error assessment components (in situ and satellite imagery).

To assess which spectral index best detects chl-a at each sampling location, we applied the four spectral indices (Table 1) to the pre-processed 33 Sentinel-2 images in Google Earth Engine. First, we extracted spectral index values from Sentinel-2 imagery by clipping these images to a 15m circular buffer that surrounded each in situ sampling location (Figure 1). Buffers were shifted by up to 15m from the original in situ sampling location when objects in the image, such

as bridges or an intake barrier curtain, obscured water visibility and impacted index reflectance values. The four spectral indices tested were: (1) the Normalized Difference Vegetation Index (NDVI), which is a ubiquitous index in terrestrial research that uses the red and NIR bands for greenness detection (Ma et al. 2021), (2) the Normalized Difference Chlorophyll Index (NDCI), which uses Sentinel-2’s first vegetation red-edge and red bands and performs well in chl-a detection of hypereutrophic water bodies (S. Mishra and Mishra 2012; Caballero et al. 2020; Watanabe et al. 2018), (3) the Band 8A-Band4 (B8AB4) index, which was inspired by studies developed to examine the differences between the red and red-edge wavelengths in Sentinel-2 measurements (Khalili and Hasanlou 2019), and (4) the Band 3 Band 2 (B3B2) index, which uses the green and blue bands for chl-a identification (Cillero Castro et al. 2020). Each of the wavelengths used within these indices has previously been tested and proven to be effective in chl-a identification.

Table 1. Sentinel-2 spectral indices used for chlorophyll-a identification. The indices used in this study include the Normalized Difference Vegetation Index (NDVI), the Normalized Difference Chlorophyll Index (NDCI), Band 8A Band 4 (B8AB4), and Band 3 Band 2 (B3B2). Rs indicates reflectance values from the satellite. The wavelengths represented include the Near-Infrared (NIR), Red, Vegetation Red Edge 1 (Veg Red Edge 1), Narrow Near-Infrared (Narrow NIR), Green, and Blue.

Algorithm	Equation	Wavelengths	Sentinel-2 Bands	Reference
NDVI	$\frac{Rs842-Rs665}{Rs842+Rs665}$	NIR, Red	(B8-B4)/(B8+B4)	<i>Ma et al 2021</i>
NDCI	$\frac{Rs705-Rs665}{Rs705+Rs665}$	Veg Red Edge 1, Red	(B5-B4)/(B5+B4)	<i>Caballero et al 2020</i>
B8AB4	$\frac{Rs865-Rs665}{Rs865+Rs665}$	Narrow NIR, Red	(B8A-B4)/(B8A+B4)	<i>Khalili & Hasanlou 2019</i>
B3B2	$\frac{Rs560-Rs490}{Rs560+Rs490}$	Green, Blue	(B3-B2)/(B3+B2)	<i>Cillero-Castro et al 2020</i>

2.4. Data Analysis

We examined the relationship between in situ chl-a measurements and the spectral index values using cubic polynomial regression models through the generalized linear model method in the ggplot2 package of the R program (R Core Team 2020; Wickham 2016). We used this regression equation because of the non-linear relationship between the spectral reflectance and chl-a values (Martinez et al. 2020; Sharma et al. 2019; Kwon et al. 2018) and its success in related studies (O’Reilly et al. 1998; Konik et al. 2020). We first categorized chl-a measurements into four temporal subgroups per sampling site: Overall (all values per time series), Wet Years (2017 and 2019), Dry Years (2015, 2016, 2018, 2020), and Cyanobacteria Season (July 1 through October 31 for each year). Wet and dry years were categorized based on years that experienced more than average (wet) or less than average (dry) river discharge (mean = 1243 cubic feet per second) based on the 5-year average (2015-2020) discharge recorded at the United States Geological Survey Klamath River Below John C. Boyle PowerPlant near Keno, Oregon, sampling station (USGS 11510700), which is upstream of all sites. We then fit a cubic

polynomial function ($y = \text{index} + \text{chl-a} + \text{chl-a}^2 + \text{chl-a}^3$) to the paired chl-a value and spectral index values, resulting in 48 models total (4 subgroups * 4 indices * 3 sites). We evaluated the significance of each relationship based on the p -value. We also calculated the root mean square error (RMSE) and coefficient of determination, adjusted for the number of terms in the model (adjusted R^2), by comparing model predictions with observed chl-a values (Tehrani, Janalipour, and Babaei 2021).

To examine higher and lower than average spectral index values per cyanobacteria season in the reservoirs, we selected the two highest-performing indices, NDVI and NDCI, and calculated their annual standardized anomalies in Google Earth Engine. Anomalies are commonly used in environmental science, such as for climate and drought monitoring, to identify large departures from a long term mean (Helama, Meriläinen, and Tuomenvirta 2009; Anyamba, Tucker, and Eastman 2001). To calculate the anomalies, we first organized the Sentinel-2 imagery into yearly composites (2016-2020) and then filtered these data to only include values from July 1 through October 31 each year, as this includes the annual cyanobacteria season in this system (Otten et al. 2015; Jacoby and Kann 2007). Next, we subtracted the overall mean per index from each yearly composite value per index. Finally, we divided this resulting value by the standard deviation for all years per index. This enabled us to calculate the Z-score of the dataset, which is a metric that describes how many standard deviations an observation is from the mean (Patel, Chopra, and Dadhwal 2007). For this study, we call the Z-score the standardized anomaly. The equation for this calculation is: [Z-Score = (Individual Year - Mean) / Standard Deviation of all Years]. The annual Standardized Anomaly is used to decipher locations within each reservoir that diverged from average Sentinel-2 spectral index values, determined per year and during the cyanobacteria season (July - October). Higher than average values can be used as a proxy to imply higher chl-a values, while lower than average values serve as a proxy for decreased quantities of chl-a.

3. Results

3.1. Satellite-based Modeling of Chl-a

Results revealed the seasonal and interannual heterogeneity of algal blooms in Copco and Iron Gate Reservoirs as detected by spectral indices applied to Sentinel-2 satellite imagery. In general, algae appeared to be highest in the spring and summer months, with the highest peaks observed in 2019 at Copco among all spectral indices, in 2019 for NDCI and B3B2 values and 2020 for NDVI and B8AB4 values at Below Copco, and in 2018 for NDCI and B3B2 values and 2020 for NDVI and B8AB4 values at Iron Gate (Figure 4). At each of the three sites, 2016 and 2017 appeared to have generally lower spectral index values (Figure 4). NDVI, NDCI, and B8AB4 registered their lowest values at Iron Gate, and both NDVI and B8AB4 experienced their highest values at Below Copco on average. NDCI had its highest values at Copco, with generally highest values on average across all spectral indices. B3B2 was fairly consistent across the three sites, with highest values at Iron Gate (Figure 4).

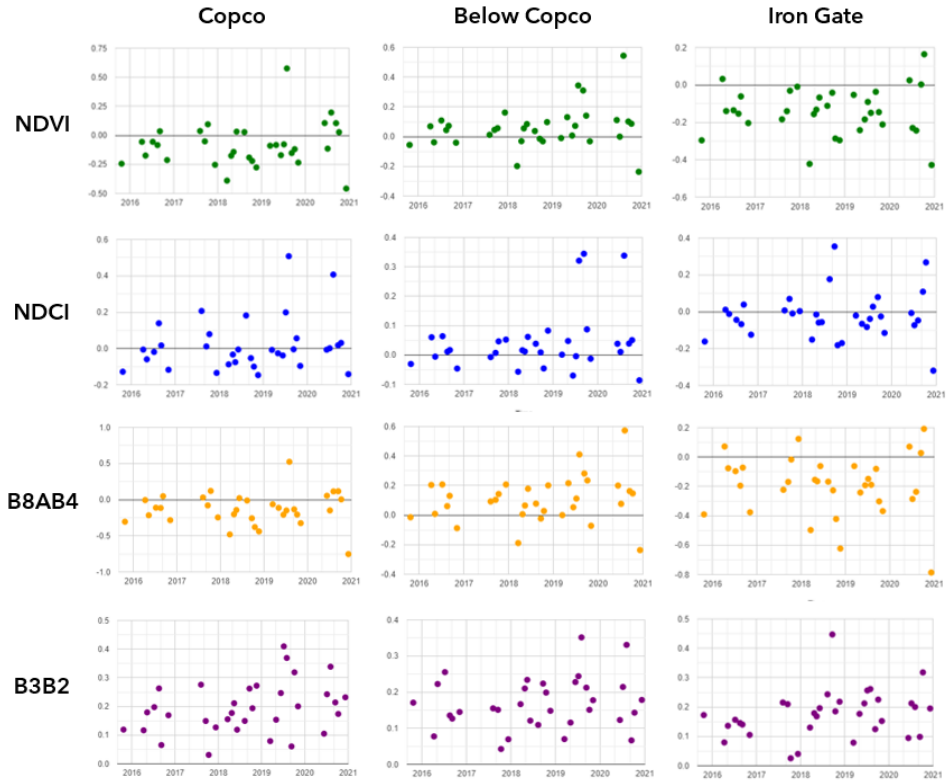





Figure 4. Time series per spectral index (rows) and in situ sampling location (columns) from October 2015 to December 2020. This demonstrates the range of values among the four indices tested in this study and how they vary per site.

NDCI was the most successful spectral index in estimating chl-a from Sentinel-2 imagery at Below Copco during the wet years (adj. $R^2 = 0.841$, RMSE = 4%, p -Value < 0.001) and Iron Gate during the wet years (adj. $R^2 = 0.782$, RMSE = 2%, p -Value < 0.01) (Figure 5). In comparison to in situ measurements, 19 of the 48 evaluated regression results had moderate to strong relationships (adj. $R^2 > 0.4$) and 26 of the 48 regression results were statistically significant (p -Value < 0.1) (Figure 5). Overall, all indices performed best at Copco (11 of 16 total regression results were statistically significant with p -Value < 0.1 and 9 of 16 total results had moderate to strong relationships with adj. $R^2 > 0.4$). NDCI was the most successful index across all sites and models (11 of 12 total regression results were statistically significant with p -Value < 0.1 and 10 of 12 total results had moderate to strong relationships with adj. $R^2 > 0.4$), particularly at Copco and Iron Gate. B3B2 had the second-highest number of statistically significant models (6 of 12 with p -Value < 0.1), performing best at Iron Gate, although relationships were not as strong across all models (3 of 12 results with adj. $R^2 > 0.4$). For this reason, NDVI appeared to perform the second-best across all sites, after NDCI, with 4 of 12 moderate to strong relationships (adj. $R^2 > 0.4$) and 5 of 12 statistically-significant values (p -Value < 0.1). B8AB4 and NDVI performed similarly to one another across several sites, with high statistical significance (p -Value < 0.01) and relatively strong relationships at Copco in the categories of Overall (entire time series), Copco Wet Year (2017 & 2019), and Copco Cyanobacteria Season (July - October) (adj. $R^2 > 0.45$ for NDVI and adj. $R^2 > 0.25$ for B8AB4). However, error was higher at these sites for NDVI and B8AB4 than in other locations (as high as 20%). Of all the

indices, B8AB4 performed the worst across all sites. NDCI and B3B2 had the lowest RMSE values across all sites (below 9%) (Figure 5). In terms of the four temporal subgroups, the Overall category (entire time series) performed best (9 of 12 with p -Value < 0.1 and 5 of 12 with $\text{adj. } R^2 > 0.4$), followed by the Wet Years (2017 & 2019) (6 of 12 with p -Value < 0.1 and 6 of 12 with $\text{adj. } R^2 > 0.4$), the Cyanobacteria Season (July - Oct) (6 of 12 with p -Value < 0.1 and 5 of 12 with $\text{adj. } R^2 > 0.4$), and finally the Dry Years (2015, 2016, 2018, 2020) (5 of 12 with p -Value < 0.1 and 3 of 12 with $\text{adj. } R^2 > 0.4$). Results indicate that pixel values that are collected within a 15-meter buffer around in situ sampling locations generally correspond well to in situ chl-a measurements within 5 days of collection.

Figure 5. Cubic polynomial regression (a) adjusted R^2 and (b) Root Mean Square Error (RMSE) Values of the four Sentinel-2 spectral indices compared to in situ chlorophyll-a data. *Green* signifies favorable values indicating high predictive potential (top 30th percentile $\text{adj. } R^2$ values, bottom 30th percentile RMSE values). Statistical significance (*) for $\text{adj. } R^2$ values is determined by: (*) $p < 0.1$; (**) $p < 0.05$; (***) $p < 0.01$; (****) $p < 0.001$.

		R^2				RMSE					
		a)	NDVI	NDCI	B8AB4	B3B2	b)	NDVI	NDCI	B8AB4	B3B2
	Copco Overall		0.467****	0.712****	0.274***	0.124*		0.13	0.07	0.18	0.08
	Copco Wet Year		0.764***	0.777**	0.606**	0.217		0.09	0.06	0.11	0.09
	Copco Dry Year		0.079	0.712****	-0.064	0.266*		0.14	0.06	0.20	0.05
	Copco July - Oct		0.668****	0.726****	0.474***	0.018		0.09	0.07	0.13	0.09
	Below Copco Overall		0.142*	0.432****	0.050**	0.100		0.12	0.07	0.14	0.06
	Below Copco Wet Year		0.619**	0.841****	0.270	0.146		0.06	0.04	0.09	0.07
	Below Copco Dry Year		0.007	0.095	-0.089	0.300**		0.14	0.07	0.16	0.05
	Below Copco July - Oct		0.053	0.389**	-0.042	0.050		0.13	0.09	0.13	0.07
	Iron Gate Overall		-0.012	0.569****	-0.051	0.429****		0.12	0.08	0.19	0.06
	Iron Gate Wet Year		-0.353	0.782***	-0.270	0.052		0.07	0.02	0.10	0.07
	Iron Gate Dry Year		0.052	0.603****	0.008	0.595****		0.13	0.09	0.21	0.05
	Iron Gate July - Oct		-0.052	0.615**	-0.041	0.445**		0.10	0.07	0.14	0.06

Strong relationships were observed between satellite-derived spectral indices and in situ chl-a data at each site (Figure 6). Below Copco had the highest relationship based on the cubic polynomial regression (NDCI $\text{adj. } R^2 = 0.841$), while Iron Gate (NDCI $\text{adj. } R^2 = 0.782$) and Copco (NDCI $\text{adj. } R^2 = 0.777$) had very similar values. There is a non-linear relationship between NDCI and chl-a, especially for chl-a values above $0.25 \mu\text{g/l}$ at Copco and Below Copco, and $0.05 \mu\text{g/l}$ at Iron Gate. While most points lie within the gray 95% confidence intervals for each location, there are about five remaining points per plot that can be considered outliers (Figure 6).

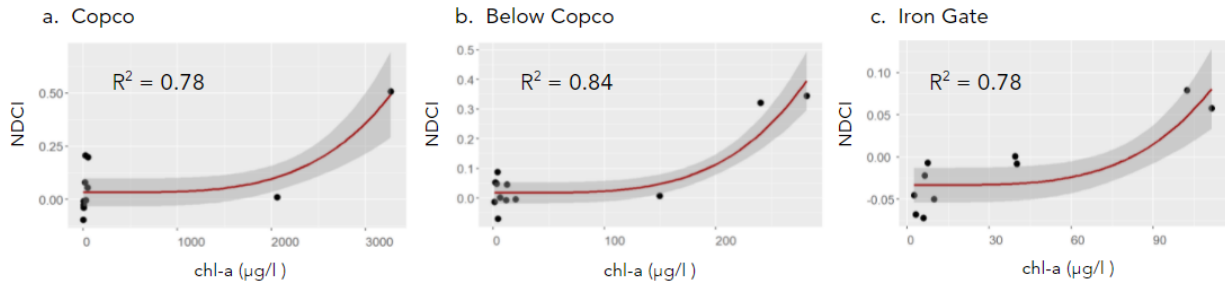


Figure 6. Regressions of the best-performing spectral index per sampling location based on the relationship between Sentinel-2 pixels and chlorophyll-a in situ data at (a) Copco (Wet Year, NDCI), (b) Below Copco (Wet Year, NDCI), and (c) Iron Gate (Wet Year, NDCI). *Gray shading:* 95% confidence intervals; *red lines* demonstrate the mean relationships for the polynomial (x^3) regressions. R^2 values represent adjusted R^2 values.

3.2. Standardized Anomalies of Chl-a Estimates

Annual standardized anomalies demonstrate the relative differences from average spectral index values across space and time (Figure 7). Specifically, the two best-performing indices across all sites, NDCI and NDVI, were used to show the biggest deviations from average annual values during the cyanobacteria season (July 1 - October 31) from 2016 to 2020. Figure 7 indicates that 2019 experienced the largest increases (positive changes from average spectral index values) across both reservoirs, especially in Copco reservoir, while 2018 shows less than average values across both reservoirs, particularly in Copco reservoir and the upstream half of Iron Gate. However, also in 2018, Iron Gate experienced higher than average values in the downstream portion of the reservoir. Iron Gate also exhibited higher standardized anomaly values in 2017 and 2020. Index values in 2016 and 2017 appear to be fairly consistent without major increases or decreases across both reservoirs, and NDVI and NDCI performed similarly to one another throughout the time series. Finally, these maps demonstrate that depending on the year, different locations within the reservoirs have various trends in anomalies. For example, during the wet years (2017 and 2019), Copco experienced higher than average trends near the Copco in situ sampling location and closer to the edges of the reservoir, while Iron Gate had higher than average values closer to the Below Copco in situ sampling location. During the dry years (2016, 2018, 2020), there were generally lower than average values across both reservoirs, but Iron Gate may have experienced higher than average values closer to the Iron Gate in situ sampling location. Standardized anomaly maps are useful in determining the seasonal, interannual, and localized spatial patterns of satellite-derived algal bloom occurrences.

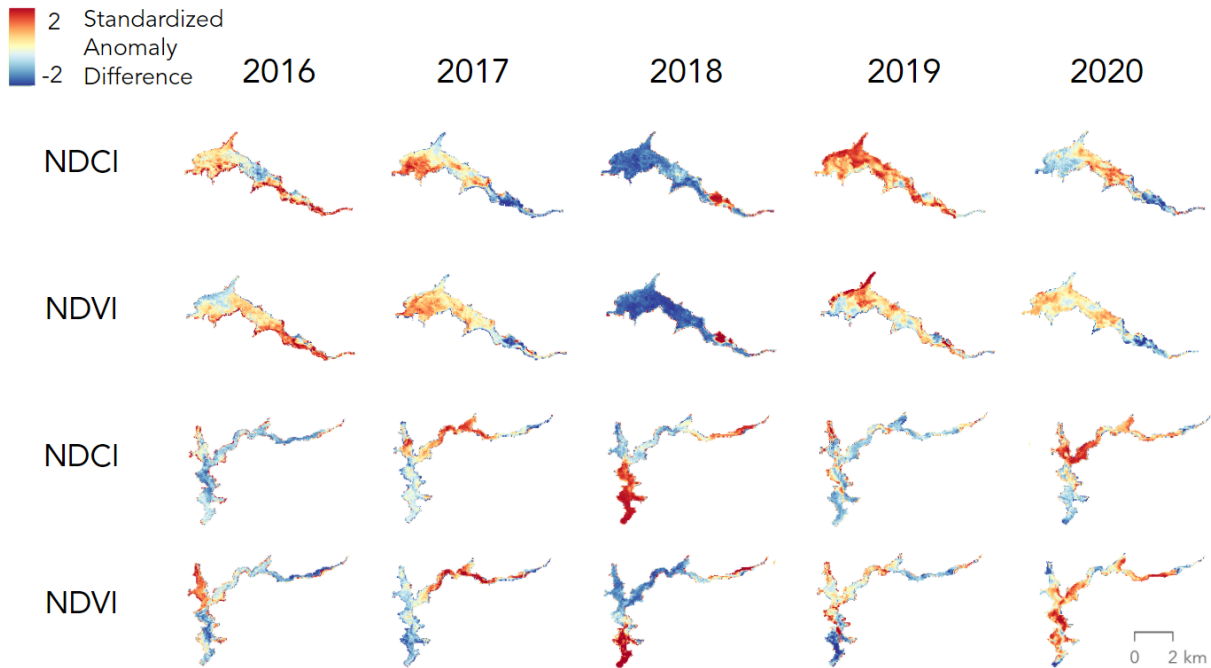


Figure 7. Annual standardized anomaly maps during the cyanobacteria season (July 1 - October 31) for the two most reliable indices tested in this study, NDVI and NDCI. An annual Standardized Anomaly depicts higher than average and lower than average Sentinel-2 spectral index values per cyanobacteria season per full year (2016 - 2020) to identify areas that likely have more and less than average chl-a.

4. Discussion

4.1. Sentinel-2 Capabilities for Algal Bloom Monitoring

This research demonstrated that Sentinel-2 imagery is effective in monitoring algal blooms in small freshwater reservoirs. NDCI successfully predicted algal concentrations in the two reservoirs, as demonstrated by moderate to strong adj. R^2 values, high statistical significance, and low RMSE values (Figure 5). This index uses the red-edge wavelength, which was originally applied in marine and coastal environments (Caballero et al. 2020; S. Mishra and Mishra 2012) and has since been tested and proven to effectively identify chl-a in a variety of freshwater environments (Caballero et al. 2020; Cillero Castro et al. 2020; Lobo et al. 2021; S. J. Weber et al. 2020; Beck et al. 2017). Red-edge and NIR wavelengths are less affected by detritus and suspended particles (M. Xu et al. 2019), which are typical components of Copco and Iron Gate reservoirs (Oliver, Dahlgren, and Deas 2014; Otten et al. 2015). This helps explain why NDCI and NDVI performed well at a majority of the sampling locations within these water bodies. NDCI was able to capture peak chl-a concentrations observed at each site (Figure 4), consistent with previous studies that have shown the index to accurately detect elevated chl-a concentrations (Gilerson et al. 2010; S. Mishra and Mishra 2012). The highest detection of chl-a compared to other sites in this study (3270 $\mu\text{g/l}$) influenced the regression model fit for Copco and led to low RMSE values (Figure 5). Similar results have been found in recent studies in

which NDCI was useful when chl-a concentrations were above 10 $\mu\text{g/l}$ and under 70 $\mu\text{g/l}$ (Lobo et al. 2021). NDCI was especially successful in identifying blooms during the wet years (2017 and 2019) (Figure 5), which included the most elevated chl-a values throughout the time series. High chl-a rates in these reservoirs during wet years were likely due to a combination of increased nutrient availability from runoff (T. Huang et al. 2014), as well as sloughing and flushing of certain aquatic grazers (Beaver et al. 2013). In this study, the efficacy of spectral indices for algal bloom detection was generally much better in wet years than dry years because of the higher and more consistent chl-a concentrations.

The red-edge wavelength outperformed NIR and narrow NIR wavelengths in algal bloom detection throughout this study. Although NDVI leverages the NIR band, it was not as useful as NDCI because this wavelength has a tendency to overestimate chl-a in high chl-a concentrations, possibly resembling the oversaturation effect of high forest canopy cover in terrestrial research (Jiang et al. 2006). High NDVI RMSE values could be linked to the increase of prediction error associated with large ranges of chl-a concentrations ($<5 \mu\text{g/l}$ or $>70 \mu\text{g/l}$) (Lobo et al. 2021). Furthermore, B8AB4, which incorporates the narrow NIR and red bands in a similar equation to NDVI (Table 1), was found to be the least effective index in this study. This poor performance is expected as Sentinel-2's narrow NIR band (B8A) has demonstrated success particularly in terrestrial studies such as leaf area index estimates (Kaplan and Rozenstein 2021) and burn severity identification (Fernández-Manso, Fernández-Manso, and Quintano 2016), while the red (B4) and red edge (B5) bands have also been applied to aquatic studies (J. Shi et al. 2022; Ambrose-Igho et al. 2021). Additionally, without a large enough difference in reflectance and absorption values between the narrow NIR and red wavelengths, spectral index values for B8AB4 become muted and generally underestimate chl-a even in high concentrations (Figure 4). Results from this study corroborate findings from similar studies (Cillero Castro et al. 2020; Caballero et al. 2020), which attribute the detection of phytoplankton blooms to high reflectance peaks in the red-edge and near-infrared bands and low reflectance values in the red band (Caballero et al. 2020). This reflectance pattern is characteristic of floating cyanobacteria blooms that appear green to the eye, which resembles reflectance peaks in healthy terrestrial vegetation (Govender, Chetty, and Bulcock 2007). Although Sentinel-2 sensors were originally created for land-based studies, findings from this research and other related studies (Cao et al. 2021; Caballero et al. 2020; Cillero Castro et al. 2020; Lobo et al. 2021) further support the notion that this satellite is appropriate and can be adapted to aquatic studies.

Indices involving the blue and green portions of the electromagnetic spectrum are often best for clearer waters with less organic material (Binding et al. 2018; Alawadi 2010). In this study, B3B2 performed poorly in terms of its relationship to in situ data, but had fairly low RMSE values (Figure 5). This index proved to be moderately successful ($\text{adj. } R^2 > 0.4$) at Iron Gate sampling location (Figure 5), most likely due to clarity of the blooms on the surface of the water in this location, but was unreliable at Copco and Below Copco sites because blue and green wavelengths tend to be affected by confounding factors of chl-a, including detritus and color dissolved organic matter (S. Mishra and Mishra 2012), which are common in these extremely productive reservoirs. B3B2 both overestimated chl-a in low concentrations (as demonstrated in similar studies (Cillero Castro et al. 2020)) and underestimated chl-a in high concentrations (Figure 4). This can be linked to the pigment packaging effect (Alcántara et al. 2016), which is a flattening effect that describes lower chl-a reflectance values under scenarios of high in situ chl-a concentrations (Stuart et al. 1998). B3B2 appeared to perform best during the dry years (2016, 2018, and 2020) when cyanobacteria levels are often reduced because of

decreased nutrient influx. Although indices that use the blue and green can penetrate the water's surface slightly farther than indices in the NIR, red-edge, and red wavelengths (Legleiter, Kinzel, and Overstreet 2011), it is likely that blue-green indices are more accurate when blooms are clearly visible directly on the water's surface instead of layered in higher concentrations below the surface due to an inability to capture the full concentration. Therefore, B3B2 is most useful when applied to locations that typically have lower chl-a concentrations ($< 5 \mu\text{g/l}$), when blooms look bright green or blue to the human eye, and when blooms proliferate in the top layer of the water column.

4.2. Limitations of Sentinel-2 Chl-a Detection

There are several limitations associated with this research. The primary concern relates to the temporal resolution mismatch inherent to the in situ and satellite data comparison. Since in situ data were only collected once a month at each of the sampling locations, it was difficult to find Sentinel-2 satellite imagery that was both unobstructed by clouds and within several days of the sampling day (Figure 2). Therefore, the five-day time difference between the in situ measurements and some of the satellite data may cause uncertainty in the analysis, and similar studies attributed error to three-day discrepancies between in situ and Sentinel-2 data (Cillero Castro et al. 2020). However, regressions run separately on satellite data captured fewer than three days from in situ measurements did not render better results in our preliminary analyses. As algal blooms can appear and vanish within hours, it is preferable to gather data on a daily or weekly timescale. Figure 2 demonstrates that once a strong relationship is established between satellite imagery and in situ data, satellite imagery can be used to fill temporal gaps and understand the large heterogeneity that is present in this system. Missions such as PlanetScope (3 m spatial resolution) and RapidEye (5 m spatial resolution) offer daily imagery (Hu 2021) and indices such as NDVI and NDCI can be applied to these images to detect algal blooms at even finer resolutions. Other options for improved algal bloom satellite detection involve a harmonized product of Sentinel-2 and Sentinel-3 or even high-resolution Planet imagery (3-5m) to leverage enhanced spatial, temporal, and spectral resolution from each mission (Nima Pahlevan et al. 2020; Caballero et al. 2020). This will help reduce the mismatch between in situ and satellite data and enable more precise monitoring of bloom dynamics in small reservoirs.

Another limitation involves the detection of chl-a as a determinant for cyanobacteria species and toxicity. While some satellite missions have spectral bands that can identify the presence of phycocyanin, a key accessory pigment in cyanobacteria (Beck et al. 2017), Sentinel-2 does not have this specificity in band wavelength. In contrast, the Sentinel-3 Ocean and Land Color Instrument sensor has a band centered at 620 nm that has been used for more precise identification of cyanobacteria blooms (Ogashawara 2019). However, these images are captured at coarser spatial resolution (300 m) and are thus less useful for small sites. This presents a tradeoff in spectral and spatial resolution that again deters the detection of bloom dynamics in small reservoirs. Although chl-a is useful in ascertaining algal biomass, the concentration of chl-a can only act as a proxy for blooms and indicates neither the species nor the toxicity level of the bloom (R. P. Stumpf et al. 2003; Gustaaf M. Hallegraeff et al. 2004). However, toxin levels in this study have a high correlation with chl-a concentrations (Figure A.2), thus supporting these methods to detect both chl-a and microcystin toxin concentrations using Sentinel-2 imagery in these reservoirs. To remotely sense algal species or genera

information, hyperspectral imagery at high spatial resolutions with daily return intervals would be optimal, although no current satellite missions fit this objective.

4.3. Algal Bloom Management Implications

Despite the above mentioned limitations, Sentinel-2 chl-a time series analysis provides a promising tool for expanding the spatial and temporal measurements of algal blooms in small reservoirs. Currently in Iron Gate Reservoir, PacifiCorp uses a physical barrier or “curtain” to curtail the downstream drift of HABs to the rest of the Klamath River (Stillwater Sciences 2020). Sentinel-2 imagery might assist this protocol by providing time series information to inform managers on when to implement the curtain. Using the Google Earth Engine time series information and standardized anomaly images (Figure 7), locations that may require special observation to potentially enact phosphate reduction (Hans W. Paerl, Otten, and Kudela 2018) or cyanobacteria removal and inactivation techniques (Westrick et al. 2010) might be assessed. Throughout this time series, chl-a measurements exceeded the “Danger” category (20 µg/l microcystins) for Trigger Levels for Human & Animal Health in California (United States Environmental Protection Agency 2019) on at least 10 separate days (Figure 2). Increased monitoring of the Klamath reservoirs through the use of open-access satellite imagery can help communities prepare for and respond to these toxic events.

This study provides information on algal biomass estimations prior to one of the largest dam removals in history (Allen 2010). As Klamath River dam removal is expected to improve overall water quality and diminish long term HAB impacts in this system (Otten et al. 2015), results from this study provide baseline data that can help managers prepare for ecological restoration projects in future dam removal scenarios. Also, as the dams are drawn down for removal, spectral indices, especially NDCI and NDVI, applied to high-resolution satellite imagery will be effective as a tool for monitoring the spatial and temporal effects on water quality, particularly if the river mimics the dynamics of a “wet” year. Sentinel-2 imagery complements in situ monitoring and can be used to improve algal bloom management in small nutrient-rich lakes, rivers, ponds, and reservoirs around the world. Google Earth Engine analysis allows researchers to easily scale up the analysis to include greater portions of the Klamath River or reservoirs to better understand the spatial extent of dam removal impacts in this region.

Finally, the benefits of augmenting sampling with satellite imagery analysis rather than only increasing field sampling are clear since there is limited money and time for additional in situ sampling efforts. Instead, strong relationships between spectral indices and in situ data can be established, allowing managers to leverage satellite-derived products (Figure 7) to expand the comprehension of the spatial and temporal dynamics of algal blooms in these systems. This study demonstrated that NDCI is a useful tool to understand cyanobacteria dynamics and patterns in small reservoirs and lakes, which can be implemented to inform localized management and mitigation strategies. Satellite imagery allows an integration of understanding of HAB dynamics over space and time and thus provides a greater perspective on the variability of the aquatic system than methods relying only on monthly in situ observations.

5. Conclusions

This research validated the use of Sentinel-2 imagery to improve algal bloom management and inform baseline water quality data before dam removal by providing greater spatial and temporal coverage of these events. By deriving a strong relationship between Sentinel-2 imagery and in situ chl-a data through the use of red-edge and NIR spectral indices, it is possible to understand the seasonal, interannual, and local patterns of blooms in such freshwater ecosystems. NDCI proved to be the optimal spectral index in this environment. We recommend that future studies use high-resolution satellite data in concert with in situ water quality sampling that occurs within five days of the satellite flyover during peak bloom events. This research promoted a greater understanding and communication of a highly dynamic system through the incorporation of a continuous satellite mission and high-performance cloud computing via Google Earth Engine, where code and analysis can be shared among researchers and water quality managers. Research in this field can benefit from increased spatial, temporal, and spectral resolution, and upcoming hyperspectral missions such as NASA’s Plankton, Aerosol, Cloud, ocean Ecosystem (PACE) paired with in situ data and high spatial resolution imagery from Sentinel and Planet missions can increase the ability to document and address future blooms. Finally, as dam removal is anticipated to reduce toxic HABs in the Klamath River Basin over time (Otten et al. 2015), results from this study allow researchers to estimate algal bloom risk aversion in future dam removal projects. Similar methods can be applied to a variety of freshwater environments, reducing the impact of potentially toxic HABs in small lakes, rivers, and reservoirs around the world.

6. Appendix

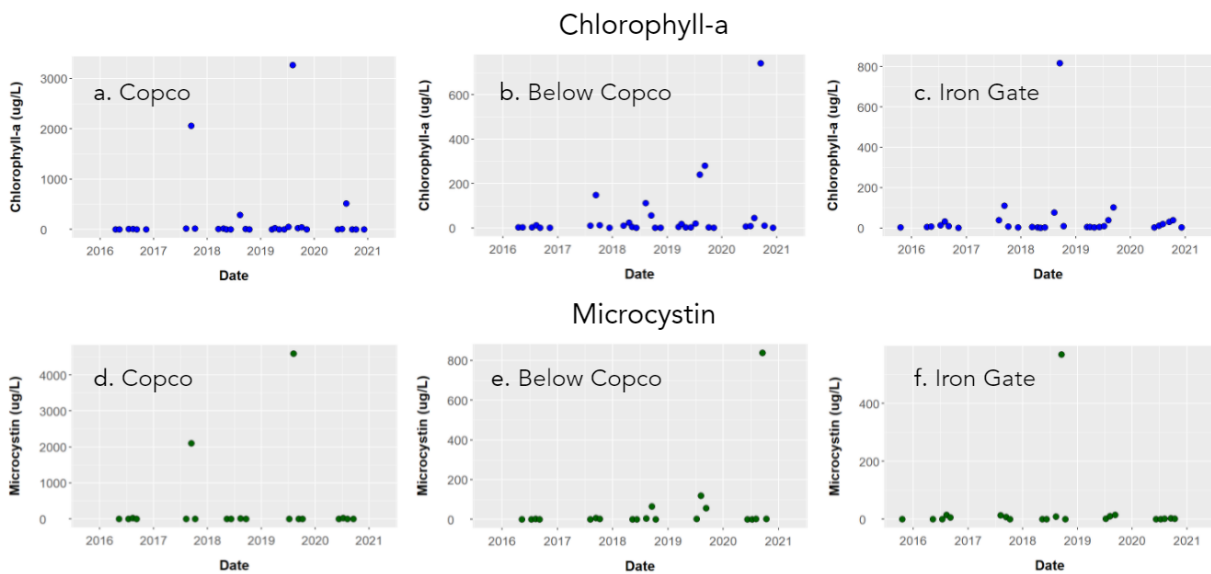


Figure A.1. In situ chlorophyll-a and microcystin values (µg/l) per sampling location from 2015-2020, measured by PacifiCorp.

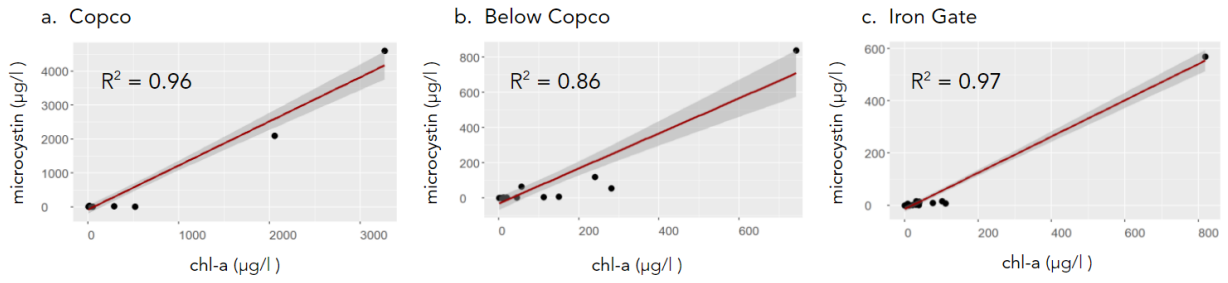


Figure A.2. Linear regressions of in situ microcystin toxin and chlorophyll-a data at (a) Copco, (b) Below Copco, and (c) Iron Gate. *Gray shading:* 95% confidence intervals; *red lines* demonstrate the mean relationships for the regression. R^2 values represent adjusted R^2 values.

Chapter 4: Integrating Crowdsourced Incident Reports with Satellite Imagery to Understand Algal Blooms in California Lakes and Reservoirs

Abstract

Freshwater harmful algal blooms (FHABs), and particularly cyanobacteria blooms that emit toxins, are associated with negative ecological, environmental, and health impacts in global lakes and reservoirs. In situ water quality sampling is necessary to monitor these blooms, but this method is often deployed infrequently due to time and financial constraints. Satellite imagery expands the capacity to evaluate bloom events at broader spatial and temporal scales, although trade offs exist between spatial and spectral resolution with current sensors. While Sentinel-3 imagery (300 m/pixel) provides the spectral resolution to identify cyanobacteria blooms using the Modified Cyanobacteria Index, its coarse spatial resolution lacks the detail to resolve smaller bodies of water ($< 2 \text{ km}^2$), which are important for drinking water, recreational activities, and aquatic ecosystems. Sentinel-2 (10 m/pixel) fills this gap with greater spatial resolution, but lacks the spectral resolution to decipher among algal bloom types. In California, there are FHAB datasets involving both crowdsourced bloom incident reports and Sentinel-3 satellite imagery of lakes and reservoirs at near-real time. Although these FHAB data are provisional, this is the first study to attempt to integrate these two datasets to determine if we can pair field reported blooms and aerially-detected blooms in California. We compared three spectral indices applied to Sentinel-2 imagery – Normalized Difference Vegetation Index (NDVI), Normalized Chlorophyll Index (NDCI), and a blue-green index (B3B2) – to reported microcystin values at two scales: a 200 m buffer around a reported bloom and at the entire lake or reservoir scale. We extracted mean spectral index values for the buffer scale to average out reflectance noise at a small scale and 90th percentile spectral index values for the lake or reservoir scale to identify highest values across the entire body of water. We also compared Sentinel-3 90th percentile Modified Cyanobacteria Index values to reported microcystin values at the lake or reservoir scale. We assessed these relationships using logarithmic regressions. For Sentinel-2 imagery, NDVI proved to be the most useful index ($R^2 = 0.34$) at the buffer scale. Sentinel-3 MCI values had a stronger relationship to reported microcystin data ($R^2 = 0.52$) than Sentinel-2, although the increased spatial resolution of Sentinel-2 greatly expands the number of monitored lakes and reservoirs. Improving the spectral and spatial resolution of future satellite missions will enhance the ability to integrate in situ reports and aerial imagery, which will help improve detection and monitoring for potentially toxic blooms in lakes and reservoirs throughout the world.

1. Introduction

Freshwater harmful algal blooms (FHABs) are increasing in frequency, duration, and severity across the globe (W. Carmichael 2008; Hans W. Paerl and Huisman 2008; J. C. Ho, Michalak, and Pahlevan 2019). FHABs are algal proliferations in freshwater environments that become harmful to humans, other animals, and the economy when they produce toxins, foul smells, anoxic zones, and excess biomass that disrupt ecological processes and recreational activities (Hudnell 2010). Lakes and reservoirs often suffer from the most severe and frequent FHABs because of upstream nutrient inputs, extended water residence times, and water column stratification that enable algal species to grow rapidly in these environments (Hans W. Paerl,

Otten, and Kudela 2018). Many FHABs in these ecosystems are composed of cyanobacteria, or blue-green algae, that can produce microcystin, a toxin that can cause acute liver damage in organisms that consume it. It has been shown to cause gastrointestinal problems, head and eye pain, nausea and vomiting, and organ damage in people, as well as mortality of dogs, cattle, fish, and birds (Wood 2016; Massey et al. 2018).

Due to the severity and increase in FHABs, new monitoring programs have been established for lakes and reservoirs across the world. New methods are also being developed to detect and monitor FHABs. Monitoring FHABs typically involves collecting water quality samples, which are then analyzed in the laboratory for the presence of toxins such as microcystin. However, this in situ method is expensive and time-intensive, and necessarily restricts the analysis to the point location at which the sample was collected (Ogashawara and Moreno-Madriñán 2014). Fortunately, new methods for monitoring FHABs are being developed that are more cost effective and have greater spatial and temporal coverage. For example, researchers have used satellite imagery (Klemas 2012; Shen, Xu, and Guo 2012), drones (Kislik et al. 2020), and other aerial methods (Strong 1974; Beck et al. 2016) to observe and analyze algal proliferations in concert with in situ monitoring. Others have shown that crowdsourced, participatory, and citizen science data from social media platforms like Twitter (D. R. Mishra et al. 2020; Skripnikov et al. 2021) and mobile device applications (Malthus, Ohmsen, and Woerd 2020; Kotovirta et al. 2014) can be used to monitor FHABs. One notable mobile device application is the Cyanobacteria Assessment Network Application (CyAN app), which pairs blue-green algae observations and satellite imagery within more than 2,000 of the biggest lakes and reservoirs throughout the United States (Schaeffer et al. 2018).

The integration of crowdsourced data with satellite imagery has the potential to extend FHAB monitoring capacity across the globe. However, spatial resolution limitations in satellite sensors have restricted applications to large lakes and reservoirs ($> 2 \text{ km}^2$) (S. Mishra, Stumpf, and Meredith 2019). For example, previous studies that focus on cyanobacteria detection in large lakes and reservoirs have used imagery from missions such as the Medium Resolution Imaging Spectrometer (MERIS) (Kutser et al. 2006; Mark W. Matthews, Bernard, and Winter 2010) and Sentinel-3 (Coffer et al. 2021; Clark et al. 2017). These satellites have sensors that leverage the reflectance peak near 700 nm or the absorption trough around 620 nm of phycocyanin, a pigment of cyanobacteria (Kutser 2009; Ogashawara 2019) (Figure 1). These wavelengths greatly improve the ability to determine if an algal bloom is composed of cyanobacteria, which can produce toxic blooms. However, the coarse resolution ($\geq 300 \text{ m/pixel}$) limits the spatial scope of analysis.

In California, there is an increasing availability of both in situ and satellite-based FHAB bloom datasets that are collected by the California Cyanobacteria and HAB (CCHAB) Network, a workgroup of the California Water Quality Monitoring Council. The Network manages and compiles crowdsourced incident reports (“FHAB Incident Reports”) (https://mywaterquality.ca.gov/habs/where/freshwater_events.html), in which water body managers and users can report a bloom online or via phone (<https://mywaterquality.ca.gov/habs/do/bloomreport.html>) with an associated advisory level that is determined by visual observation, laboratory analysis, or both. These advisory levels in California include Caution (0.8 $\mu\text{g/l}$ microcystins or observational greenness), Warning (6 $\mu\text{g/l}$

microcystins), and Danger (20 µg/l or more microcystins), and were originally established by the U.S. Environmental Protection Agency as health guidelines for swimming and recreational activities (United States Environmental Protection Agency 2019). These FHAB incident reports are then displayed in an online interactive map that is updated weekly, enabling recreational water users and water quality managers to view which bodies of water are currently at risk of potentially toxic algal blooms in California. The Network also hosts a HAB Data Viewer (“FHAB Data Viewer”) (https://mywaterquality.ca.gov/habs/data_viewer/), which uses Sentinel-3 Ocean and Land Colour Instrument (300 m/pixel) imagery to monitor cyanobacteria blooms in approximately 255 large lakes and reservoirs throughout California (<https://fhab.sfei.org/>). With increased spatial resolution, the FHAB Data Viewer can improve its ability to resolve all sizes of lakes and reservoirs throughout the state. It should be noted that both of these FHAB monitoring systems use provisional data that are neither validated nor intended for use in analytical or research settings. However, they serve a vital purpose in alerting water users, dog owners, and environmental managers of the immediate dangers of potentially toxic blooms in California. Despite their importance and utility, little attention has been given to comparing these two statewide programs.

Higher-resolution imagery from Sentinel-2 offers the capability to detect FHABs at smaller spatial scales. Sentinel-2 captures imagery at 10, 20, and 60 m/pixel, depending on the band (Rodríguez-Benito, Navarro, and Caballero 2020). However, Sentinel-2 cannot specifically identify phycocyanin due to limited spectral resolution (Sòria-Perpinyà et al. 2021). Instead, bands 2 (blue), 3 (green), 4 (red), 5 (red edge), and 8 (near-infrared; NIR) from this satellite (Figure 1) are commonly used to detect chlorophyll-a (chl-a), a measure of greenness in photosynthesizing organisms, as a proxy for FHAB biomass (Bramich, Bolch, and Fischer 2021; Ansper and Alikas 2018; Alawadi 2010; Beck et al. 2016; Pirasteh et al. 2020; Cillero Castro et al. 2020). Previous studies have leveraged spectral indices applied to Sentinel-2 imagery to expand their understanding of the location, frequency, and duration of FHABs (Cao et al. 2021; Viso-Vázquez et al. 2021). Furthermore, studies have linked chl-a measurements with microcystin measurements and have found predictive relationships (Hollister and Kreakie 2016; Qian et al. 2021), demonstrating that Sentinel-2 can be used as a tool to monitor cyanobacteria blooms. However, additional validation from in situ field measurements is needed to determine the contexts in which data from Sentinel-2 can reliably be used to infer the presence of microcystin associated with FHABs.

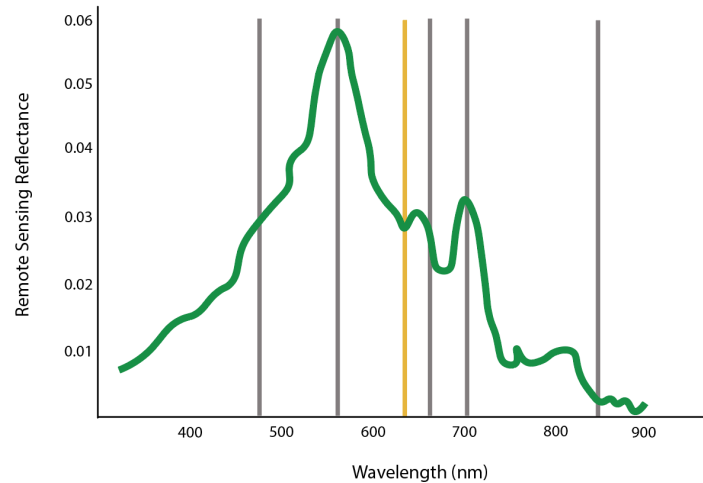


Figure 1. An example spectral reflectance curve of cyanobacteria (shown as the *green line*) in a freshwater lake, modified from Stumpf et al. 2016. *Gray lines* denote the central wavelengths of the Sentinel-2 bands used in this study (blue, green, red, red-edge, near-infrared), and the *yellow line* denotes the absorption trough at 620 nm that indicates phycocyanin, a key pigment of cyanobacteria.

To understand the extent to which remotely-sensed imagery can reliably predict the presence of FHABs at relatively small spatial scales, we compared three spectral indices applied to Sentinel-2 imagery with FHAB incident report microcystin data from 68 lakes and reservoirs across California, USA. This analysis was conducted both within a 200 meter buffer around each sample and at the lake or reservoir scale to understand how we can use remotely-sensed imagery to capture both local water quality characteristics around in situ sampling locations and broad-scale dynamics across the entire water body. We also compared the Modified Cyanobacteria Index applied to Sentinel-3 data with FHAB reported microcystin data from 5 lakes and reservoirs of various sizes (e.g., from ~0.5 - 264 km²) across the state to understand the difference in scale of existing FHAB monitoring practices. The specific objectives for this study were to: (1) determine which Sentinel-2 spectral index is most effective in identifying potentially toxin-producing blooms in California from 2019 to 2021; (2) assess the relationship between current Sentinel-3 satellite imagery and FHAB-reported microcystin data; and (3) identify the spatial scale at which toxic blooms can be most reliably detected with satellite data. Our study attempts to integrate two distinct statewide datasets through the incorporation of a higher spatial resolution dataset to improve toxic algal bloom monitoring in near-real time within California.

2. Methods & Materials

2.1. FHAB Incident Report Data

To evaluate the relationships between satellite indices and FHAB reported data, we first gathered the reported data. FHAB incident reports from 2016 to present (2022) were obtained through the California Open Data Portal (<https://data.ca.gov/dataset/surface-water-freshwater-harmful-algal-blooms>). These data are voluntarily submitted to the California State Water Resources Control Board (Water Boards) using the Freshwater Incident Form on the California Harmful Algal Blooms Portal, operated by

the CCHAB Network. Reports within this dataset include different types of water bodies, advisory levels, methods of analysis, and information about each bloom event. From 2016 to January 26, 2022, there were 1,350 reports in this database. To focus on algal blooms in lakes and reservoirs throughout California from 2019 through 2021, we first refined this raw dataset in Excel by selecting blooms from January 1, 2019 to December 31, 2021 (to align with Sentinel-2 surface reflectance data availability) and then by eliminating any entries that did not include a latitude and longitude (Figure 2).

FHAB Incident Report Database Search Queries

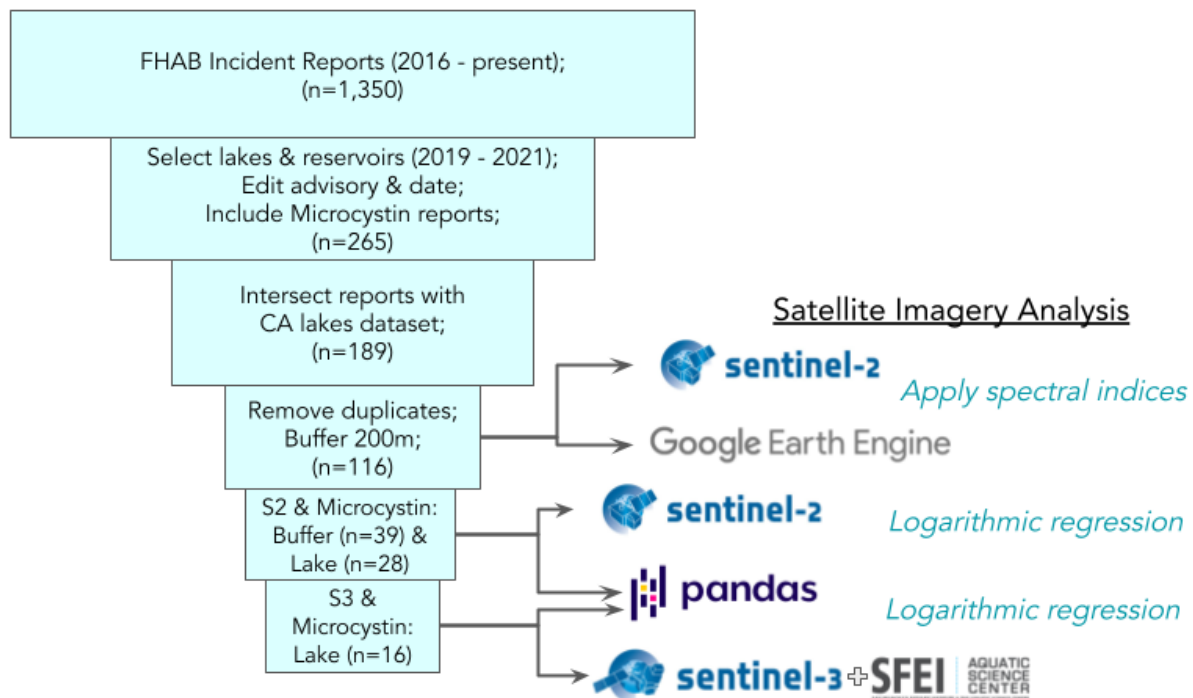


Figure 2. Conceptual graphic showing the steps involved in data cleaning, processing, and analysis phases of the study. The number of incident reports is listed for each step. Note: S2 = Sentinel-2 satellite imagery and S3 = Sentinel-3 satellite imagery. For Sentinel-2, spectral index values acquired at both the 200 m buffer and lake or reservoir scale were compared to microcystin values, while Sentinel-3 spectral index values were only compared to microcystin values at the lake or reservoir scale. The reduction in the number of comparisons between microcystin values and spectral index values for Sentinel-2 and Sentinel-3 is based on satellite imagery availability for each bloom event and pixel size limitations.

We further organized and prepared the FHAB incident reports prior to comparing these data to satellite-derived spectral indices. We discarded any FHAB report entries that did not pertain to lakes and reservoirs (i.e., we removed all rivers, creeks, ponds, gulches, irrigation ditches, and canals, and eliminated any bays, lagoons, marinas, deltas, sloughs, and ports that were not located within a lake or reservoir). We also removed any bloom that had an advisory level (using

the field “TypeofSign” in the database) of None or NA. This left us with 265 FHAB reports. We then read through each report description (“IncidentInformation” in the database) and identified a date and bloom advisory level for each event (Figure 2). In some cases, reports included multiple dates and events, so we selected those that contained microcystin toxin level information. We created a separate column in this refined dataset for microcystin toxin values that were included in the report descriptions, when available (n = 45). These toxins were measured through quantitative real-time polymerase chain reaction (qPCR) and enzyme-linked immunosorbent assays (ELISA) methods. For report descriptions that indicated that further analysis was warranted or that observations were likely but unsure, we designated the advisory level as “Precaution” to distinguish these reports from others with higher certainty. We cleaned and consolidated several data categories including analysis type (“BloomDeterminedBy” in the database), date, and advisory level, to properly reflect the bloom description information. Finally, we summarized the FHAB incident reports by bloom advisory level, bloom analysis type, bloom reports per year, and bloom reports per month.

Next, in ArcGIS Pro 2.9.1 (ESRI 2022), we continued to refine the FHAB incident reports in preparation for satellite imagery comparison. We used the latitude and longitude information from the FHAB incident reports to plot the location of each in situ measurement and we then removed any duplicates. Next, we buffered each FHAB report in situ measurement location by 200 m using the Buffer tool. This 200 m buffer width has been used in previous studies to extract inland water quality parameters from remotely-sensed imagery (Ross et al. 2019; Yu et al. 2016). We then intersected and clipped the buffered incident reports to the California Lakes shapefile from the California Department of Fish and Wildlife (<https://gis.data.ca.gov/datasets/CDFW::california-lakes/about>) to constrain buffered incident reports to lake and reservoir boundaries. We selected a date for “non-blooms” after reviewing incident report descriptions and finding a day that was at least two weeks after and at least two weeks before any reported FHAB incidents (February 19, 2020). This non-bloom date was selected to evaluate statistical significance between bloom and background spectral index values. We added this non-bloom date as a column in the buffered incident reports shapefile. To assess each body of water at the lake or reservoir scale, we created a separate shapefile by spatially joining the buffered incident reports to the California Lakes shapefile. Finally, for both of these new shapefiles, we converted the dates of each bloom or non-bloom event to “yyyy-mm-dd” format (as a string, with dashes) using the Convert Time Field tool in ArcGIS Pro to align with Google Earth Engine’s date format requirements. After this, we exported the two shapefiles (one at the buffer scale with blooms and non-blooms columns and one at the lake or reservoir scale with blooms columns) for further analysis in Google Earth Engine (Gorelick et al. 2017).

2.2. Satellite Data Processing

We used Google Earth Engine to determine which spectral index applied to Sentinel-2 satellite data is most effective in identifying reported FHAB blooms. Here, we paired Sentinel-2 satellite data with FHAB incident report dates to extract spectral index values per event at various scales. We used the Sentinel-2 MultiSpectral Instrument Level-2A surface reflectance image collection in Google Earth Engine (Asset ID: COPERNICUS/S2_SR) to understand reported algal blooms in California with high resolution satellite imagery from 2019 to 2021 (Figure 2). We first implemented a cloud mask on this collection by using the QA60 band to remove dense and cirrus

clouds from the imagery, and then applied spectral indices to each image in the collection. These indices include the Normalized Difference Vegetation Index (NDVI) $[(\text{NIR} - \text{Red}) / (\text{NIR} + \text{Red})]$, which uses the near-infrared and red wavelengths to assess greenness in terrestrial vegetation and aquatic algae (Oyama, Matsushita, and Fukushima 2015), the Normalized Difference Chlorophyll Index (NDCI) $[(\text{Red Edge} - \text{Red}) / (\text{Red Edge} + \text{Red})]$, which uses the red edge and red wavelengths to identify algal blooms in turbid environments (S. Mishra and Mishra 2012), and Band 3 Band 2 (B3B2) $[(\text{Green} - \text{Blue}) / (\text{Green} + \text{Blue})]$, which uses the green and blue wavelengths to assess chl-a in freshwater ecosystems (Cillero Castro et al. 2020). We then applied the European Commission's Joint Research Centre's Global Surface Water Mapping Layers water mask (Asset ID: JRC/GSW1_0/GlobalSurfaceWater) with a 70% water occurrence threshold to the image collection. This water mask was originally created using 30 m Landsat pixels and is used to distinguish land and shoreline from areas inundated with water (Pekel et al. 2016). We used this surface water mask in Google Earth Engine to further improve our ability to exclude neighboring shoreline and land pixels from our analysis.

We then spatially and temporally aligned reported FHAB incident data with the Sentinel-2 satellite imagery to evaluate the relationship between these two datasets. First, we imported the ArcGIS Pro shapefiles as assets into our Google Earth Engine project and assigned a variable for the bloom dates. For each FHAB incident, we filtered the Sentinel-2 imagery to include four images (two images before and two images on or after) its reported date. Four images were selected to ensure that crowdsourced bloom reports would be captured by satellite imagery within a large enough time frame. We then calculated the mean spectral index value within the 200 m buffer area per FHAB event (using the 'reduceRegion' and 'Reducer.mean' functions in Google Earth Engine), as well as the number of cloud free pixels within each buffer and the number of day(s) between the FHAB incident and each of the four associated satellite image capture dates. We repeated this process for "non-bloom" events. We excluded imagery in which a large percentage of pixels were composed of non-water items when the 30 m water mask was unable to detect these objects. We also calculated the 90th percentile of spectral index values within the lake or reservoir boundary per FHAB event (using the 'reduceRegion' and 'Reducer.percentile([90])' tools in Google Earth Engine) to understand the highest values per spectral index at the lake or reservoir scale and to better compare them with the CCHAB Sentinel-3 methodology. Pixel counts within each body of water and the number of day(s) between the FHAB incident and associated satellite image capture date were also calculated. Data from the buffered values (blooms and non-blooms) and lake or reservoir scale values were exported as CSV files outside of Google Earth Engine for further analysis using Jupyter Notebooks (Python 3.0).

We used Jupyter Notebooks for the final stage of data preparation before we evaluated the relationships between Sentinel-2 spectral indices and FHAB incident reports, as well as the relationships between Sentinel-2 blooms and non-blooms. In this environment, we imported the CSV files created in Google Earth Engine containing the spectral index values for each FHAB event. We computed the average value of Image 2 (the soonest available image before the FHAB incident) and Image 3 (the soonest available image on or just after the FHAB incident) for every FHAB incident and for each spectral index. This process was completed for buffered values (blooms and non-blooms) and lake or reservoir scale blooms. We used this averaged value of Images 2 and 3 as the primary value of analysis in this study for each spectral index at the 200 m

buffer scale because it improved data quality by reducing artifacts common to remotely sensed imagery such as missing cloud-masked pixels due to clouds and erroneous reflectance values from solar glint and atmospheric properties (Alawadi 2010).

To evaluate how Sentinel-3 Ocean and Land Colour Instrument imagery from the FHAB Data Viewer can be used in relation to crowdsourced incident reports, we selected FHAB incident reports that contained microcystin values. We then paired these blooms with data from the FHAB Data Viewer website (<https://fhab.sfei.org/>) by searching for the water body, viewing the satellite data, and evaluating the Sentinel-3 spectral index values. The spectral index used in the FHAB Data Viewer is the Modified Cyanobacteria Index (MCI), which is an index that was developed for MERIS imagery to identify the spectral shape at 681 nm; higher curvature indicates higher cyanobacteria concentrations and there is also a corresponding elevated reflectance at 709 nm for cyanobacteria species (Timothy T. Wynne et al. 2010). MCI has proven useful in previous algal bloom detection studies involving species that produce microcystin (Vander Woude et al. 2019; Timothy T. Wynne and Stumpf 2015; Timothy T. Wynne et al. 2013, 2010; T. T. Wynne et al. 2008). We then downloaded the 90th percentile MCI values for the 10-day interval that overlapped with each FHAB incident date ($n = 16$) (Figure 2). The Sentinel-3 imagery used on this website is not atmospherically corrected because previous studies have shown that these types of corrections applied over inland waters can produce errors that are worse than top-of-atmosphere values for algal blooms (Nima Pahlevan et al. 2020). Sentinel-3 values from the FHAB Data Viewer assess cyanobacteria blooms at the lake or reservoir scale, and we therefore only compared Sentinel-3 spectral index values to Sentinel-2 values at the same scale (rather than at the 200 m buffer scale) ($n = 14$).

2.3. Satellite and In Situ Data Comparison

To determine if non-bloom events and bloom events characterized by Sentinel-2 imagery at the 200 m buffer scale were statistically different, we conducted paired t-tests on the spectral values from each of the three indices (NDVI, NDCI, B3B2) extracted from 116 reported FHAB events per group (Kim 2015). We calculated this test to determine if the spectral indices applied to Sentinel-2 imagery in this study can distinguish blooms from non-blooms. This analysis was performed using the Python pandas (McKinney and Others 2010) and scipy (Virtanen et al. 2020) packages.

We used linear regression analysis to assess the relationships between the various datasets at different scales. We wanted to understand how well Sentinel-2 spectral index values and Sentinel-3 MCI values could predict microcystin values from the FHAB incident reports. To do this, we used logarithmic regression model coefficient of determination values (R^2) for each comparison: Sentinel-2 index values and microcystin at the 200 m buffer scale, Sentinel-2 index values and microcystin at the lake or reservoir scale, and Sentinel-3 MCI values at the lake or reservoir scale. The logarithmic model equation can be described as: $y = a + b \cdot \ln(x)$, in which y is the responses variable, x is the predictor variable, and a and b are the regression coefficients (Godfrey and Wickens 1981). We selected this equation to describe the relationship between these predictor and response variables because it linearizes the model, as spectral index values and the log of microcystin values have a relatively linear relationship (Ostrovsky et al. 2020). Previous related studies have used logarithmic regressions to evaluate spectral index predictions

of algal blooms (Van der Merwe and Price 2015; Chang, Shen, and Chen 2004; Ekstrand 1992; Bakker et al. 2010). We also compared Sentinel-3 MCI values to Sentinel-2 spectral index values using a standard linear regression equation ($y = a + bx$) (Krutchkoff 1967).

3. Results

3.1. Descriptive Statistics of FHAB Incidents

Of the 116 FHAB incidents reported in this study (2019 - 2021), the majority were labeled at the “Caution” bloom advisory level ($n = 50$), followed by an equal number designated as “Precaution” ($n = 25$) and “Danger” ($n = 25$). The fewest reports ($n = 16$) had a “Warning” advisory level (Figure 3). Most reported blooms were analyzed by both visual observation and water quality sampling analysis ($n = 74$), followed by those that were only visually observed ($n = 23$), and others that only had either laboratory or test strip analysis ($n = 19$). The number of reported incidents increased in each year of the study, from 2019 ($n = 20$) to 2020 ($n = 46$) to 2021 ($n = 50$). The majority of reports occurred in the summer months with August having the highest number ($n = 36$), followed by September ($n = 20$), and July ($n = 16$). The fewest reports occurred in January ($n = 1$), February ($n = 1$), and March ($n = 2$).

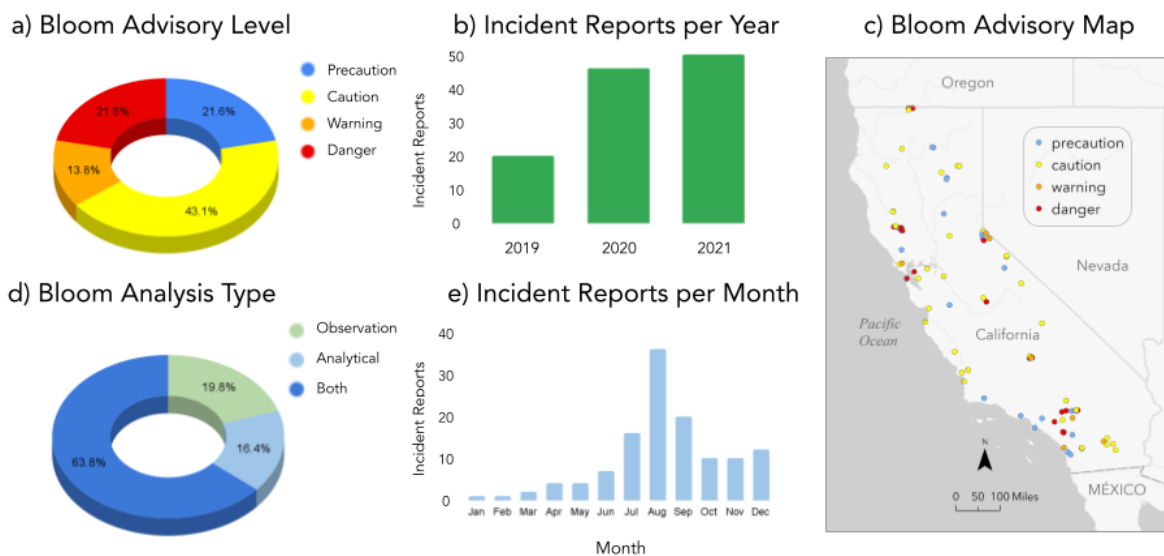


Figure 3. Descriptive statistics for the 116 FHAB incident reports analyzed in this study (2019 - 2021). These are categorized by: a) bloom advisory level, b) reports per year, c) bloom advisory location, d) bloom analysis type, and e) reports per month.

Lakes and reservoirs with the highest microcystin levels ($\geq 100 \mu\text{g/l}$) recorded in the FHAB incident reports for this study included Clear Lake (160,377.5 $\mu\text{g/l}$, 4940 $\mu\text{g/l}$, 1449.5 $\mu\text{g/l}$, 517.2 $\mu\text{g/l}$, 506.6 $\mu\text{g/l}$, 135.02 $\mu\text{g/l}$), Isabella Lake (9,452.8 $\mu\text{g/l}$, 1,192.5 $\mu\text{g/l}$, 91 $\mu\text{g/l}$), Copco Reservoir (3,600 $\mu\text{g/l}$), Red Lake (2,389.5 $\mu\text{g/l}$), Hensley Lake (1,510.1 $\mu\text{g/l}$), Iron Gate

Reservoir (220 $\mu\text{g/l}$), Glen Helen (99 $\mu\text{g/l}$), and Lake Chabot (50 $\mu\text{g/l}$) (Figure 4). Each of these lakes and reservoirs vary by size; Clear Lake is about 264 km^2 , Isabella Lake is about 48 km^2 , Copco Reservoir is about 7 km^2 , Red Lake is about 0.5 km^2 , Hensley Lake is about 10 km^2 , Iron Gate is about 7 km^2 , Glen Helen is about 0.06 km^2 , and Lake Chabot is about 2 km^2 . Each of these microcystin values is associated with a Danger bloom advisory level. Of the top 15 microcystin values analyzed in this study, 6 are from Clear Lake and 3 are from Isabella Lake. Figure 4 displays the four reservoirs with the highest reported microcystin values (Clear Lake, Isabella Lake, Copco Reservoir, and Red Lake) in this study using Sentinel-2 imagery on the day of or closest to the reported bloom. All four of these blooms occurred in August or September of 2020 or 2021. One of the largest microcystin levels ever recorded occurred in Clear Lake on September 7, 2021, and the green cyanobacteria bloom is clearly visible in the Sentinel-2 imagery, particularly in the southeastern portion of the lake (Figure 4).

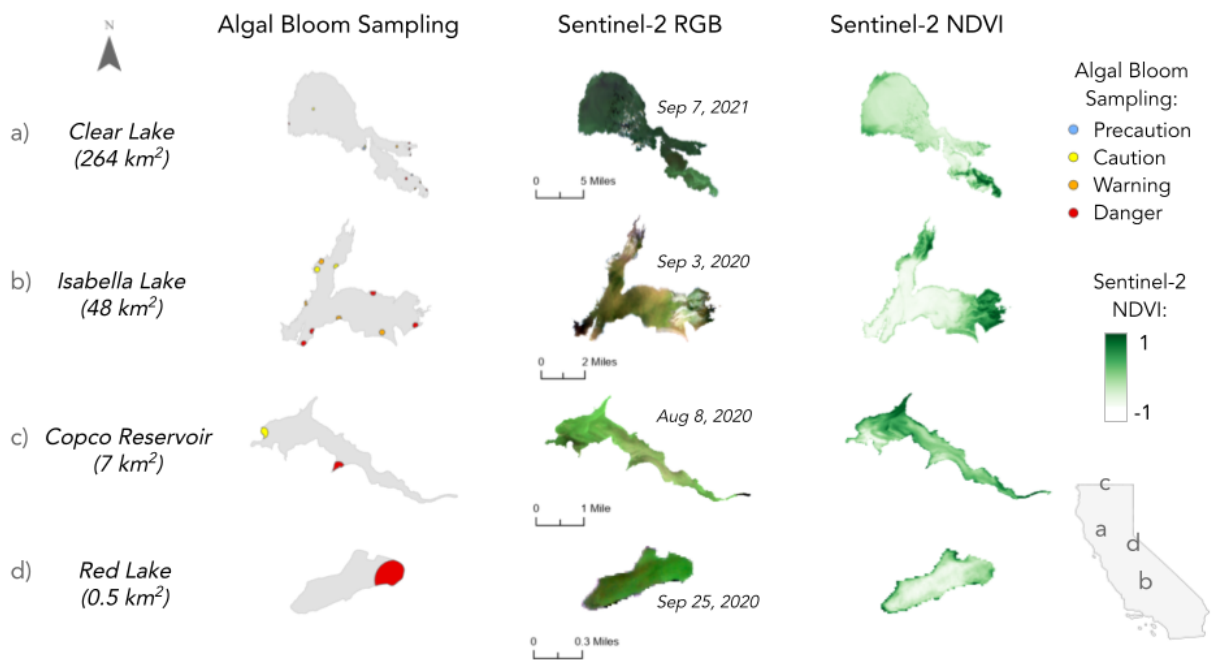


Figure 4. Sampling locations, bloom advisory levels, and Sentinel-2 imagery of the reservoirs and lakes with the highest microcystin values during this study: a) Clear Lake: 160,377.5 $\mu\text{g/l}$ recorded on September 7, 2021; b) Isabella Lake: 9,452.8 $\mu\text{g/l}$ recorded on September 3, 2020; c) Copco Reservoir: 3,600 $\mu\text{g/l}$ recorded on August 18, 2020; and d) Red Lake: 2389.5 $\mu\text{g/l}$ recorded on September 25, 2020. The algal bloom sampling maps show where water quality samples for the crowdsourced reports were collected throughout this study (2019 - 2021), with associated colors representing the bloom advisory level of each sample. The Sentinel-2 RGB (red-green-blue) imagery displays what the naked eye can see, and the Sentinel-2 NDVI imagery has the Normalized Difference Vegetation Index applied to the RGB imagery to depict spectral index values from the best of the three indices tested in this study. All satellite images were captured within 3 days of each bloom event (either on or after the event was recorded).

3.2. Sentinel-2 Satellite Comparison to FHAB Microcystin and Non-Bloom Values

The FHAB incident reports included microcystin values from 45 total bloom events in 19 different lakes and reservoirs across California. Sentinel-2 imagery aligned with 39 of these bloom events at the 200 m buffer scale and 28 of these events at the lake or reservoir scale (Figure 2). NDVI applied to Sentinel-2 imagery had the strongest relationship to reported FHAB microcystin levels of the three spectral indices tested in this study, although this relationship was moderate to low at the 200 m buffer scale ($R^2 = 0.34$) and lake or reservoir scale ($R^2 = 0.22$) (Figure 5). All other index values had low or negligible relationships (NDCI: $R^2 = 0.17$ at the buffer scale, $R^2 = 0.24$ at the lake or reservoir scale; B3B2: $R^2 = 0$ at the buffer scale, $R^2 = 0.11$ at the lake or reservoir scale). NDVI detected microcystins between about 100 and 1,000 $\mu\text{g/l}$ at the 200 m buffer scale, and over 10 $\mu\text{g/l}$ at the lake or reservoir scale, while NDCI was best at microcystin levels between 10 and 100 $\mu\text{g/l}$ at the buffer scale and under 10 $\mu\text{g/l}$ at the lake or reservoir scale. B3B2 did not perform particularly well in any microcystin level category.

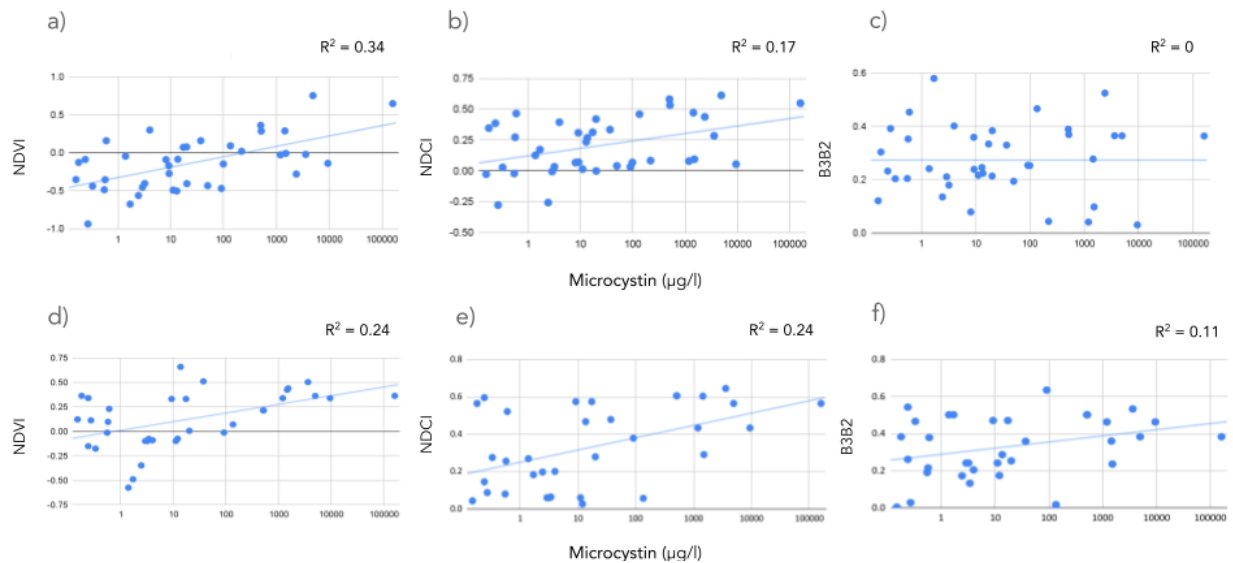


Figure 5. Sentinel-2 spectral index comparisons to FHAB incident report microcystin data using logarithmic regressions for: a) NDVI at the 200 m buffer scale [$y = -0.328 + 0.0594 \ln x$], b) NDCI at the 200 m buffer scale [$y = 0.121 + 0.0263 \ln x$], c) B3B2 at the 200 m buffer scale [$y = 0.273 + -1.64E-05 \ln x$], d) NDVI at the lake or reservoir scale [$y = 0.0111 + 0.0384 \ln x$], e) NDCI at the lake or reservoir scale [$y = 0.25 + 0.0285 \ln x$], and f) B3B2 at the lake or reservoir scale [$y = 0.29 + 0.0144 \ln x$]. Buffer values were calculated by averaging the values of Image 2 and 3 per bloom, while lake or reservoir values were calculated using the 90th percentile values per bloom. The x-axis is shown using a logarithmic scale.

Results comparing paired population means between blooms and non-blooms indicated that NDVI and NDCI can distinguish between the two categories and B3B2 cannot. The paired t-test

result for NDVI returns a statistic of -3.86 and a p-value of 0.0001. The NDVI algal bloom mean is -0.16 while the non-bloom mean is -0.30 (Figure 6). For NDCI, the statistic is -5.86 with a p-value of 3.67e-08. The NDCI algal bloom mean is 0.13 while the non-bloom mean is 0.01. The p-values of both of these spectral indices indicate statistical significance and signify that the mean bloom values are significantly higher than the non-bloom values. For B3B2, the difference between the means of algal blooms versus non-blooms is not significant (p-value > 0.1), and the algal bloom mean is 0.23 while the non-bloom mean is 0.27.

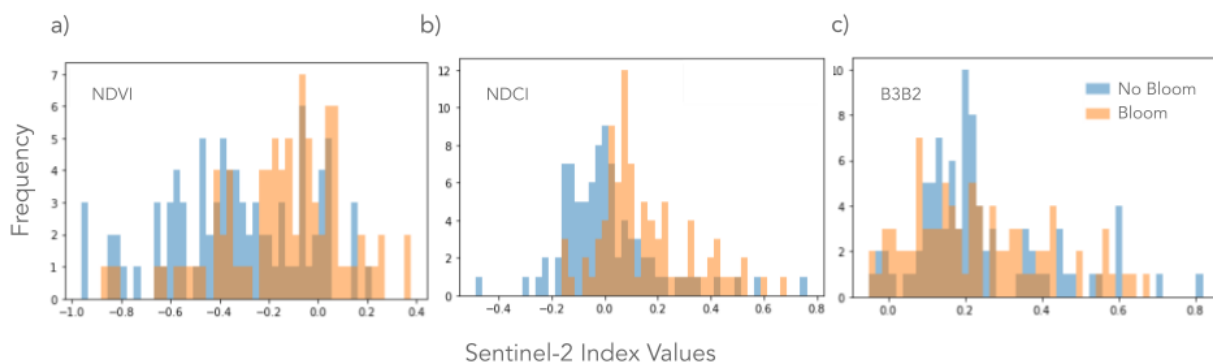


Figure 6. Population distribution comparisons for bloom events and non-bloom events with Sentinel-2 spectral index values for: a) NDVI, b) NDCI, and c) B3B2. Bloom events correspond to the average values of Images 2 and 3 and non-bloom events correspond to index values captured on February 19, 2020.

3.3. Sentinel-3 Satellite Comparison to FHAB Microcystin and Sentinel-2 Values

Sentinel-3 MCI values at the lake or reservoir scale aligned with 16 of the reported bloom events that had associated microcystin data from 5 different lakes and reservoirs across California (Clear Lake, Copco Reservoir, Hensley Lake, Iron Gate Reservoir, and Isabella Lake). Several lakes and reservoirs that had associated microcystin data were not available on the FHAB Data Viewer (Ewing Reservoir, Glen Helen Lake, Laguna Lake, Lake Chabot, Lake Merced, Pelican Lake, Red Lake, Stafford Lake, and Whelan Lake) because they are too small to be captured by the Sentinel-3 satellite imagery. Sentinel-3 mean and 90th percentile MCI values had moderately strong relationships to FHAB incident report microcystin values ($R^2 = 0.51$ and $R^2 = 0.52$, respectively) (Figure 7). The mean values appeared to detect microcystin best below 10 $\mu\text{g/l}$ while the 90th percentile MCI values detected microcystin at higher values, between 100 and 1,000 $\mu\text{g/l}$. NDCI had the strongest relationship with Sentinel-3 MCI values of the three Sentinel-2 spectral indices tested in this study, although this was a weak correlation ($R^2 = 0.18$ for mean MCI values and $R^2 = 0.14$ for 90th percentile values) (Figure 8). The highest agreement between Sentinel-3 MCI and Sentinel-2 NDCI values exist in low (near 0) and midrange (300-400 MCI values and 0.2-0.4 NDCI values) for the 90th percentile comparison.

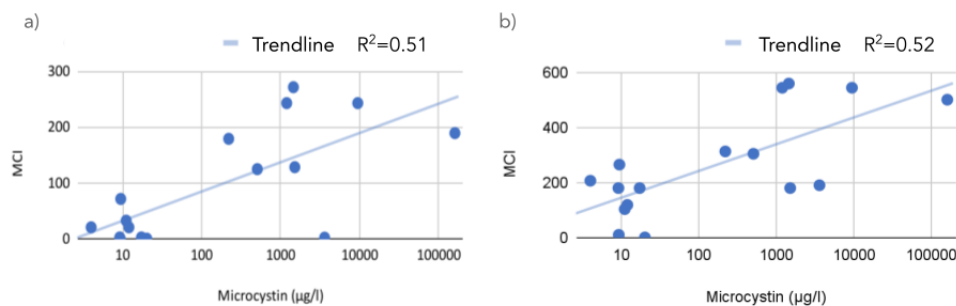


Figure 7. Sentinel-3 comparisons with FHAB incident report microcystin values using logarithmic regressions for: a) mean MCI values [$y = -19.4 + 22.8 \ln x$], and b) 90th percentile MCI values at the lake or reservoir scale [$y = 48 + 42.2 \ln x$]. The x-axis is shown using a logarithmic scale.

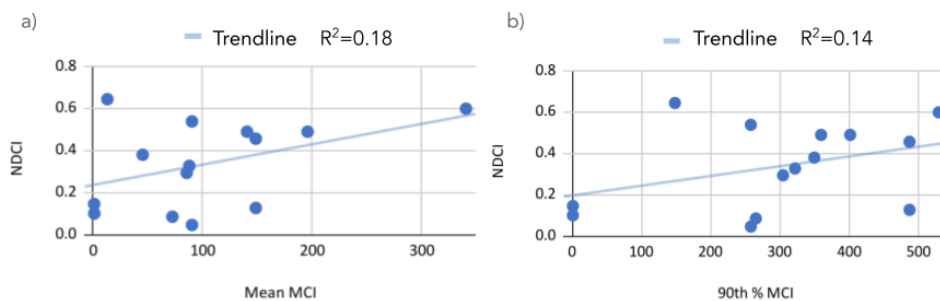


Figure 8. Sentinel-3 comparisons to 90th percentile NDCI Sentinel-2 values using linear regressions for: a) mean MCI values [$y = 9.68E-04*x + 0.235$], and b) 90th percentile MCI values at the lake or reservoir scale [$y = 4.72E-04*x + 0.196$].

4. Discussion

4.1. Sentinel-2 Satellite's Ability to Assess FHAB Incident Reports

The best fit between the Sentinel-2 spectral indices tested in this study and the FHAB blooms from the FHAB Incident Reports database was NDVI ($R^2 = 0.34$) at the buffer (200m) scale. This index leverages the near-infrared and red wavelengths, which have been used in line height algorithm estimates of chlorophyll-a in turbid waters (Zeng and Binding 2019), but have also been used to assess microcystin-producing algal species (Ma et al. 2021; Teta et al. 2016, 2021; Douglas Greene, LeFevre, and Markfort 2021). Although NDVI is not sensitive to phycocyanin as MCI is, this index was relatively successful in identifying FHABs with microcystin levels between 100 and 1,000 $\mu\text{g/l}$ at the 200 m buffer scale in this study. NDVI did not accurately predict lower microcystin values because this index tends to overestimate low chl-a values due to a saturation phenomenon (S. Huang et al. 2021; Viso-Vázquez et al. 2021). NDVI performed best with “warning” and “danger” advisory levels, as these reports tend to correspond to high

(median: 64 $\mu\text{g/l}$) microcystin values. Specifically, this index was best able to predict microcystin levels in several sampling locations of Glen Helen, Clear Lake, and Iron Gate Reservoir because images associated with these blooms had little atmospheric effect, meaning Rayleigh scattering and noise in the red band were reduced (S. Huang et al. 2021), and because of the high microcystin values (99 $\mu\text{g/l}$, 135 $\mu\text{g/l}$, and 220 $\mu\text{g/l}$, respectively) of these events. Also, the statistical significance between this index and non-bloom events demonstrates that it can distinguish algal blooms from background reflectance values.

However, it was surprising that NDVI outperformed NDCI, as the latter index has been largely successful in other related studies (Page, Kumar, and Mishra 2018; Beck et al. 2016; Rodríguez-Benito, Navarro, and Caballero 2020; S. J. Weber et al. 2020). The reasons for this may involve the clarity of the lakes and reservoirs, as NDCI was developed for more turbid waters (S. Mishra and Mishra 2012), and the concentrations of microcystins evaluated in this study, as NDCI was not as successful at predicting many blooms over 10 $\mu\text{g/l}$. Despite the diminished performance of NDCI in predicting microcystin levels in this analysis, we recommend future researchers consider this spectral index in their algal bloom monitoring assessments, especially in studies that involve chl-a measurements and low to moderate microcystin concentrations. Furthermore, R^2 values observed in this study may improve by leveraging a more automated model selection and ranking approach to arrive at a best-fit parsimonious multivariate model in which all predictors are significant (Marques Ramos et al. 2020; C. Yang et al. 2019; Calcagno and de Mazancourt 2010). This could entail using a stepwise multiple regression that involves a combination of forward selection and backward elimination to identify significant variables (Olusegun, Dikko, and Gulumbe 2015; Ghani and Ahmad 2010; Zhang 2016). Resulting model performance could be evaluated using the Bayesian information criterion (BIC) and Akaike's information criterion (AIC) (Kuha 2004) to improve the goodness of fit in this study. Results from this research would also likely improve if the FHAB incident reports included chl-a measurements, or if chl-a measurements from other sources such as the National Water Quality Monitoring Council's Water Quality Portal were available for our study period in California (Papenfus et al. 2020), as the Sentinel-2 indices we tested are used to evaluate chl-a and general greenness rather than microcystin.

Overall, Sentinel-2 indices performed fairly well at the lake or reservoir scale across the three indices. We evaluated lakes and reservoirs at the 90th percentile index value, while buffers were evaluated by computing the mean index value of Images 2 and 3 per bloom. The 90th percentile index value may be a better measure of potentially toxic blooms because it identifies the highest pixel values which likely reflect localized regions of high microcystin concentrations, while the average may dilute these values. The B3B2 index did not perform well in this study because the green and blue wavelengths could not distinguish between blooms and non-blooms (Figure 6). Finally, although relationships between microcystin values and spectral index values were stronger at the lake or reservoir scale, the 200 m buffer scale allowed for a greater number of comparisons ($n = 39$ compared to $n = 28$) using Sentinel-2 imagery (Figure 2). This increase in comparisons is because the buffered areas were less frequently impacted by cloud interference and we could therefore derive spectral index values from these satellite images. The buffered areas allowed us to expand our monitoring capacity by nearly 40%, which is helpful particularly during cloudy periods of the year.

4.2. Sentinel-3 Satellite's Ability to Assess FHAB Incident Reports

The Sentinel-3 MCI performed best in Clear Lake and Isabella Lakes when compared to FHAB incident reports because these are large lakes with microcystin data in their reports. Smaller bodies of water including Iron Gate and Hensley Lake also had microcystin data and were large enough to be included in the FHAB Data Viewer, although there were many missing pixels that led to less accurate 90th percentile MCI values. Sentinel-3's coarse resolution was unable to resolve smaller bodies of water ($< 2 \text{ km}^2$) with high microcystin values that Sentinel-2 was able to capture, including Red Lake and Lake Chabot. The FHAB Data Viewer Sentinel-3 satellite imagery analysis is currently available at the lake or reservoir scale, so we therefore did not evaluate blooms at the 200 m buffer scale using Sentinel-3 data. MCI outperformed all of the Sentinel-2 indices in comparison to FHAB microcystin data because of its use of the spectral shape at 681 nm, which can identify chlorophyll-a absorption as a proxy for cyanobacteria biomass (S. Mishra et al. 2019). Other wavelengths that are useful in cyanobacteria identification include 620 nm and 665 nm (S. Mishra et al. 2019), and the Sentinel-2 spectral indices tested in this study do not center on either of these wavelengths. Previous studies have successfully used the Cyanobacteria Index applied to Sentinel-3 Ocean and Land Colour Instrument data to estimate cyanobacteria distributions (Vander Woude et al. 2019; Sharp et al. 2021; Timothy T. Wynne and Stumpf 2015; T. T. Wynne et al. 2008). Finally, in comparison to Sentinel-2 imagery, NDCI had the strongest relationship to microcystin values ($R^2 = 0.18$), although this is relatively low because of the differences in wavelengths used in both indices. Therefore, Sentinel-3 data from the FHAB Viewer can be used with moderate confidence to examine microcystin levels in larger lakes such as Clear Lake and Lake Isabella.

4.3. Implications for Cyanobacteria Monitoring with Satellite Imagery

This study provides the first attempt to integrate two statewide HAB monitoring efforts: the FHAB incident reports and the FHAB Data Viewer. The methods suggested in this study can allow water quality managers to assess potentially toxic blooms at higher spatial scales than currently available. The use of Google Earth Engine provides a rapid assessment of both current and historical blooms across a large study area such as the state of California, and additional time series analyses such as monthly, seasonal, and interannual assessments can be made to further understand particular bloom dynamics. Furthermore, the downscaling of cyanobacteria bloom detection enables water quality managers to locate specific regions within a lake or reservoir to focus sampling efforts and alert recreational users to avoid hazardous areas. The integration of Sentinel-2 imagery into the existing FHAB Data Viewer would expand analysis from 255 to over 14,000 lakes and reservoirs, which would greatly improve our understanding of algal blooms in California.

As other spectral indices and machine-learning algorithms continue to be evaluated for their use in FHAB detection, the potential for high resolution imagery from Sentinel-2 or PlanetScope's 8-band mission to integrate into the existing FHAB Data Viewer will become a closer reality. PlanetScope's 8-band imagery at 3 m spatial resolution includes a new coastal blue, green, yellow, and red-edge band (in addition to pre-existing PlanetScope bands) that could be applicable to algal bloom monitoring, and this mission includes near-daily global coverage since August 2021. Spectral indices such as the Floating Algal Index (Hu 2009; Cao et al. 2021),

Surface Algal Bloom Index (Alawadi 2010), Fluorescence Line Height (Beck et al. 2016), and the Maximum Chlorophyll Index (Pirasteh et al. 2020) can also be explored further and applied to high spatial resolution data like the PlanetScope 8-band imagery. Harmonizing products from PlanetScope, Sentinel-2, and Landsat can result in high spatial (3 m), spectral (including red edge, near-infrared, and shortwave infrared bands), and temporal (daily) (Johansen et al. 2022) imagery for algal bloom monitoring. Incorporating higher-resolution satellite imagery into algal bloom monitoring apps will enable greater pairing with crowdsourced and participatory observations, thereby expanding the number of lakes and reservoirs that are monitored not only within the FHAB Data Viewer but also on other platforms such as CyAN.

Future satellite missions such as Landsat 10, which is proposed to include an orange phycocyanin band, will revolutionize this field by providing greater spatial and spectral resolution to enable cyanobacteria detection in concert with in situ analysis. However, while phycocyanin identification through Sentinel-3 and the proposed Landsat 10 sensors can detect cyanobacteria, this type of data cannot determine whether the identified cyanobacteria will create microcystins or other cyanotoxins. Therefore, hyperspectral imagery at high spatial resolutions, such as an upgraded version of the International Space Station's Hyperspectral Imager for the Coastal Ocean, will allow detection to the level of cyanobacteria genera that will enable a better understanding of the potential toxins produced (Dierssen et al. 2020; Wolny et al. 2020). Integration of these higher spatial and spectral resolution missions into the existing FHAB Data Viewer will allow for greater mitigation of toxic bloom events in a variety of lakes and reservoirs throughout California, thereby reducing the risk of illness and mortality for humans and animals such as dogs and cattle that reside and recreate around these waters.

5. Conclusions

This study demonstrates how high resolution satellite imagery can be used to fill in the gaps of two very useful and different FHAB datasets within the state of California. Improving the spatial capabilities of algal bloom detection in conjunction with on-the-ground bloom reporting will expand the ability to rapidly monitor and manage potentially dangerous public health events. Although there remains a spectral mismatch between incident reports of smaller lakes and reservoirs and high resolution satellite imagery bloom detection, we can use indices such as NDVI to monitor a majority of blooms with high levels of microcystin ($> 100 \mu\text{g/l}$) at the 200 m buffer scale. Furthermore, the use of Google Earth Engine in this study provides an efficient, cost-effective, and widespread methodology for assessing algal blooms across California, promoting the ultimate goal of creating accurate, near-real time alerts of algal blooms within the state. The current FHAB data resources in California are incredibly helpful in reducing the exposure of humans and animals to toxic algal blooms using crowdsourced and participatory data. High spatial resolution imagery will broaden satellite detection capacity of lakes and reservoirs by nearly 55 times within the state of California, and methods from this study can be adapted to help water quality managers, dog owners, and swimmers stay safe from potentially toxic blooms in water bodies throughout the world.

Chapter 5: Lessons Learned and Future Directions of High-Resolution Remote Sensing of Algal Blooms

Freshwater algal blooms, both harmful and non-harmful, are important topics of study within the remote sensing community. Whether it is to evaluate the spatial distribution of filamentous algae in riverine ecosystems or the potentially toxic algae in reservoirs and lakes, it is vital to be able to map the spatial and temporal characteristics of such blooms. Rivers are the main arteries in freshwater ecosystems, transporting nutrients, gasses, water, and aquatic life to the ocean (Meybeck 2003), and lakes and reservoirs are vital because they store most of Earth's liquid surface freshwater (Gao 2015). We want to preserve and manage these environments not only for their ecological value but also for their ecosystem services such as transport of goods, irrigation supply, and recreational opportunities (Daily 2012). Remotely sensed methods to monitor freshwater harmful algal blooms in rivers, lakes, and reservoirs have involved red-green-blue (RGB), multispectral, and hyperspectral sensors on UAVs, airplanes, and satellites over the past several decades. This dissertation examined algae and aquatic plants in a non-wadeable river using a drone (Chapter 2: Application of UAV Imagery to Detect and Quantify Submerged Filamentous Algae and Rooted Macrophytes in a Non-Wadeable River), algal bloom dynamics in two reservoirs using Sentinel-2 satellite imagery (Chapter 3: Mapping Algal Bloom Dynamics in Small Reservoirs using Sentinel-2 Imagery in Google Earth Engine), and compared two statewide datasets of freshwater harmful algal blooms in California using Sentinel-2 data (Chapter 4: Integrating Crowdsourced Incident Reports with Satellite Imagery to Understand Algal Blooms in California Lakes and Reservoirs). This work investigated both “good” and “bad” algae in various freshwater environments of California using high-resolution imagery to understand how algal dynamics differ across landscapes, bodies of water, seasons, and years. Here I discuss the primary results, lessons learned, challenges, and future areas of research for improved management of algal bloom remote sensing.

There are many lessons learned throughout this dissertation. Chapter 2 taught me that there is a greater distribution of aquatic plants than filamentous algae just below the most downstream dam of the Klamath River, Iron Gate, and there is a greater distribution of filamentous algae than aquatic plants closer to the Pacific Ocean within this body of water. I learned lessons about collecting quality UAV data. For example, flying a drone in the morning (between about 10 and 11:30 am during the summer months in mid-latitude regions) helped reduce solar glare and made it possible to capture the best images over water. I was able to detect algae down to nearly 2 m under the surface of the water in a clear portion of the Klamath River, which provides promising evidence for benthic algal surveys in deep rivers. In terms of algal bloom classification, I found that pixel-based supervised classification worked better than object-based image analysis and unsupervised classification when using drone imagery. Chapter 3 demonstrated that the highest concentration of chl-a and microcystin toxins detected in Copco and Iron Gate Reservoirs from 2015 to 2020 occurred during wet years, particularly in August 2019, likely due to nutrient influx from runoff during these wet years. The Normalized Difference Vegetation Index (NDVI) and the Normalized Difference Chlorophyll Index (NDCI) were the best spectral indices applied to Sentinel-2 imagery for surface bloom detection in this study. Chapter 4 demonstrated that crowdsourced reports of freshwater blooms in lakes and reservoirs have been increasing throughout California since 2019, with the majority of blooms occurring in August and September. About 30% of these reported blooms contain microcystin

toxins at the Warning (6 $\mu\text{g}/\text{l}$ microcystins) and Danger (20 $\mu\text{g}/\text{l}$ microcystins) bloom advisory levels and Sentinel-3 imagery is moderately successful at capturing these toxic blooms in larger ($> 2 \text{ km}^2$) lakes and reservoirs. ArcGIS Pro, R, and Python in a Jupyter Notebook were efficient tools to process drone and satellite imagery in each of these studies, and Google Earth Engine was the favored tool among all projects because it enabled rapid time series analyses for multiple years of satellite imagery, eliminated the time needed to back up data, and did not require the storage of hundreds of gigabytes of satellite data on a harddrive. Scale was a prominent theme throughout this dissertation. UAV imagery was able to resolve features within centimeters, while Sentinel-2 and 3 imagery was limited to between 10 and 300 m per pixel. I recommend using drone imagery for studies that require the democratization of data (choosing when to fly and how close to fly to the target, thereby selecting the spatial resolution), with the caveat that drone image processing can be more cumbersome and storage-heavy than the cloud computing of satellite imagery collections available on Google Earth Engine (such as Landsat, Sentinel-2, and Sentinel-3). I recommend processing satellite imagery in Google Earth Engine when more than 10 images are involved, otherwise ArcGIS Pro (and the Planet ArcGIS Pro Add-In v2.2) are great for this endeavor.

The biggest challenges observed throughout this dissertation involved solar glint, clouds, and resolution limitations. In Chapter 2, it proved difficult to stitch images over homogeneous scenes of water, so I chose to capture individual images with the drone and process them separately instead of building mosaicked images. I also found it more difficult to obtain clear imagery over a fast-moving river than over lakes and reservoirs because of the ripples, currents, and impacts of wind on the water's surface. The biggest limitations in Chapter 3 involved the temporal mismatch between in situ water quality observations, which were monthly, and cloud-free Sentinel-2 images within five days of the sample. Although the five-day time difference did not negatively impact results as I had anticipated, I recommend finding imagery that coincides with as close to the sampling date as possible. In Chapters 3 and 4, I discussed how Sentinel-2 imagery, and even Sentinel-3 imagery, cannot identify algal species and therefore cannot determine the toxicity of a bloom. These are limitations inherent to the sensors themselves, and improvements in the spectral properties of future sensors can help resolve this issue.

A final limitation concerns the likelihood of inaccurate landscape representations and spectral noise in the satellite imagery. Pixels located on the edges of an image or land cover category can present reflectance value artifacts which may alter the validity of the satellite-derived data. Differences in pixel brightness, including within mixed pixels, can create false positives for algal bloom detection, although they sometimes can be detected and removed using the NIR and red-edge wavelengths (S. Mishra et al. 2019). Additionally, certain atmospheric correction algorithms, such as iCOR, can account for adjacency effect issues, or the influence of neighboring pixels on a given pixel's spectral value, for Sentinel-2 imagery and have been proven to succeed in inland aquatic environments (Cillero Castro et al. 2020). Fortunately, edge effect and land adjacency issues did not pose large concerns in our studies because satellite data were captured in small regions that did not overlap with pixel values from adjacent bridges, shorelines, or image edges. Addressing these challenges and considering future directions of research in this field will enable more precise algal bloom monitoring in rivers, lakes, and reservoirs, also helping us achieve several of the United Nations' Sustainable Development Goals (L. T. Ho and Goethals 2019).

The first future direction proposed for algal bloom investigations involves *improved spectral resolution* to gain greater information on the algal genus and potential toxin production of each bloom. Hyperspectral imaging offers large advantages to multispectral mapping of algal blooms because instead of analyzing several broad wavelengths, researchers can derive specific phytoplankton group information from hundreds of narrow wavelengths. Several hyperspectral satellite sensors that have been used in this field include Hyperion, the Compact High Resolution Imaging Spectrometer (CHRIS), and Hyperspectral Imager for the Coastal Ocean (HICO) (Shen, Xu, and Guo 2012; Kutser 2009), although these missions are not always sensitive to aquatic environments (Dierssen et al. 2020). The National Aeronautics and Space Administration (NASA)'s planned launch of the Pre-Aerosol Clouds and Ocean Ecosystem (PACE) sensors will provide greater spectral resolution, with 90 bands ranging from 350 to 800 nm (Kudela et al. 2015). Other hyperspectral missions that may be useful for algal bloom monitoring include Sentinel 5's TROPOspheric Monitoring Instrument (TROPOMI), The University of Tokyo, Japan's Picosatellite for Remote-sensing and Innovative Space Missions (PRISMA), the German Environmental Mapping and Analysis Program (EnMAP), the European Space Agency's Copernicus Hyperspectral Imaging Mission for the Environment (CHIME), and NASA's Surface Biology and Geology mission (SBG), previously known as HypIRI (Dierssen et al. 2020). Dierssen et al. proposes a hyperspectral database to track algal diversity across the world that includes standardized correction algorithms, in situ data, aerial imagery, algal taxa, water quality parameters, and metadata information (Dierssen et al. 2020). This type of database, perhaps similar to the open-sourced OpenAerialMap (<https://openaerialmap.org/>) database for UAV imagery, would revolutionize the ability to access high spectral and spatial data for blooms across the globe.

The second future direction of freshwater algal bloom monitoring involves strengthening our *understanding of the causes of blooms*, especially for toxic algae. While we know that most algae respond positively to increased temperatures and irradiance, water column stratification, and nitrogen, phosphorus, and silicate availability, we still do not fully understand why toxins are expressed in certain species and at specific times (D. M. Anderson, Cembella, and Hallegraeff 2012). Furthermore, we do not understand how different stages of toxicity during an algal bloom affect trophic cascades within aquatic food webs (Berdalet et al. 2014). It is important to grasp why specific algal bloom groups (i.e. cyanobacteria, diatoms) have variable responses in terms of nutrient inputs and toxin production in different environments across the world (Elser, Marzolf, and Goldman 1990). The impacts of grazing and predation on algae also need further exploration, as these dynamics have been shown to alter relationships between algal proliferation, depending on the season (X.-L. Wang et al. 2007). Methods that could improve this inquiry include dynamic factor analysis (Zuur, Tuck, and Bailey 2003) applied to high-resolution imagery of algal blooms to explore relationships between chl-a or bloom toxin data and factors such as nutrients, water temperature, and water residence times. Another statistical technique that has been developed to analyze aquatic time series data is the Multivariate Autoregressive Space-State (MARSS) model, which has been applied to systems including fisheries (Nally et al. 2010; Hampton et al. 2013), freshwater phytoplankton communities (Scheef et al. 2012), and turtle migration (Holmes, Ward, and Wills 2012). This technique is helpful in analyzing ecological time series data to discern species' interactions and responses to human influences and environmental drivers (Hampton et al. 2013), and thus it can be used to understand factors that contribute to freshwater HAB events. With improved covariate and variate data to ascertain

causes of blooms, freshwater algal bloom research can help water quality managers understand why proliferations occur to better monitor and predict future events.

My final recommended future direction is the promotion of *freshwater algal bloom forecasting*. State-of-the-art modeling of future blooms involves estimating water residence times, nutrient inputs, chl-a concentrations, currents, and weather patterns (Janssen et al. 2019; Stauffer et al. 2019). One existing algal bloom forecasting tool is the California-Harmful Algae RiskMapping program (CHARM), which provides near-real time 3 km forecasts of *Pseudo-nitzschia* spp. blooms and potential for a toxin called domoic acid along the California coast (C. R. Anderson et al. 2016). However, many algal bloom forecasting tools are developed for marine environments because they can be paired with oceanic models and satellite missions that are designed for large-scale marine analysis. Future research should involve a greater focus on freshwater algal bloom alert systems. Also, freshwater data involving nutrient loads, water temperatures, and residence times are infrequently collected due to financial and time constraints inherent to in situ data acquisition (Kroeze et al. 2016; Fink et al. 2018). Therefore, remotely-sensed products that can estimate these parameters at relatively high spatial and temporal scales would vastly improve the ability to forecast these blooms. Furthermore, tools that leverage online cloud computing such as Google Earth Engine would enable these predictions to be near-real time. Machine-learning algorithms used within these environments, such as support vector machines, random forest, and artificial neural networks, would also increase the detection capabilities of forecasted models (R. C. Cruz et al. 2021). The ability to more accurately predict blooms and potentially toxic occurrences will open the door to greater collaboration with agriculturists who may be adding nutrients into the water system during critical algal proliferation periods. Improved forecasts will also impact regulatory policies such as Total Maximum Daily Loads (TMDLs), which are designed to limit the total pollutants that enter impaired waters as defined by the Clean Water Act (Karr James R. and Yoder Chris O. 2004). Finally, near-real time forecasts will help communicate to the public when water quality may be dangerous, reducing illnesses and even death by decreasing exposure to toxic blooms.

In conclusion, the remote sensing of algal blooms has drastically improved with the inclusion of higher spectral, spatial, and temporal sensors on UAVs, airplanes, and satellites. In particular, hyperspectral sensors allow for more accurate detection to the genus level, which gets closer to identifying toxin-producing species. Gaining a greater understanding of the factors that contribute to blooms helps us interpret and predict future blooms for more informed management. As climate change and industrial farming are projected to contribute to greater freshwater algal growth with warming waters, lower oxygen levels, and higher terrestrial and atmospheric nutrient additions (Gobler 2020; Glibert 2020), it is imperative that methods to monitor these events become more frequent and accurate. Methods tested in this dissertation can be implemented at local, state, and national levels to integrate into the management of algal species, fisheries, nutrient inputs, shoreline erosion, and recreational activities (L. T. Ho and Goethals 2019). Increased resolution in freshwater bloom monitoring has implications in dam removal restoration efforts, reducing public health risks, and protecting our drinking and irrigation water from potential poisons in rivers, lakes, and reservoirs across the globe.

References

- Abati, Silverio, Maria Rita Minciardi, Simone Ciadamidaro, Simone Fattorini, and Simona Ceschin. 2016. "Response of Macrophyte Communities to Flow Regulation in Mountain Streams." *Environmental Monitoring and Assessment*.
<https://doi.org/10.1007/s10661-016-5420-2>.
- Aguirre-Gómez, R., O. Salmerón-García, G. Gómez-Rodríguez, and A. Peralta-Higuera. 2017. "Use of Unmanned Aerial Vehicles and Remote Sensors in Urban Lakes Studies in Mexico." *International Journal of Remote Sensing* 38 (8-10): 2771–79.
- Ahmad, Asmala, and Shaun Quegan. 2013. "Comparative Analysis of Supervised and Unsupervised Classification on Multispectral Data." *Applied Mathematical Sciences* 7 (74): 3681–94.
- Alawadi, F. 2010. "Detection of Surface Algal Blooms Using the Newly Developed Algorithm Surface Algal Bloom Index (SABI)." *Remote Sensing of the Ocean, Sea Ice, and Large*.
https://www.spiedigitallibrary.org/conference-proceedings-of-spie/7825/782506/Detection-of-surface-algal-blooms-using-the-newly-developed/10.1117/12.862096.short?casa_token=31BwWn03zRAAAAAA:qa9_4LSZiAB16C-yoWjBZ7vz-t-bXPxnDfMr5BhiB1hAzlL2p0GMHEvBXP2Y7ZDqOmxJIIT07w.
- Alcântara, Enner, Fernanda Watanabe, Thanan Rodrigues, and Nariane Bernardo. 2016. "An Investigation into the Phytoplankton Package Effect on the Chlorophyll-a Specific Absorption Coefficient in Barra Bonita Reservoir, Brazil." *Remote Sensing Letters* 7 (8): 761–70.
- Algal Ecology: Freshwater Benthic Ecosystem*. 1996. Academic Press.
- Allen, David N. 2010. "The Klamath Hydroelectric Settlement Agreement: Federal Law, Local Compromise, and the Largest Dam Removal Project in History." *Hastings W. -Nw. J. Env't'l L. & Pol'y* 16: 427.
- Ambrose-Igho, Gare, Wondwosen M. Seyoum, William L. Perry, and Catherine M. O'Reilly. 2021. "Spatiotemporal Analysis of Water Quality Indicators in Small Lakes Using Sentinel-2 Satellite Data: Lake Bloomington and Evergreen Lake, Central Illinois, USA." *Environmental Processes* 8 (2): 637–60.
- Anderson, Clarissa R., Raphael M. Kudela, Mati Kahru, Yi Chao, Leslie K. Rosenfeld, Frederick L. Bahr, David M. Anderson, and Tenaya A. Norris. 2016. "Initial Skill Assessment of the California Harmful Algae Risk Mapping (C-HARM) System." *Harmful Algae* 59 (November): 1–18.
- Anderson, Donald M. 2009. "Approaches to Monitoring, Control and Management of Harmful Algal Blooms (HABs)." *Ocean & Coastal Management* 52 (7): 342.
- Anderson, Donald M., Allan D. Cembella, and Gustaaf M. Hallegraeff. 2012. "Progress in Understanding Harmful Algal Blooms: Paradigm Shifts and New Technologies for Research, Monitoring, and Management." *Annual Review of Marine Science* 4: 143–76.
- Anderson, Donald M., Elizabeth Fensin, Christopher J. Gobler, Alicia E. Hoeglund, Katherine A. Hubbard, David M. Kulis, Jan H. Landsberg, et al. 2021. "Marine Harmful Algal Blooms (HABs) in the United States: History, Current Status and Future Trends." *Harmful Algae* 102 (February): 101975.
- Anderson, Donald M., Patricia M. Glibert, and Joann M. Burkholder. 2002. "Harmful Algal Blooms and Eutrophication: Nutrient Sources, Composition, and Consequences." *Estuaries* 25 (4): 704–26.

- Andrew Lyons and the R Development Core Team. 2020. "Uasing: Drone Images Utilities." *R Package Version 1.3.4*. <https://github.com/ucaer-igis/uasing>.
- Ansdell, Vernon. 2019. "49 - Seafood Poisoning." In *Travel Medicine (Fourth Edition)*, edited by Jay S. Keystone, Phyllis E. Kozarsky, Bradley A. Connor, Hans D. Nothdurft, Marc Mendelson, and Karin Leder, 449–56. London: Elsevier.
- Ansper, Ave, and Krista Alikas. 2018. "Retrieval of Chlorophyll a from Sentinel-2 MSI Data for the European Union Water Framework Directive Reporting Purposes." *Remote Sensing* 11 (1): 64.
- Anyamba, A., C. J. Tucker, and J. R. Eastman. 2001. "NDVI Anomaly Patterns over Africa during the 1997/98 ENSO Warm Event." *International Journal of Remote Sensing* 22 (10): 1847–60.
- Asarian, E., and J. Kann. 2011. "Phytoplankton and Nutrient Dynamics in Iron Gate and Copco Reservoirs 2005- 2010." Prepared by Kier Associates and Aquatic Ecosystem Sciences for the Klamath Basin Tribal Water Quality Work Group.
- Asarian, E., Kann, J. and W. Walker. 2009. "Multi-Year Nutrient Budget Dynamics for Iron Gate and Copco Reservoirs, California." Prepared by Riverbend Sciences, Kier Associates, Aquatic Ecosystem Sciences, and William Walker for the Karuk Tribe Department of Natural Resources, Orleans, CA.
- Asarian, J. Eli, Yangdong Pan, Nadia D. Gillett, and Jacob Kann. 2014. "Spatial and Temporal Variation of Periphyton Assemblages in the Klamath River 2004-2012." *Prepared by Kier Associates, Portland State University, and Aquatic Ecosystem Sciences LLC. for the Klamath Basin Tribal Water Quality Work Group. 50p. + Appendices.* https://www.researchgate.net/profile/J_Asarian/publication/272788109_Spatial_and_temporal_variation_of_periphyton_assemblages_in_the_Klamath_River_2004-2012/links/5eb032c845851592d6b880e8/Spatial-and-temporal-variation-of-periphyton-assemblages-in-the-Klamath-River-2004-2012.pdf.
- Backer, Lorraine C. 2002. "Cyanobacterial Harmful Algal Blooms (CyanoHABs): Developing a Public Health Response." *Lake and Reservoir Management* 18 (1): 20–31.
- Backer, Lorraine C., Jan H. Landsberg, Melissa Miller, Kevin Keel, and Tegwin K. Taylor. 2013. "Canine Cyanotoxin Poisonings in the United States (1920s–2012): Review of Suspected and Confirmed Cases from Three Data Sources." *Toxins* 5 (9): 1597–1628.
- Bakker, E. S., E. Van Donk, S. A. J. Declerck, N. R. Helmsing, B. Hidding, and B. A. Nolet. 2010. "Effect of Macrophyte Community Composition and Nutrient Enrichment on Plant Biomass and Algal Blooms." *Basic and Applied Ecology* 11 (5): 432–39.
- Bandini, Filippo, Jakob Jakobsen, Daniel Olesen, Jose Antonio Reyna-Gutierrez, and Peter Bauer-Gottwein. 2017. "Measuring Water Level in Rivers and Lakes from Lightweight Unmanned Aerial Vehicles." *Journal of Hydrology* 548 (May): 237–50.
- Banish, Nicholas J. 2017. "Factors Influencing Cladophora Biomass Abundance in the Upper Clark Fork River, Montana." <https://scholarworks.umt.edu/cgi/viewcontent.cgi?article=12162&context=etd>.
- Bartholow, John M., Sharon G. Campbell, and Marshall Flug. 2004. "Predicting the Thermal Effects of Dam Removal on the Klamath River." *Environmental Management* 34 (6): 856–74.
- Bates, S. S., D. J. Douglas, G. J. Doucette, and C. Léger. 1995. "Enhancement of Domoic Acid Production by Reintroducing Bacteria to Axenic Cultures of the Diatom Pseudo-Nitzschia Multiseriis." *Natural Toxins* 3 (6): 428–35.

- Bates, Stephen S., Jonathan Gaudet, Irena Kaczmarek, and James M. Ehrman. 2004. "Interaction between Bacteria and the Domoic-Acid-Producing Diatom Pseudo-Nitzschia Multiseriata (Hasle) Hasle; Can Bacteria Produce Domoic Acid Autonomously?" *Harmful Algae*. <https://doi.org/10.1016/j.hal.2003.08.001>.
- Beaver, John R., David E. Jensen, Dale A. Casamatta, Claudia E. Tausz, Kyle C. Scotese, Kristen M. Buccier, Catherine E. Teacher, Teodoro C. Rosati, Alison D. Minerovic, and Thomas R. Renicker. 2013. "Response of Phytoplankton and Zooplankton Communities in Six Reservoirs of the Middle Missouri River (USA) to Drought Conditions and a Major Flood Event." *Hydrobiologia* 705 (1): 173–89.
- Becker, Richard H., Michael Sayers, Dustin Dehm, Robert Shuchman, Kaydian Quintero, Karl Bosse, and Reid Sawtell. 2019. "Unmanned Aerial System Based Spectroradiometer for Monitoring Harmful Algal Blooms: A New Paradigm in Water Quality Monitoring." *Journal of Great Lakes Research* 45 (3): 444–53.
- Beck, Richard, Min Xu, Shengan Zhan, Hongxing Liu, Richard Johansen, Susanna Tong, Bo Yang, et al. 2017. "Comparison of Satellite Reflectance Algorithms for Estimating Phycocyanin Values and Cyanobacterial Total Biovolume in a Temperate Reservoir Using Coincident Hyperspectral Aircraft Imagery and Dense Coincident Surface Observations." *Remote Sensing*. <https://doi.org/10.3390/rs9060538>.
- Beck, Richard, Shengan Zhan, Hongxing Liu, Susanna Tong, Bo Yang, Min Xu, Zhaoxia Ye, et al. 2016. "Comparison of Satellite Reflectance Algorithms for Estimating Chlorophyll-a in a Temperate Reservoir Using Coincident Hyperspectral Aircraft Imagery and Dense Coincident Surface Observations." *Remote Sensing of Environment* 178 (June): 15–30.
- Beijbom, Oscar, Peter J. Edmunds, Chris Roelfsema, Jennifer Smith, David I. Kline, Benjamin P. Neal, Matthew J. Dunlap, et al. 2015. "Towards Automated Annotation of Benthic Survey Images: Variability of Human Experts and Operational Modes of Automation." *PloS One* 10 (7): e0130312.
- Bellmore, J. Ryan, George R. Pess, Jeffrey J. Duda, Jim E. O'Connor, Amy E. East, Melissa M. Foley, Andrew C. Wilcox, et al. 2019. "Conceptualizing Ecological Responses to Dam Removal: If You Remove It, What's to Come?" *Bioscience* 69 (1): 26–39.
- Benavides, Martin T., F. Joel Fodrie, and David W. Johnston. 2020. "Shark Detection Probability from Aerial Drone Surveys within a Temperate Estuary." *Journal of Unmanned Vehicle Systems* 8 (1): 44–56.
- Benediktsson, Jon Atli, Jocelyn Chanussot, and Mathieu Fauvel. 2007. "Multiple Classifier Systems in Remote Sensing: From Basics to Recent Developments." In *Multiple Classifier Systems*, 501–12. Springer Berlin Heidelberg.
- Berdalet, E., M. A. McManus, O. N. Ross, H. Burchard, F. P. Chavez, J. S. Jaffe, I. R. Jenkinson, et al. 2014. "Understanding Harmful Algae in Stratified Systems: Review of Progress and Future Directions." *Deep-Sea Research. Part II, Topical Studies in Oceanography* 101 (March): 4–20.
- Biggs, Barry J. F. 1996. "Patterns in Benthic Algae of Streams." *Algal Ecology: Freshwater Benthic Ecosystems*, 31–56.
- . 2000. "Eutrophication of Streams and Rivers: Dissolved Nutrient-Chlorophyll Relationships for Benthic Algae." *Journal of the North American Benthological Society* 19 (1): 17–31.
- Biggs, B. J., and Cathy Kilroy. 2000. *Stream Periphyton Monitoring Manual*. Niwa.
- Binding, C. E., T. A. Greenberg, G. McCullough, S. B. Watson, and E. Page. 2018. "An Analysis

- of Satellite-Derived Chlorophyll and Algal Bloom Indices on Lake Winnipeg.” *Journal of Great Lakes Research* 44 (3): 436–46.
- Blinn, Dean W., Joseph P. Shannon, Peggy L. Benenati, and Kevin P. Wilson. 1998. “Algal Ecology in Tailwater Stream Communities: The Colorado River below Glen Canyon Dam, Arizona.” *Journal of Phycology* 34 (5): 734–40.
- Blondeau-Patissier, David, James F. R. Gower, Arnold G. Dekker, Stuart R. Phinn, and Vittorio E. Brando. 2014. “A Review of Ocean Color Remote Sensing Methods and Statistical Techniques for the Detection, Mapping and Analysis of Phytoplankton Blooms in Coastal and Open Oceans.” *Progress in Oceanography* 123 (April): 123–44.
- Bollard-Breen, Barbara, John D. Brooks, Matthew R. L. Jones, John Robertson, Sonja Betschart, Olivier Kung, S. Craig Cary, Charles K. Lee, and Stephen B. Pointing. 2015. “Application of an Unmanned Aerial Vehicle in Spatial Mapping of Terrestrial Biology and Human Disturbance in the McMurdo Dry Valleys, East Antarctica.” *Polar Biology* 38 (4): 573–78.
- Boon, M. A., A. P. Drijfhout, and Solomon Tesfamichael. 2017. “Comparison of a Fixed-Wing and Multi-Rotor Uav for Environmental Mapping Applications: A Case Study.” *The International Archives of Photogrammetry, Remote Sensing and Spatial Information Sciences* 42: 47.
- Boyer, Gregory L., Mary C. Watzin, Angela D. Shambaugh, Michael F. Satchwell, Barry H. Rosen, and Timothy Mihuc. 2004. “The Occurrence of Cyanobacterial Toxins in Lake Champlain.” In *Lake Champlain: Partnerships and Research in the New Millennium*, 241–57. Springer US.
- Bozarth, Connie S., Andrew D. Schwartz, Jonathan W. Shepardson, Frederick S. Colwell, and Theo W. Dreher. 2010. “Population Turnover in a Microcystis Bloom Results in Predominantly Nontoxic Variants Late in the Season.” *Applied and Environmental Microbiology* 76 (15): 5207–13.
- Bramich, James, Christopher J. S. Bolch, and Andrew Fischer. 2021. “Improved Red-Edge Chlorophyll-a Detection for Sentinel 2.” *Ecological Indicators* 120 (January): 106876.
- Bresciani, M., I. Cazzaniga, M. Austoni, T. Sforzi, F. Buzzi, G. Morabito, and C. Giardino. 2018. “Mapping Phytoplankton Blooms in Deep Subalpine Lakes from Sentinel-2A and Landsat-8.” *Hydrobiologia* 824 (1): 197–214.
- Brinkhoff, James, John Hornbuckle, and Jan L. Barton. 2018. “Assessment of Aquatic Weed in Irrigation Channels Using UAV and Satellite Imagery.” *WATER* 10 (11): 1497.
- Brooks, B. W., J. M. Lazorchak, and M. D. A. Howard. 2016. “Are Harmful Algal Blooms Becoming the Greatest Inland Water Quality Threat to Public Health and Aquatic Ecosystems?” *The Environmentalist*.
[https://setac.onlinelibrary.wiley.com/doi/abs/10.1002/etc.3220@10.1002/\(ISSN\)1552-8618.FOCUS?casa_token=Yr1RtIMLqhgAAAAA:AiRvCCDUz9s1hboUsyI7qE_TXH6YuvKRSED1Ec6m2Ksp-Eo3FPYhrMpUiyWocqfnqHGybQtcNBhnZ0M](https://setac.onlinelibrary.wiley.com/doi/abs/10.1002/etc.3220@10.1002/(ISSN)1552-8618.FOCUS?casa_token=Yr1RtIMLqhgAAAAA:AiRvCCDUz9s1hboUsyI7qE_TXH6YuvKRSED1Ec6m2Ksp-Eo3FPYhrMpUiyWocqfnqHGybQtcNBhnZ0M).
- Brooks, Colin N., Amanda G. Grimm, Amy M. Marcarelli, and Richard J. Dobson. 2019. “Multiscale Collection and Analysis of Submerged Aquatic Vegetation Spectral Profiles for Eurasian Watermilfoil Detection.” *Journal of Applied Remote Sensing* 13 (3): 037501.
- Bunn, S. E., E. G. Abal, M. J. Smith, S. C. Choy, C. S. Fellows, B. D. Harch, M. J. Kennard, and F. Sheldon. 2010. “Integration of Science and Monitoring of River Ecosystem Health to Guide Investments in Catchment Protection and Rehabilitation.” *Freshwater Biology* 55 (January): 223–40.
- Caballero, Isabel, Raúl Fernández, Oscar Moreno Escalante, Luz Mamán, and Gabriel Navarro.

2020. “New Capabilities of Sentinel-2A/B Satellites Combined with in Situ Data for Monitoring Small Harmful Algal Blooms in Complex Coastal Waters.” *Scientific Reports* 10 (1): 8743.
- Caballero, Isabel, and Richard P. Stumpf. 2020. “Towards Routine Mapping of Shallow Bathymetry in Environments with Variable Turbidity: Contribution of Sentinel-2A/B Satellites Mission.” *Remote Sensing* 12 (3): 451.
- Calcagno, Vincent, and Claire de Mazancourt. 2010. “Glmulti: An R Package for Easy Automated Model Selection with (generalized) Linear Models.” *Journal of Statistical Software* 34 (12): 1–29.
- Cao, Mengmeng, Song Qing, Eerdemutu Jin, Yanling Hao, and Wenjing Zhao. 2021. “A Spectral Index for the Detection of Algal Blooms Using Sentinel-2 Multispectral Instrument (MSI) Imagery: A Case Study of Hulun Lake, China.” *International Journal of Remote Sensing* 42 (12): 4514–35.
- Carmichael, Wayne. 2008. “A World Overview — One-Hundred-Twenty-Seven Years of Research on Toxic Cyanobacteria — Where Do We Go from Here?” *Advances in Experimental Medicine and Biology*. https://doi.org/10.1007/978-0-387-75865-7_4.
- Carmichael, W. W. 1992. “Cyanobacteria Secondary Metabolites--the Cyanotoxins.” *The Journal of Applied Bacteriology* 72 (6): 445–59.
- Carpenter, Stephen R., and David M. Lodge. 1986. “Effects of Submersed Macrophytes on Ecosystem Processes.” *Aquatic Botany* 26 (January): 341–70.
- Chabot, Dominique, Christopher Dillon, Oumer Ahmed, and Adam Shemrock. 2017. “Object-Based Analysis of UAS Imagery to Map Emergent and Submerged Invasive Aquatic Vegetation: A Case Study.” *Journal of Unmanned Vehicle Systems* 5 (1): 27–33.
- Chan, Cheong-Xin, Chai-Ling Ho, and Siew-Moi Phang. 2006. “Trends in Seaweed Research.” *Trends in Plant Science* 11 (4): 165–66.
- Chang, K-W, Y. Shen, and P-C Chen. 2004. “Predicting Algal Bloom in the Techi Reservoir Using Landsat TM Data.” *International Journal of Remote Sensing* 25 (17): 3411–22.
- Chapman, Russell Leonard. 2013. “Algae: The World’s Most Important ‘plants’—an Introduction.” *Mitigation and Adaptation Strategies for Global Change*. <https://doi.org/10.1007/s11027-010-9255-9>.
- Chorus, I., I. R. Falconer, H. J. Salas, and J. Bartram. 2000. “Health Risks Caused by Freshwater Cyanobacteria in Recreational Waters.” *Journal of Toxicology and Environmental Health. Part B, Critical Reviews* 3 (4): 323–47.
- Cillero Castro, Carmen, Jose Antonio Domínguez Gómez, Jordi Delgado Martín, Boris Alejandro Hinojo Sánchez, Jose Luis Cereijo Arango, Federico Andrés Cheda Tuya, and Ramon Díaz-Varela. 2020. “An UAV and Satellite Multispectral Data Approach to Monitor Water Quality in Small Reservoirs.” *Remote Sensing* 12 (9): 1514.
- Clark, John M., Blake A. Schaeffer, John A. Darling, Erin A. Urquhart, John M. Johnston, Amber R. Ignatius, Mark H. Myer, Keith A. Loftin, P. Jeremy Werdell, and Richard P. Stumpf. 2017. “Satellite Monitoring of Cyanobacterial Harmful Algal Bloom Frequency in Recreational Waters and Drinking Water Sources.” *Ecological Indicators* 80 (September): 84–95.
- Cloern, James E. 1996. “Phytoplankton Bloom Dynamics in Coastal Ecosystems: A Review with Some General Lessons from Sustained Investigation of San Francisco Bay, California.” *Reviews of Geophysics*. <https://doi.org/10.1029/96rg00986>.
- Coffer, Megan M., Blake A. Schaeffer, John A. Darling, Erin A. Urquhart, and Wilson B. Salls.

2020. “Quantifying National and Regional Cyanobacterial Occurrence in US Lakes Using Satellite Remote Sensing.” *Ecological Indicators* 111 (April): 105976.
- Coffer, Megan M., Blake A. Schaeffer, Wilson B. Salls, Erin Urquhart, Keith A. Loftin, Richard P. Stumpf, P. Jeremy Werdell, and John A. Darling. 2021. “Satellite Remote Sensing to Assess Cyanobacterial Bloom Frequency across the United States at Multiple Spatial Scales.” *Ecological Indicators* 128 (September): 107822.
- Core Team, Rctr, and Others. 2013. “R: A Language and Environment for Statistical Computing.” *R Foundation for Statistical Computing, Vienna*.
- Crisci, C., B. Ghattas, and G. Perera. 2012. “A Review of Supervised Machine Learning Algorithms and Their Applications to Ecological Data.” *Ecological Modelling* 240 (August): 113–22.
- Cruz, Armah de la, Rachael Logsdon, Dennis Lye, Stefania Guglielmi, Alexis Rice, and Miriam Steinitz Kannan. 2017. “Harmful Algae Bloom Occurrence in Urban Ponds: Relationship of Toxin Levels with Cell Density and Species Composition.” *Journal of Earth Sciences and Environment* 25 (November): 704–26.
- Cruz, Rafaela C., Pedro Reis Costa, Susana Vinga, Ludwig Krippahl, and Marta B. Lopes. 2021. “A Review of Recent Machine Learning Advances for Forecasting Harmful Algal Blooms and Shellfish Contamination.” *Journal of Marine Science and Engineering* 9 (3): 283.
- Daily, Gretchen Cara. 2012. *Nature's Services: Societal Dependence On Natural Ecosystems*. Island Press.
- Dalu, Tatenda, and Ryan J. Wasserman. 2018. “Cyanobacteria Dynamics in a Small Tropical Reservoir: Understanding Spatio-Temporal Variability and Influence of Environmental Variables.” *The Science of the Total Environment* 643 (December): 835–41.
- Davidson, Keith, Richard J. Gowen, Paul J. Harrison, Lora E. Fleming, Porter Hoagland, and Grigorios Moschonas. 2014. “Anthropogenic Nutrients and Harmful Algae in Coastal Waters.” *Journal of Environmental Management* 146 (December): 206–16.
- Deas, Michael, and Jennifer Vaughn. 2006. “Characterization of Organic Matter Fate and Transport in the Klamath River below Link Dam to Assess Treatment/reduction Potential.” *Inc. Davis, CA*.
https://www.researchgate.net/profile/Michael_Deas/publication/228985030_Characterization_of_organic_matter_fate_and_transport_in_the_Klamath_River_below_Link_Dam_to_assess_treatmentreduction_potential/links/00b7d534ffacabfad8000000/Characterization-of-organic-matter-fate-and-transport-in-the-Klamath-River-below-Link-Dam-to-assess-treatment-reduction-potential.pdf.
- DeBell, L., K. Anderson, R. E. Brazier, N. King, and L. Jones. 2015. “Water Resource Management at Catchment Scales Using Lightweight UAVs: Current Capabilities and Future Perspectives.” *Journal of Unmanned Vehicle Systems* 4 (1): 7–30.
- Dennison, William C., Robert J. Orth, Kenneth A. Moore, J. Court Stevenson, Virginia Carter, Stan Kollar, Peter W. Bergstrom, and Richard A. Batiuk. 1993. “Assessing Water Quality with Submersed Aquatic Vegetation Habitat Requirements as Barometers of Chesapeake Bay Health.” *Bioscience* 43 (2): 86–94.
- Díaz-Delgado, Ricardo, Gábor Ónodi, György Kröel-Dulay, and Miklós Kertész. 2019. “Enhancement of Ecological Field Experimental Research by Means of UAV Multispectral Sensing.” *Drones* 3 (1): 7.
- Dierssen, Heidi, Astrid Bracher, Vittorio Brando, Hubert Loisel, and Kevin Ruddick. 2020. “DATA NEEDS FOR HYPERSPECTRAL DETECTION OF ALGAL DIVERSITY

- ACROSS THE GLOBE.” *Oceanography* 33 (1): 74–79.
- Dodds, Walter K., and Dolly A. Gudder. 1992. “The Ecology of Cladophora.” *Journal of Phycology*. <https://doi.org/10.1111/j.0022-3646.1992.00415.x>.
- Dogliotti, Ana I., Juan I. Gossn, Quinten Vanhellemont, and Kevin G. Ruddick. 2018. “Detecting and Quantifying a Massive Invasion of Floating Aquatic Plants in the Río de La Plata Turbid Waters Using High Spatial Resolution Ocean Color Imagery.” *Remote Sensing* 10 (7): 1140.
- Douglas Greene, Sarah B., Gregory H. LeFevre, and Corey D. Markfort. 2021. “Improving the Spatial and Temporal Monitoring of Cyanotoxins in Iowa Lakes Using a Multiscale and Multi-Modal Monitoring Approach.” *The Science of the Total Environment* 760 (March): 143327.
- Dronova, Iryna. 2015. “Object-Based Image Analysis in Wetland Research: A Review.” *Remote Sensing* 7 (5): 6380–6413.
- Duarte, Carlos M. 1995. “Submerged Aquatic Vegetation in Relation to Different Nutrient Regimes.” *Ophelia* 41 (1): 87–112.
- Duffy, James P., Laura Pratt, Karen Anderson, Peter E. Land, and Jamie D. Shutler. 2018. “Spatial Assessment of Intertidal Seagrass Meadows Using Optical Imaging Systems and a Lightweight Drone.” *Estuarine, Coastal and Shelf Science* 200 (January): 169–80.
- Ebert, Demian, David Austin, Mike Deas, and Ken Carlson. 2016. “Interim Measure 11, Activity 6--Study of Algal Conditions Management within a Reservoir Cove Using Physical Measures.”
[https://www.pacificorp.com/content/dam/pacorp/documents/en/pacificorp/energy/hydro/klamath-river/khsa-implementation/technical-documents/2016-IM11-Act6TRptF\(7-12-16_v3\).pdf](https://www.pacificorp.com/content/dam/pacorp/documents/en/pacificorp/energy/hydro/klamath-river/khsa-implementation/technical-documents/2016-IM11-Act6TRptF(7-12-16_v3).pdf).
- Ekstrand, S. 1992. “Landsat TM Based Quantification of Chlorophyll-a during Algae Blooms in Coastal Waters.” *International Journal of Remote Sensing* 13 (10): 1913–26.
- Elser, James J., Erich R. Marzolf, and Charles R. Goldman. 1990. “Phosphorus and Nitrogen Limitation of Phytoplankton Growth in the Freshwaters of North America: A Review and Critique of Experimental Enrichments.” *Canadian Journal of Fisheries and Aquatic Sciences*. <https://doi.org/10.1139/f90-165>.
- ESRI. 2022. *ArcGIS Pro* (version 2.9.1). Redlands, CA: Environmental Systems Research Institute.
- Fernández-Manso, Alfonso, Oscar Fernández-Manso, and Carmen Quintano. 2016. “SENTINEL-2A Red-Edge Spectral Indices Suitability for Discriminating Burn Severity.” *International Journal of Applied Earth Observation and Geoinformation* 50 (August): 170–75.
- Filatova, Daria, Massimo Picardo, Oscar Núñez, and Marinella Farré. 2020. “Analysis, Levels and Seasonal Variation of Cyanotoxins in Freshwater Ecosystems.” *Trends in Environmental Analytical Chemistry* 26 (June): e00091.
- Fink, Gabriel, Joseph Alcamo, Martina Flörke, and Klara Reder. 2018. “Phosphorus Loadings to the World’s Largest Lakes: Sources and Trends.” *Global Biogeochemical Cycles* 32 (4): 617–34.
- Flinders, Camille A., and David D. Hart. 2009. “Effects of Pulsed Flows on Nuisance Periphyton Growths in Rivers: A Mesocosm Study.” *River Research and Applications* 25 (10): 1320–30.
- Flynn, Kyle F., and Steven C. Chapra. 2014. “Remote Sensing of Submerged Aquatic Vegetation

- in a Shallow Non-Turbid River Using an Unmanned Aerial Vehicle.” *Remote Sensing* 6 (12): 12815–36.
- Flynn Kyle F., and Chapra Steven C. 2020. “Evaluating Hydraulic Habitat Suitability of Filamentous Algae Using an Unmanned Aerial Vehicle and Acoustic Doppler Current Profiler.” *Journal of Environmental Engineering* 146 (3): 04019126.
- Foody, Giles M. 2020. “Explaining the Unsuitability of the Kappa Coefficient in the Assessment and Comparison of the Accuracy of Thematic Maps Obtained by Image Classification.” *Remote Sensing of Environment* 239 (March): 111630.
- Gallant, Alisa L. 2015. “The Challenges of Remote Monitoring of Wetlands.” *Remote Sensing* 7 (8): 10938–50.
- Gao, Huilin. 2015. “Satellite Remote Sensing of Large Lakes and Reservoirs: From Elevation and Area to Storage.” *WIREs. Water* 2 (2): 147–57.
- Genzoli, Laurel, and Robert O. Hall. 2016. “Shifts in Klamath River Metabolism Following a Reservoir Cyanobacterial Bloom.” *Freshwater Science*. <https://doi.org/10.1086/687752>.
- Gerke, Markus. 2011. “Supervised Classification of Multiple View Images in Object Space for Seismic Damage Assessment.” In *Photogrammetric Image Analysis*, 221–32. Springer Berlin Heidelberg.
- Ghani, Intan Martina, and Sabri Ahmad. 2010. “Stepwise Multiple Regression Method to Forecast Fish Landing.” *Procedia - Social and Behavioral Sciences* 8 (January): 549–54.
- Ghimire, B., J. Rogan, and J. Miller. 2010. “Contextual Land-Cover Classification: Incorporating Spatial Dependence in Land-Cover Classification Models Using Random Forests and the Getis Statistic.” *Remote Sensing Letters* 1 (1): 45–54.
- Gilerson, Alexander A., Anatoly A. Gitelson, Jing Zhou, Daniela Gurlin, Wesley Moses, Ioannis Ioannou, and Samir A. Ahmed. 2010. “Algorithms for Remote Estimation of Chlorophyll-a in Coastal and Inland Waters Using Red and near Infrared Bands.” *Optics Express* 18 (23): 24109–25.
- Gillett, Nadia D., Yangdong Pan, J. Eli Asarian, and Jacob Kann. 2016. “Spatial and Temporal Variability of River Periphyton below a Hypereutrophic Lake and a Series of Dams.” *The Science of the Total Environment* 541 (January): 1382–92.
- Glibert, Patricia M. 2020. “From Hogs to HABs: Impacts of Industrial Farming in the US on Nitrogen and Phosphorus and Greenhouse Gas Pollution.” *Biogeochemistry* 150 (2): 139–80.
- Gobler, Christopher J. 2020. “Climate Change and Harmful Algal Blooms: Insights and Perspective.” *Harmful Algae* 91 (January): 101731.
- Gobler, Christopher J., Owen M. Doherty, Theresa K. Hattenrath-Lehmann, Andrew W. Griffith, Yoonja Kang, and R. Wayne Litaker. 2017. “Ocean Warming since 1982 Has Expanded the Niche of Toxic Algal Blooms in the North Atlantic and North Pacific Oceans.” *Proceedings of the National Academy of Sciences of the United States of America* 114 (19): 4975–80.
- Godfrey, L. G., and M. R. Wickens. 1981. “Testing Linear and Log-Linear Regressions for Functional Form.” *The Review of Economic Studies* 48 (3): 487–96.
- Goldberg, Scott J., Jordan T. Kirby, and Stephen C. Licht. 2016. “Applications of Aerial Multi-Spectral Imagery for Algal Bloom Monitoring in Rhode Island.” *SURFO Technical Report No. 16-01*, 28.
- Gómez-Chova, Luis, Jordi Muñoz-Marí, Valero Laparra, Jesús Malo-López, and Gustavo Camps-Valls. 2011. “A Review of Kernel Methods in Remote Sensing Data Analysis.” In *Optical Remote Sensing: Advances in Signal Processing and Exploitation Techniques*,

- edited by Saurabh Prasad, Lori M. Bruce, and Jocelyn Chanusot, 171–206. Berlin, Heidelberg: Springer Berlin Heidelberg.
- Gorelick, Noel, Matt Hancher, Mike Dixon, Simon Ilyushchenko, David Thau, and Rebecca Moore. 2017. “Google Earth Engine: Planetary-Scale Geospatial Analysis for Everyone.” *Remote Sensing of Environment* 202 (December): 18–27.
- Govender, M., K. Chetty, and H. Bulcock. 2007. “A Review of Hyperspectral Remote Sensing and Its Application in Vegetation and Water Resource Studies.” *Water SA* 33 (2). <https://doi.org/10.4314/wsa.v33i2.49049>.
- Green, David R. 2020. *Unmanned Aerial Remote Sensing: UAS for Environmental Applications*. CRC Press.
- Guiry, Michael D. 2012. “How Many Species of Algae Are There?” *Journal of Phycology* 48 (5): 1057–63.
- Hallegraeff, G. M. 1993. “A Review of Harmful Algal Blooms and Their Apparent Global Increase.” *Phycologia* 32 (2): 79–99.
- . 2003. “Harmful Algal Blooms: A Global Overview.” *Manual on Harmful Marine Microalgae* 33: 1–22.
- Hallegraeff, Gustaaf M., Donald Mark Anderson, Allan D. Cembella, and H. O. Enevoldsen. 2004. *Manual on Harmful Marine Microalgae*. Unesco.
- Hallegraeff, Gustaaf M., Donald M. Anderson, Catherine Belin, Marie-Yasmine Dechraoui Bottein, Eileen Bresnan, Mireille Chinain, Henrik Enevoldsen, et al. 2021. “Perceived Global Increase in Algal Blooms Is Attributable to Intensified Monitoring and Emerging Bloom Impacts.” *Communications Earth & Environment* 2 (1): 1–10.
- Hampton, Stephanie E., Elizabeth E. Holmes, Lindsay P. Scheef, Mark D. Scheuerell, Stephen L. Katz, Daniel E. Pendleton, and Eric J. Ward. 2013. “Quantifying Effects of Abiotic and Biotic Drivers on Community Dynamics with Multivariate Autoregressive (MAR) Models.” *Ecology* 94 (12): 2663–69.
- Ha, Nguyen Thi Thu, Nguyen Thien Phuong Thao, Katsuaki Koike, and Mai Trong Nhuan. 2017. “Selecting the Best Band Ratio to Estimate Chlorophyll-a Concentration in a Tropical Freshwater Lake Using Sentinel 2A Images from a Case Study of Lake Ba Be (Northern Vietnam).” *ISPRS International Journal of Geo-Information*. <https://doi.org/10.3390/ijgi6090290>.
- Hardin, Perry J., and Ryan R. Jensen. 2011. “Small-Scale Unmanned Aerial Vehicles in Environmental Remote Sensing: Challenges and Opportunities.” *GIScience and Remote Sensing* 48 (1): 99–111.
- Harke, Matthew J., Morgan M. Steffen, Christopher J. Gobler, Timothy G. Otten, Steven W. Wilhelm, Susanna A. Wood, and Hans W. Paerl. 2016. “A Review of the Global Ecology, Genomics, and Biogeography of the Toxic Cyanobacterium, *Microcystis* Spp.” *Harmful Algae* 54 (April): 4–20.
- Hashemi-Beni, Leila, Jeffery Jones, Gary Thompson, Curt Johnson, and Asmamaw Gebrehiwot. 2018. “Challenges and Opportunities for UAV-Based Digital Elevation Model Generation for Flood-Risk Management: A Case of Princeville, North Carolina.” *Sensors* 18 (11). <https://doi.org/10.3390/s18113843>.
- Helama, Samuli, Jouko Meriläinen, and Heikki Tuomenvirta. 2009. “Multicentennial Megadrought in Northern Europe Coincided with a Global El Niño–Southern Oscillation Drought Pattern during the Medieval Climate Anomaly.” *Geology* 37 (2): 175–78.
- Hilton, John, Matthew O’Hare, Michael J. Bowes, and J. Iwan Jones. 2006. “How Green Is My

- River? A New Paradigm of Eutrophication in Rivers.” *The Science of the Total Environment* 365 (1-3): 66–83.
- Ho, Jeff C., and Anna M. Michalak. 2015. “Challenges in Tracking Harmful Algal Blooms: A Synthesis of Evidence from Lake Erie.” *Journal of Great Lakes Research* 41 (2): 317–25.
- Ho, Jeff C., Anna M. Michalak, and Nima Pahlevan. 2019. “Widespread Global Increase in Intense Lake Phytoplankton Blooms since the 1980s.” *Nature* 574 (7780): 667–70.
- Hollister, Jeffrey W., and Betty J. Kreakie. 2016. “Associations between Chlorophyll a and Various Microcystin Health Advisory Concentrations.” *F1000Research* 5 (February): 151.
- Holmes, Elizabeth E., Eric J. Ward, and Kellie Wills. 2012. “MARSS: Multivariate Autoregressive State-Space Models for Analyzing Time-Series Data.” *The R Journal* 4 (1). https://www.academia.edu/download/30588864/rjournal_2012-1_holmes_et_al.pdf.
- Holmquist-Johnson, Christopher L., and Robert T. Milhous. 2010. “Channel Maintenance and Flushing Flows for the Klamath River below Iron Gate Dam, California.” <https://pubs.usgs.gov/of/2010/1086/>.
- Ho, Long T., and Peter L. M. Goethals. 2019. “Opportunities and Challenges for the Sustainability of Lakes and Reservoirs in Relation to the Sustainable Development Goals (SDGs).” *WATER* 11 (7): 1462.
- Honkavaara, E., T. Hakala, J. Kirjasniemi, A. Lindfors, J. Mäkynen, K. Nurminen, P. Ruokokoski, H. Saari, and L. Markelin. 2013. “New Light-Weight Stereoscopic Spectrometric Airborne Imaging Technology for High-Resolution Environmental Remote Sensing Case Studies in Water Quality Mapping.” *International Archives of the Photogrammetry, Remote Sensing and Spatial Information Sciences* 1: W1.
- Hook, Simon J., Jeffrey J. Myers, Kurtis J. Thome, Michael Fitzgerald, and Anne B. Kahle. 2001. “The MODIS/ASTER Airborne Simulator (MASTER) — a New Instrument for Earth Science Studies.” *Remote Sensing of Environment* 76 (1): 93–102.
- Huang, Sha, Lina Tang, Joseph P. Hupy, Yang Wang, and Guofan Shao. 2021. “A Commentary Review on the Use of Normalized Difference Vegetation Index (NDVI) in the Era of Popular Remote Sensing.” *Research Journal of Forestry* 32 (1): 1–6.
- Huang, Tinglin, Xuan Li, Huub Rijnaarts, Tim Grotenhuis, Weixing Ma, Xin Sun, and Jinlan Xu. 2014. “Effects of Storm Runoff on the Thermal Regime and Water Quality of a Deep, Stratified Reservoir in a Temperate Monsoon Zone, in Northwest China.” *The Science of the Total Environment* 485-486 (July): 820–27.
- Hu, Chuanmin. 2009. “A Novel Ocean Color Index to Detect Floating Algae in the Global Oceans.” *Remote Sensing of Environment* 113 (10): 2118–29.
- . 2021. “Remote Detection of Marine Debris Using Satellite Observations in the Visible and near Infrared Spectral Range: Challenges and Potentials.” *Remote Sensing of Environment* 259 (June): 112414.
- Hudnell, H. Kenneth. 2010. “The State of U.S. Freshwater Harmful Algal Blooms Assessments, Policy and Legislation.” *Toxicon: Official Journal of the International Society on Toxinology* 55 (5): 1024–34.
- Hughes, B. B., J. C. Haskins, K. Wasson, and E. Watson. 2011. “Identifying Factors That Influence Expression of Eutrophication in a Central California Estuary.” *Marine Ecology Progress Series* 439 (October): 31–43.
- Husson, Eva, Frauke Ecke, and Heather Reese. 2016. “Comparison of Manual Mapping and Automated Object-Based Image Analysis of Non-Submerged Aquatic Vegetation from Very-High-Resolution UAS Images.” *Remote Sensing* 8 (9): 724.

- Husson, Eva, Olle Hagner, and Frauke Ecke. 2014. "Unmanned Aircraft Systems Help to Map Aquatic Vegetation." Edited by Sebastian Schmidlein. *Applied Vegetation Science* 17 (3): 567–77.
- I, Mohd Hasmadi, H. Z. Pakhriazad, and M. F. Shahrin. 2009. "Evaluating Supervised and Unsupervised Techniques for Land Cover Mapping Using Remote Sensing Data." *Geografia : Malaysian Journal of Society and Space* 5 (1): 1–10.
- Jacoby, J. M., and J. Kann. 2007. "The Occurrence and Response to Toxic Cyanobacteria in the Pacific Northwest, North America." *Lake and Reservoir Management* 23 (2): 123–43.
- Jang, Seon Woong, Hong Joo Yoon, Seok Nam Kwak, Byeong Yong Sohn, Se Geun Kim, and Dae Hyun Kim. 2016. "Algal Bloom Monitoring Using UAVs Imagery." http://onlinepresent.org/proceedings/vol138_2016/8.pdf.
- Janssen, Annette B. G., Jan H. Janse, Arthur H. W. Beusen, Manqi Chang, John A. Harrison, Inese Huttunen, Xiangzhen Kong, et al. 2019. "How to Model Algal Blooms in Any Lake on Earth." *Current Opinion in Environmental Sustainability* 36 (February): 1–10.
- Jay Kerns, G. 2010. *Introduction to Probability and Statistics Using R*. Lulu.com.
- Jiang, Zhangyan, Alfredo R. Huete, Jin Chen, Yunhao Chen, Jing Li, Guangjian Yan, and Xiaoyu Zhang. 2006. "Analysis of NDVI and Scaled Difference Vegetation Index Retrievals of Vegetation Fraction." *Remote Sensing of Environment* 101 (3): 366–78.
- Jia, Tianxia, Xueqi Zhang, and Rencai Dong. 2019. "Long-Term Spatial and Temporal Monitoring of Cyanobacteria Blooms Using MODIS on Google Earth Engine: A Case Study in Taihu Lake." *Remote Sensing* 11 (19): 2269.
- Jochens, Ann E., Thomas C. Malone, Richard P. Stumpf, Barbara M. Hickey, Melissa Carter, Ru Morrison, Juli Dyble, Burt Jones, and Vera L. Trainer. 2010. "Integrated Ocean Observing System in Support of Forecasting Harmful Algal Blooms." *Marine Technology Society Journal* 44 (6): 99–121.
- Johansen, Kasper, Matteo G. Ziliani, Rasmus Houborg, Trenton E. Franz, and Matthew F. McCabe. 2022. "CubeSat Constellations Provide Enhanced Crop Phenology and Digital Agricultural Insights Using Daily Leaf Area Index Retrievals." *Scientific Reports* 12 (1): 5244.
- Johnston, David W. 2018. "Unoccupied Aircraft Systems in Marine Science and Conservation." *Annual Review of Marine Science*, July. <https://doi.org/10.1146/annurev-marine-010318-095323>.
- Jones, J. I., A. L. Collins, P. S. Naden, and D. A. Sear. 2012. "The Relationship between Fine Sediment and Macrophytes in Rivers." *River Research and Applications* 28 (7): 1006–18.
- Joyce, K. E., S. Duce, S. M. Leahy, J. Leon, and S. W. Maier. 2019. "Principles and Practice of Acquiring Drone-Based Image Data in Marine Environments." *Marine and Freshwater Research* 70 (7): 952–63.
- Kann, J., and S. Corum. 2006. "Summary of 2005 Toxic Microcystis Aeruginosa Trends in Copco and Iron Gate Reservoirs on the Klamath River, CA." Prepared by Aquatic Ecosystem Sciences and the Karuk Tribe Department of Natural Resources for the Karuk Tribe, Orleans, CA.
- Kaplan, Gregoriy, and Offer Rozenstein. 2021. "Spaceborne Estimation of Leaf Area Index in Cotton, Tomato, and Wheat Using Sentinel-2." *Land* 10 (5): 505.
- Karlson, B., C. Cusack, and E. Bresnan. 2010. "Microscopic and Molecular Methods for Quantitative Phytoplankton Analysis," 303.
- Karr James R., and Yoder Chris O. 2004. "Biological Assessment and Criteria Improve Total

- Maximum Daily Load Decision Making.” *Journal of Environmental Engineering* 130 (6): 594–604.
- Kay, Susan, John D. Hedley, and Samantha Lavender. 2009. “Sun Glint Correction of High and Low Spatial Resolution Images of Aquatic Scenes: A Review of Methods for Visible and Near-Infrared Wavelengths.” *Remote Sensing* 1 (4): 697–730.
- Kenneth Hudnell, H. 2008. *Cyanobacterial Harmful Algal Blooms: State of the Science and Research Needs*. Springer Science & Business Media.
- Keshava, Nirmal. 2003. “A Survey of Spectral Unmixing Algorithms.” *Lincoln Laboratory Journal* 14 (1): 55–78.
- Khalili, M. H., and M. Hasanlou. 2019. “Harmful Algal Blooms Monitoring Using Sentinel-2 Satellite Images.” *ISPRS - International Archives of the Photogrammetry Remote Sensing and Spatial Information Sciences XLII-4/W18* (October): 609–13.
- Kim, Tae Kyun. 2015. “T Test as a Parametric Statistic.” *Korean Journal of Anesthesiology* 68 (6): 540–46.
- Kirkpatrick, Barbara, Lora E. Fleming, Dominick Squicciarini, Lorrie C. Backer, Richard Clark, William Abraham, Janet Benson, et al. 2004. “Literature Review of Florida Red Tide: Implications for Human Health Effects.” *Harmful Algae* 3 (2): 99–115.
- Kislik, Chippie, Iryna Dronova, and Maggi Kelly. 2018. “UAVs in Support of Algal Bloom Research: A Review of Current Applications and Future Opportunities.” *Drones* 2 (4): 35.
- Kislik, Chippie, Laurel Genzoli, Andy Lyons, and Maggi Kelly. 2020. “Application of UAV Imagery to Detect and Quantify Submerged Filamentous Algae and Rooted Macrophytes in a Non-Wadeable River.” *Remote Sensing* 12 (20): 3332.
- Klamath River Renewal Corporation. n.d. “Lower Klamath Project Exhibit A-1: Definite Decommissioning Plan.” FERC No. 14803.
- . 2018. “Definite Plan for the Lower Klamath Project.” <https://play.google.com/store/books/details?id=9HXEvQEACAAJ>.
- Klemas, Victor. 2012. “Remote Sensing of Algal Blooms: An Overview with Case Studies.” *Journal of Coastal Research*, January, 34–43.
- Konik, Marta, Piotr Kowalczyk, Monika Zabłocka, Anna Makarewicz, Justyna Meler, Agnieszka Zdun, and Mirosław Darecki. 2020. “Empirical Relationships between Remote-Sensing Reflectance and Selected Inherent Optical Properties in Nordic Sea Surface Waters for the MODIS and OLCI Ocean Colour Sensors.” *Remote Sensing* 12 (17): 2774.
- Kornijow, Ryszard, Ramesh D. Gulati, and Teresa Ozimek. 1995. “Food Preference of Freshwater Invertebrates: Comparing Fresh and Decomposed Angiosperm and a Filamentous Alga.” *Freshwater Biology* 33 (2): 205–12.
- Kotovirta, Ville, Timo Toivanen, Marko Järvinen, Matti Lindholm, and Kari Kallio. 2014. “Participatory Surface Algal Bloom Monitoring in Finland in 2011–2013.” *Environmental Systems Research* 3 (1): 24.
- Kroeze, Carolien, Silke Gabbert, Nynke Hofstra, Albert A. Koelmans, Ang Li, Ansje Löhr, Fulco Ludwig, et al. 2016. “Global Modelling of Surface Water Quality: A Multi-Pollutant Approach.” *Current Opinion in Environmental Sustainability* 23 (December): 35–45.
- Krutchkoff, R. G. 1967. “Classical and Inverse Regression Methods of Calibration.” *Technometrics*. <https://doi.org/10.1080/00401706.1967.10490486>.
- Kudela, Raphael M., Sherry L. Palacios, David C. Austerberry, Emma K. Accorsi, Liane S. Guild, and Juan Torres-Perez. 2015. “Application of Hyperspectral Remote Sensing to Cyanobacterial Blooms in Inland Waters.” *Remote Sensing of Environment* 167

- (September): 196–205.
- Kudela, Raphael M., Richard P. Stumpf, and Peter Petrov. 2017. “Acquisition and Analysis of Remote Sensing Imagery of Harmful Algal Blooms.” <https://repository.oceanbestpractices.org/handle/11329/648>.
- Kuha, Jouni. 2004. “AIC and BIC: Comparisons of Assumptions and Performance.” *Sociological Methods & Research* 33 (2): 188–229.
- Kutser, Tiit. 2009. “Passive Optical Remote Sensing of Cyanobacteria and Other Intense Phytoplankton Blooms in Coastal and Inland Waters.” *International Journal of Remote Sensing* 30 (17): 4401–25.
- Kutser, Tiit, Liisa Metsamaa, Niklas Strömbeck, and Ele Vahtmäe. 2006. “Monitoring Cyanobacterial Blooms by Satellite Remote Sensing.” *Estuarine, Coastal and Shelf Science* 67 (1): 303–12.
- Kutser, Tiit, Ele Vahtmäe, and Georg Martin. 2006. “Assessing Suitability of Multispectral Satellites for Mapping Benthic Macroalgal Cover in Turbid Coastal Waters by Means of Model Simulations.” *Estuarine, Coastal and Shelf Science* 67 (3): 521–29.
- Kutser, Tiit, Ele Vahtmäe, and Jaan Praks. 2009. “A Sun Glint Correction Method for Hyperspectral Imagery Containing Areas with Non-Negligible Water Leaving NIR Signal.” *Remote Sensing of Environment* 113 (10): 2267–74.
- Kwon, Yong Sung, Seung Ho Baek, Young Kyun Lim, Jongcheol Pyo, Mayzonee Ligaray, Yongeun Park, and Kyung Hwa Cho. 2018. “Monitoring Coastal Chlorophyll-a Concentrations in Coastal Areas Using Machine Learning Models.” *WATER* 10 (8): 1020.
- Kwon, Yong Sung, Jongcheol Pyo, Yong-Hwan Kwon, Hongtao Duan, Kyung Hwa Cho, and Yongeun Park. 2020. “Drone-Based Hyperspectral Remote Sensing of Cyanobacteria Using Vertical Cumulative Pigment Concentration in a Deep Reservoir.” *Remote Sensing of Environment* 236 (January): 111517.
- Laughrey, Zachary R., Victoria G. Christensen, Robert J. Dusek, Sarena Senegal, Julia S. Lankton, Tracy A. Ziegler, Lee C. Jones, et al. 2021. “A Review of Algal Toxin Exposures on Reserved Federal Lands and among Trust Species in the United States.” *Critical Reviews in Environmental Science and Technology*, December, 1–24.
- Lavery, Amy M., Lorraine C. Backer, Virginia A. Roberts, Jourdan DeVies, Johnni Daniel, and DHSc. 2021. “Evaluation of Syndromic Surveillance Data for Studying Harmful Algal Bloom-Associated Illnesses — United States, 2017–2019.” *MMWR. Morbidity and Mortality Weekly Report*. <https://doi.org/10.15585/mmwr.mm7035a2>.
- Lee, Zhongping, John Marra, Mary Jane Perry, and Mati Kahru. 2015. “Estimating Oceanic Primary Productivity from Ocean Color Remote Sensing: A Strategic Assessment.” *Journal of Marine Systems* 149 (September): 50–59.
- Legleiter, Carl J., Paul J. Kinzel, and Brandon T. Overstreet. 2011. “Evaluating the Potential for Remote Bathymetric Mapping of a Turbid, Sand-Bed River: 1. Field Spectroscopy and Radiative Transfer Modeling.” *Water Resources Research*. <https://doi.org/10.1029/2011wr010591>.
- Legleiter, Carl J., Dar A. Roberts, W. Andrew Marcus, and Mark A. Fonstad. 2004. “Passive Optical Remote Sensing of River Channel Morphology and in-Stream Habitat: Physical Basis and Feasibility.” *Remote Sensing of Environment* 93 (4): 493–510.
- “Lm Function | R Documentation.” 2017. 2017. <https://www.rdocumentation.org/packages/stats/versions/3.6.2/topics/lm>.
- Lobo, Felipe de Lucia, Gustavo Willy Nagel, Daniel Andrade Maciel, Lino Augusto Sander de

- Carvalho, Vitor Souza Martins, Cláudio Clemente Faria Barbosa, and Evlyn Márcia Leão de Moraes Novo. 2021. "AlgaeMAP: Algae Bloom Monitoring Application for Inland Waters in Latin America." *Remote Sensing* 13 (15): 2874.
- Lopez, C. B., E. B. Jewett, Qtwb Dortch, B. T. Walton, and H. K. Hudnell. 2008. "Scientific Assessment of Freshwater Harmful Algal Blooms." <https://aquadocs.org/handle/1834/30787>.
- Lusardi, Robert A., Carson A. Jeffres, and Peter B. Moyle. 2018. "Stream Macrophytes Increase Invertebrate Production and Fish Habitat Utilization in a California Stream." *River Research and Applications* 34 (8): 1003–12.
- Macaya, E. C., and G. C. Zuccarello. 2010. "Genetic Structure of the Giant Kelp *Macrocystis Pyrifera* along the Southeastern Pacific." *Marine Ecology Progress Series* 420 (December): 103–12.
- Maeda, Eduardo Eiji, Filipe Lisboa, Laura Kaikkonen, Kari Kallio, Sampsa Koponen, Vanda Brotas, and Sakari Kuikka. 2019. "Temporal Patterns of Phytoplankton Phenology across High Latitude Lakes Unveiled by Long-Term Time Series of Satellite Data." *Remote Sensing of Environment* 221 (February): 609–20.
- Ma, Jieying, Shuanggen Jin, Jian Li, Yang He, and Wei Shang. 2021. "Spatio-Temporal Variations and Driving Forces of Harmful Algal Blooms in Chaohu Lake: A Multi-Source Remote Sensing Approach." *Remote Sensing* 13 (3): 427.
- Makino, Tomoyo, Ryo Matsuzaki, Shigekatsu Suzuki, Haruyo Yamaguchi, Masanobu Kawachi, and Hisayoshi Nozaki. 2019. "Taxonomic Re-Examination of Two NIES Strains of 'Chlamydomonas' within the Reticulata Group of the Genus *Chloromonas* (Volvocales Chlorophyceae)." *Microb Resour Syst* 35: 13–23.
- Malthus, Tim J., Renee Ohmsen, and Hendrik J. van der Woerd. 2020. "An Evaluation of Citizen Science Smartphone Apps for Inland Water Quality Assessment." *Remote Sensing* 12 (10): 1578.
- Manfreda, Salvatore, Matthew F. McCabe, Pauline E. Miller, Richard Lucas, Victor Pajuelo Madrigal, Giorgos Mallinis, Eyal Ben Dor, et al. 2018. "On the Use of Unmanned Aerial Systems for Environmental Monitoring." *Remote Sensing* 10 (4): 641.
- Marcus, W. Andrew, and Mark A. Fonstad. 2008. "Optical Remote Mapping of Rivers at Sub-Meter Resolutions and Watershed Extents." *Earth Surface Processes and Landforms: The Journal of the British Geomorphological Research Group* 33 (1): 4–24.
- Marques Ramos, Ana Paula, Lucas Prado Osco, Danielle Elis Garcia Furuya, Wesley Nunes Gonçalves, Dthenifer Cordeiro Santana, Larissa Pereira Ribeiro Teodoro, Carlos Antonio da Silva Junior, et al. 2020. "A Random Forest Ranking Approach to Predict Yield in Maize with Uav-Based Vegetation Spectral Indices." *Computers and Electronics in Agriculture* 178 (November): 105791.
- Martinez, Elodie, Thomas Gorgues, Matthieu Lengaigne, Clement Fontana, Raphaëlle Sauzède, Christophe Menkes, Julia Uitz, Emanuele Di Lorenzo, and Ronan Fablet. 2020. "Reconstructing Global Chlorophyll-a Variations Using a Non-Linear Statistical Approach." *Frontiers in Marine Science* 7: 464.
- Massey, Isaac Yaw, Fei Yang, Zhen Ding, Shu Yang, Jian Guo, Clara Tezi, Muwaffak Al-Osman, Robert Boukem Kamegni, and Weiming Zeng. 2018. "Exposure Routes and Health Effects of Microcystins on Animals and Humans: A Mini-Review." *Toxicon: Official Journal of the International Society on Toxinology* 151 (September): 156–62.
- Matthews, Mark W., Stewart Bernard, and Kevin Winter. 2010. "Remote Sensing of

- Cyanobacteria-Dominant Algal Blooms and Water Quality Parameters in Zeekoevlei, a Small Hypertrophic Lake, Using MERIS.” *Remote Sensing of Environment* 114 (9): 2070–87.
- Matthews, Mark William, Stewart Bernard, and Lisl Robertson. 2012. “An Algorithm for Detecting Trophic Status (chlorophyll-A), Cyanobacterial-Dominance, Surface Scums and Floating Vegetation in Inland and Coastal Waters.” *Remote Sensing of Environment* 124 (September): 637–52.
- Maxwell, Aaron E., Timothy A. Warner, and Fang Fang. 2018. “Implementation of Machine-Learning Classification in Remote Sensing: An Applied Review.” *International Journal of Remote Sensing* 39 (9): 2784–2817.
- McKinney, Wes, and Others. 2010. “Data Structures for Statistical Computing in Python.” In *Proceedings of the 9th Python in Science Conference*, 445:51–56. Austin, TX.
- Meybeck, Michel. 2003. “Global Analysis of River Systems: From Earth System Controls to Anthropocene Syndromes.” *Philosophical Transactions of the Royal Society of London. Series B, Biological Sciences* 358 (1440): 1935–55.
- Mishra, Deepak R., Abhishek Kumar, Lakshmi Ramaswamy, Vinay K. Boddula, Moumita C. Das, Benjamin P. Page, and Samuel J. Weber. 2020. “CyanoTRACKER: A Cloud-Based Integrated Multi-Platform Architecture for Global Observation of Cyanobacterial Harmful Algal Blooms.” *Harmful Algae* 96 (June): 101828.
- Mishra, Sachidananda, and Deepak R. Mishra. 2012. “Normalized Difference Chlorophyll Index: A Novel Model for Remote Estimation of Chlorophyll-a Concentration in Turbid Productive Waters.” *Remote Sensing of Environment* 117 (February): 394–406.
- Mishra, Sachidananda, Richard P. Stumpf, and Andrew Meredith. 2019. “Evaluation of RapidEye Data for Mapping Algal Blooms in Inland Waters.” *International Journal of Remote Sensing* 40 (7): 2811–29.
- Mishra, Sachidananda, Richard P. Stumpf, Blake A. Schaeffer, P. Jeremy Werdell, Keith A. Loftin, and Andrew Meredith. 2019. “Measurement of Cyanobacterial Bloom Magnitude Using Satellite Remote Sensing.” *Scientific Reports* 9 (1): 18310.
- Mishra, Sachidananda, Richard P. Stumpf, Blake Schaeffer, P. Jeremy Werdell, Keith A. Loftin, and Andrew Meredith. 2021. “Evaluation of a Satellite-Based Cyanobacteria Bloom Detection Algorithm Using Field-Measured Microcystin Data.” *The Science of the Total Environment* 774 (June): 145462.
- Moisander, Pia H., Mari Ochiai, and Andrew Lincoff. 2009. “Nutrient Limitation of *Microcystis Aeruginosa* in Northern California Klamath River Reservoirs.” *Harmful Algae* 8 (6): 889–97.
- Moore, Stephanie K., Vera L. Trainer, Nathan J. Mantua, Micaela S. Parker, Edward A. Laws, Lorraine C. Backer, and Lora E. Fleming. 2008. “Impacts of Climate Variability and Future Climate Change on Harmful Algal Blooms and Human Health.” *Environmental Health: A Global Access Science Source* 7 Suppl 2 (November): S4.
- Mora-Soto, Alejandra, Mauricio Palacios, Erasmo C. Macaya, Iván Gómez, Pirjo Huovinen, Alejandro Pérez-Matus, Mary Young, et al. 2020. “A High-Resolution Global Map of Giant Kelp (*Macrocystis Pyrifera*) Forests and Intertidal Green Algae (*Ulvophyceae*) with Sentinel-2 Imagery.” *Remote Sensing* 12 (4): 694.
- Mos, L. 2001. “Domoic Acid: A Fascinating Marine Toxin.” *Environmental Toxicology and Pharmacology* 9 (3): 79–85.
- Mount, Richard. 2005. “Acquisition of Through-Water Aerial Survey Images.” *Photogrammetric*

- Engineering & Remote Sensing* 71 (12): 1407–15.
- Mwaura, Francis, Anderson O. Koyo, and Ben Zech. 2004. “Cyanobacterial Blooms and the Presence of Cyanotoxins in Small High Altitude Tropical Headwater Reservoirs in Kenya.” *Journal of Water and Health* 2 (1): 49–57.
- Nahirnick, Natasha K., Paul Hunter, Maycira Costa, Sarah Schroeder, and Tara Sharma. 2019. “Benefits and Challenges of UAS Imagery for Eelgrass (*Zostera Marina*) Mapping in Small Estuaries of the Canadian West Coast.” *Journal of Coastal Research*. <https://doi.org/10.2112/jcoastres-d-18-00079.1>.
- Nally, Ralph Mac, James R. Thomson, Wim J. Kimmerer, Frederick Feyrer, Ken B. Newman, Andy Sih, William A. Bennett, et al. 2010. “Analysis of Pelagic Species Decline in the Upper San Francisco Estuary Using Multivariate Autoregressive Modeling (MAR).” *Ecological Applications*. <https://doi.org/10.1890/09-1724.1>.
- Nelson, Stacy A. C., Kendra Spence Cheruvellil, and Patricia A. Soranno. 2006. “Satellite Remote Sensing of Freshwater Macrophytes and the Influence of Water Clarity.” *Aquatic Botany* 85 (4): 289–98.
- Nowak, Maciej M., Katarzyna Dziób, and Paweł Bogawski. 2019. “Unmanned Aerial Vehicles (UAVs) in Environmental Biology: A Review.” *European Journal of Ecology* 4 (2): 56–74.
- Ode, Peter R., A. Elizabeth Fetscher, and Lilian B. Busse. 2016. “Standard Operating Procedures (SOP) for the Collection of Field Data for Bioassessments of California Wadeable Streams: Benthic Macroinvertebrates, Algae, and Physical Habitat.” *California State Water Resources Control Board Surface Water Ambient Monitoring Program, Sacramento, Calif., USA*. https://meadows.ucdavis.edu/files/SWAMP_combined_sop_031116_reduced.pdf.
- Ogashawara, Igor. 2019. “The Use of Sentinel-3 Imagery to Monitor Cyanobacterial Blooms.” *Environments* 6 (6): 60.
- Ogashawara, Igor, and Max J. Moreno-Madriñán. 2014. “Improving Inland Water Quality Monitoring through Remote Sensing Techniques.” *ISPRS International Journal of Geo-Information* 3 (4): 1234–55.
- Okada, Hisako, and Yasunori Watanabe. 2007. “Distribution of *Cladophora Glomerata* in the Riffle with Reference to the Stability of Streambed Substrata.” *Landscape and Ecological Engineering* 3 (1): 15–20.
- Oliver, Allison A., Randy A. Dahlgren, and Michael L. Deas. 2014. “The Upside-down River: Reservoirs, Algal Blooms, and Tributaries Affect Temporal and Spatial Patterns in Nitrogen and Phosphorus in the Klamath River, USA.” *Journal of Hydrology* 519 (November): 164–76.
- Olusegun, Akinwande Michael, Hussaini Garba Dikko, and Shehu Usman Gulumbe. 2015. “Identifying the Limitation of Stepwise Selection for Variable Selection in Regression Analysis.” *American Journal of Theoretical and Applied Statistics* 4 (5): 414–19.
- O’Reilly, John E., Stéphane Maritorena, B. Greg Mitchell, David A. Siegel, Kendall L. Carder, Sara A. Garver, Mati Kahru, and Charles McClain. 1998. “Ocean Color Chlorophyll Algorithms for SeaWiFS.” *Journal of Geophysical Research* 103 (C11): 24937–53.
- Ostrovsky, Ilia, Sha Wu, Lin Li, and Lirong Song. 2020. “Bloom-Forming Toxic Cyanobacterium *Microcystis*: Quantification and Monitoring with a High-Frequency Echosounder.” *Water Research* 183 (September): 116091.
- Otten, Timothy G., Joseph R. Crosswell, Sam Mackey, and Theo W. Dreher. 2015. “Application of Molecular Tools for Microbial Source Tracking and Public Health Risk Assessment of a *Microcystis* Bloom Traversing 300 Km of the Klamath River.” *Harmful Algae* 46: 71–81.

- Oyama, Yoichi, Bunkei Matsushita, and Takehiko Fukushima. 2015. "Distinguishing Surface Cyanobacterial Blooms and Aquatic Macrophytes Using Landsat/TM and ETM+ Shortwave Infrared Bands." *Remote Sensing of Environment* 157 (February): 35–47.
- PacificCorp. 2020. "2019 KHSA Final Datasets (August 14, 2020)." <https://www.pacificcorp.com/energy/hydro/klamath-river/water-quality.html>.
- Paerl, Hans W., and Jef Huisman. 2008. "Climate. Blooms like It Hot." *Science* 320 (5872): 57–58.
- Paerl, Hans W., Timothy G. Otten, and Raphael Kudela. 2018. "Mitigating the Expansion of Harmful Algal Blooms Across the Freshwater-to-Marine Continuum." *Environmental Science & Technology* 52 (10): 5519–29.
- Paerl, H. W., R. S. Fulton 3rd, P. H. Moisaner, and J. Dyble. 2001. "Harmful Freshwater Algal Blooms, with an Emphasis on Cyanobacteria." *TheScientificWorldJournal* 1 (April): 76–113.
- Page, Benjamin P., Abhishek Kumar, and Deepak R. Mishra. 2018. "A Novel Cross-Satellite Based Assessment of the Spatio-Temporal Development of a Cyanobacterial Harmful Algal Bloom." *International Journal of Applied Earth Observation and Geoinformation* 66 (April): 69–81.
- Pahlevan, Nima, Brandon Smith, John Schalles, Caren Binding, Zhigang Cao, Ronghua Ma, Krista Alikas, et al. 2020. "Seamless Retrievals of Chlorophyll-a from Sentinel-2 (MSI) and Sentinel-3 (OLCI) in Inland and Coastal Waters: A Machine-Learning Approach." *Remote Sensing of Environment* 240 (April): 111604.
- Pahlevan, N., S. Sarkar, B. A. Franz, S. V. Balasubramanian, and J. He. 2017. "Sentinel-2 MultiSpectral Instrument (MSI) Data Processing for Aquatic Science Applications: Demonstrations and Validations." *Remote Sensing of Environment* 201 (November): 47–56.
- Papenfuss, Michael, Blake Schaeffer, Amina I. Pollard, and Keith Loftin. 2020. "Exploring the Potential Value of Satellite Remote Sensing to Monitor Chlorophyll-a for US Lakes and Reservoirs." *Environmental Monitoring and Assessment* 192 (12): 808.
- Papenfuss, George. 1992. "Landmarks in Pacific North American Marine Phycology." *Marine Algae of California*. <https://doi.org/10.1515/9781503621053-002>.
- Patel, N. R., P. Chopra, and V. K. Dadhwal. 2007. "Analyzing Spatial Patterns of Meteorological Drought Using Standardized Precipitation Index." *Meteorological Applications* 14 (4): 329–36.
- Peacock, Melissa B., Corinne M. Gobble, David B. Senn, James E. Cloern, and Raphael M. Kudela. 2018. "Blurred Lines: Multiple Freshwater and Marine Algal Toxins at the Land-Sea Interface of San Francisco Bay, California." *Harmful Algae* 73 (March): 138–47.
- Pekel, Jean-François, Andrew Cottam, Noel Gorelick, and Alan S. Belward. 2016. "High-Resolution Mapping of Global Surface Water and Its Long-Term Changes." *Nature* 540 (7633): 418–22.
- Pennuto, C. M., E. T. Howell, and J. C. Makarewicz. 2012. "Relationships among Round Gobies, Dreissena Mussels, and Benthic Algae in the South Nearshore of Lake Ontario." *Journal of Great Lakes Research* 38 (January): 154–60.
- Peppas, M. V., J. Hall, J. Goodyear, and J. P. Mills. 2019. "Photogrammetric Assessment and Comparison of DJI Phantom 4 pro and Phantom 4 RTK Small Unmanned Aircraft Systems." *ISPRS Geospatial Week 2019*. https://eprints.ncl.ac.uk/file_store/production/258436/916EAB96-2294-430D-A832-CA872DB0A2CD.pdf.

- Pirasteh, Saied, Somayeh Mollaei, Sarah Narges Fatholahi, and Jonathan Li. 2020. "Estimation of Phytoplankton Chlorophyll-a Concentrations in the Western Basin of Lake Erie Using Sentinel-2 and Sentinel-3 Data." *Canadian Journal of Remote Sensing* 46 (5): 585–602.
- Pitois, S., M. H. Jackson, and B. J. B. Wood. 2000. "Problems Associated with the Presence of Cyanobacteria in Recreational and Drinking Waters." *International Journal of Environmental Health Research* 10 (3): 203–18.
- Poikane, Sandra, Martyn Kelly, and Marco Cantonati. 2016. "Benthic Algal Assessment of Ecological Status in European Lakes and Rivers: Challenges and Opportunities." *The Science of the Total Environment* 568 (October): 603–13.
- Pölonen, I., H. -H. Puupponen, Eija Honkavaara, A. Lindfors, H. Saari, L. Markelin, T. Hakala, and K. Nurminen. 2014. "UAV-Based Hyperspectral Monitoring of Small Freshwater Area." In *Remote Sensing for Agriculture, Ecosystems, and Hydrology XVI*, 9239:923912. International Society for Optics and Photonics.
- Pontius, Robert Gilmore, and Marco Millones. 2011. "Death to Kappa: Birth of Quantity Disagreement and Allocation Disagreement for Accuracy Assessment." *International Journal of Remote Sensing* 32 (15): 4407–29.
- Power, Mary E., Michael S. Parker, and William E. Dietrich. 2008. "Seasonal Reassembly of a River Food Web: Floods, Droughts, and Impacts of Fish." *Ecological Monographs* 78 (2): 263–82.
- Preskitt, Linda B., Peter S. Vroom, and Celia Marie Smith. 2004. "A Rapid Ecological Assessment (REA) Quantitative Survey Method for Benthic Algae Using Photoquadrats with Scuba." *Pacific Science* 58 (2): 201–9.
- Price, Douglas W., Kenneth W. Kizer, and K. H. Hansgen. 1991. "California's Paralytic Shellfish Poisoning Prevention Program, 1927-89." *Journal of Shellfish Research* 10 (1): 119–45.
- Pridle, J. 1980. "The Production Ecology of Benthic Plants in Some Antarctic Lakes: I. In Situ Production Studies." *The Journal of Ecology*. <https://doi.org/10.2307/2259248>.
- Qian, Song S., Craig A. Stow, Freya E. Rowland, Qianqian Liu, Mark D. Rowe, Eric J. Anderson, Richard P. Stumpf, and Thomas H. Johengen. 2021. "Chlorophyll a as an Indicator of Microcystin: Short-Term Forecasting and Risk Assessment in Lake Erie." *Ecological Indicators* 130 (November): 108055.
- Quesada, Antonio, Enrique Moreno, David Carrasco, Tamar Paniagua, Lars Wormer, Caridad de Hoyos, and Assaf Sukenik. 2006. "Toxicity of *Aphanizomenon ovalisporum* (Cyanobacteria) in a Spanish Water Reservoir." *European Journal of Phycology* 41 (1): 39–45.
- Ramaraj, Rameshprabu, Rungthip Kawaree, and Yuwalee Unpaprom. 2016. "Direct Transesterification of Microalga *Botryococcus Braunii* Biomass for Biodiesel Production." *Emergent Life Sciences Research* 2: 1–7.
- Ramazanov, Arthur, and Zakir Ramazanov. 2006. "Isolation and Characterization of a Starchless Mutant of *Chlorella Pyrenoidosa* STL-PI with a High Growth Rate, and High Protein and Polyunsaturated Fatty Acid Content." *Phycological Research* 54 (4): 255–59.
- Ranjbar, Mohammad Hassan, David P. Hamilton, Amir Etemad-Shahidi, and Fernanda Helfer. 2021. "Individual-Based Modelling of Cyanobacteria Blooms: Physical and Physiological Processes." *The Science of the Total Environment* 792 (October): 148418.
- R Core Team. 2020. *R: A Language and Environment for Statistical Computing*. R Foundation for Statistical Computing, Vienna, Austria. <https://www.R-project.org/>.
- Rodríguez-Benito, Cristina V., Gabriel Navarro, and Isabel Caballero. 2020. "Using Copernicus

- Sentinel-2 and Sentinel-3 Data to Monitor Harmful Algal Blooms in Southern Chile during the COVID-19 Lockdown.” *Marine Pollution Bulletin* 161 (Pt A): 111722.
- Rodríguez-Puerta, Francisco, Rafael Alonso Ponce, Fernando Pérez-Rodríguez, Beatriz Águeda, Saray Martín-García, Raquel Martínez-Rodrigo, and Iñigo Lizarralde. 2020. “Comparison of Machine Learning Algorithms for Wildland-Urban Interface Fuelbreak Planning Integrating ALS and UAV-Borne LiDAR Data and Multispectral Images.” *Drones* 4 (2): 21.
- Rørslett, Bjørn, and Stein W. Johansen. 1996. “Remedial Measures Connected with Aquatic Macrophytes in Norwegian Regulated Rivers and Reservoirs.” *Regulated Rivers: Research & Management* 12 (4-5): 509–22.
- Rossiter, Thomas, Thomas Furey, Tim McCarthy, and Dagmar B. Stengel. 2020. “UAV-Mounted Hyperspectral Mapping of Intertidal Macroalgae.” *Estuarine, Coastal and Shelf Science* 242 (September): 106789.
- Ross, Matthew R. V., Simon N. Topp, Alison P. Appling, Xiao Yang, Catherine Kuhn, David Butman, Marc Simard, and Tamlin M. Pavelsky. 2019. “AquaSat: A Data Set to Enable Remote Sensing of Water Quality for Inland Waters.” *Water Resources Research* 55 (11): 10012–25.
- Rusnák, Miloš, Ján Sládek, Anna Kidová, and Milan Lehotský. 2018. “Template for High-Resolution River Landscape Mapping Using UAV Technology.” *Measurement*. <https://doi.org/10.1016/j.measurement.2017.10.023>.
- Sabater, S., F. Bregoli, V. Acuña, D. Barceló, A. Elosegi, A. Ginebreda, R. Marce, I. Muñoz, L. Sabater-Liesa, and V. Ferreira. 2018. “Effects of Human-Driven Water Stress on River Ecosystems: A Meta-Analysis. *Sci. Rep.* 8, 1--11.”
- Saberioon, Mohammadmehdi, Jakub Brom, Václav Nedbal, Pavel Souček, and Petr Císař. 2020. “Chlorophyll-a and Total Suspended Solids Retrieval and Mapping Using Sentinel-2A and Machine Learning for Inland Waters.” *Ecological Indicators* 113 (June): 106236.
- Schaeffer, Blake A., Sean W. Bailey, Robyn N. Conmy, Michael Galvin, Amber R. Ignatius, John M. Johnston, Darryl J. Keith, et al. 2018. “Mobile Device Application for Monitoring Cyanobacteria Harmful Algal Blooms Using Sentinel-3 Satellite Ocean and Land Colour Instruments.” *Environmental Modelling and Software[R]* 109: 93–103.
- Scheef, Lindsay P., Daniel E. Pendleton, Stephanie E. Hampton, Stephen L. Katz, Elizabeth E. Holmes, Mark D. Scheuerell, and David G. Johns. 2012. “Assessing Marine Plankton Community Structure from Long-Term Monitoring Data with Multivariate Autoregressive (MAR) Models: A Comparison of Fixed Station versus Spatially Distributed Sampling Data.” *Limnology and Oceanography: Methods*. <https://doi.org/10.4319/lom.2012.10.54>.
- Schneider, Susanne C., Sabine Hilt, Jan E. Vermaat, and Martyn Kelly. 2017. “The ‘Forgotten’ Ecology Behind Ecological Status Evaluation: Re-Assessing the Roles of Aquatic Plants and Benthic Algae in Ecosystem Functioning.” In *Progress in Botany Vol. 78*, edited by Francisco M. Cánovas, Ulrich Lüttge, and Rainer Matyssek, 285–304. Cham: Springer International Publishing.
- Schopf, J. W., and B. M. Packer. 1987. “Early Archean (3.3-Billion to 3.5-Billion-Year-Old) Microfossils from Warrawoona Group, Australia.” *Science* 237 (July): 70–73.
- Sebastiá-Frasquet, María-Teresa, Jesús-A Aguilar-Maldonado, Iván Herrero-Durá, Eduardo Santamaría-del-Ángel, Sergio Morell-Monzó, and Javier Estornell. 2020. “Advances in the Monitoring of Algal Blooms by Remote Sensing: A Bibliometric Analysis.” *NATO Advanced Science Institutes Series E: Applied Sciences* 10 (21): 7877.
- Shang, Shaoling, Zhongping Lee, Gong Lin, Chuanmin Hu, Lianghai Shi, Yongnian Zhang,

- Xueding Li, Jingyu Wu, and Jing Yan. 2017. "Sensing an Intense Phytoplankton Bloom in the Western Taiwan Strait from Radiometric Measurements on a UAV." *Remote Sensing of Environment* 198 (September): 85–94.
- Sharma, Pratistha, Attachai Ueranantasun, Phattrawan Tongkumchum, and Mayuening Eso. 2019. "Modelling of Chlorophyll-a Concentration Patterns from Satellite Data Using Cubic Spline Function in Pattani Bay, Thailand." *Nature, Environment and Pollution Technology* 18 (3). [http://www.neptjournal.com/upload-images/NL-69-47-\(45\)-D-898.pdf](http://www.neptjournal.com/upload-images/NL-69-47-(45)-D-898.pdf).
- Sharp, Samantha L., Alexander L. Forrest, Keith Bouma-Gregson, Yufang Jin, Alicia Cortés, and S. Geoffrey Schladow. 2021. "Quantifying Scales of Spatial Variability of Cyanobacteria in a Large, Eutrophic Lake Using Multiplatform Remote Sensing Tools." *Frontiers of Environmental Science & Engineering in China* 9. <https://doi.org/10.3389/fenvs.2021.612934>.
- Shen, Li, Huiping Xu, and Xulin Guo. 2012. "Satellite Remote Sensing of Harmful Algal Blooms (HABs) and a Potential Synthesized Framework." *Sensors* 12 (6): 7778–7803.
- Shi, Di, and Xiaojun Yang. 2016. "An Assessment of Algorithmic Parameters Affecting Image Classification Accuracy by Random Forests." *Photogrammetric Engineering & Remote Sensing* 82 (6): 407–17.
- Shi, Jiarui, Qian Shen, Yue Yao, Junsheng Li, Fu Chen, Ru Wang, Wenting Xu, Zuoyan Gao, Libing Wang, and Yuting Zhou. 2022. "Estimation of Chlorophyll-a Concentrations in Small Water Bodies: Comparison of Fused Gaofen-6 and Sentinel-2 Sensors." *Remote Sensing* 14 (1): 229.
- Shintani, Christina, and Mark A. Fonstad. 2017. "Comparing Remote-Sensing Techniques Collecting Bathymetric Data from a Gravel-Bed River." *International Journal of Remote Sensing* 38 (8-10): 2883–2902.
- Silva, Thiago S. F., Maycira P. F. Costa, John M. Melack, and Evlyn M. L. M. Novo. 2008. "Remote Sensing of Aquatic Vegetation: Theory and Applications." *Environmental Monitoring and Assessment* 140 (1-3): 131–45.
- Simis, Stefan G. H., Steef W. M. Peters, and Herman J. Gons. 2005. "Remote Sensing of the Cyanobacterial Pigment Phycocyanin in Turbid Inland Water." *Limnology and Oceanography* 50 (1): 237–45.
- Skripnikov, A., N. Wagner, J. Shafer, M. Beck, E. Sherwood, and M. Burke. 2021. "Using Localized Twitter Activity to Assess Harmful Algal Bloom Impacts of *Karenia Brevis* in Florida, USA." *Harmful Algae* 110 (December): 102118.
- Slocum, R. K., W. Wright, C. Parrish, B. Costa, M. Sharr, and T. A. Battista. 2019. "Guidelines for Bathymetric Mapping and Orthoimage Generation Using sUAS and SfM, An Approach for Conducting Nearshore Coastal Mapping." <https://repository.library.noaa.gov/view/noaa/22923>.
- Smayda, Theodore J. 1997. "Bloom Dynamics: Physiology, Behavior, Trophic Effects." *Limnology and Oceanography* 42 (5 part 2): 1132–36.
- Smith, V. H., G. D. Tilman, and J. C. Nekola. 1999. "Eutrophication: Impacts of Excess Nutrient Inputs on Freshwater, Marine, and Terrestrial Ecosystems." *Environmental Pollution* 100 (1-3): 179–96.
- Snyder, Daniel T., and Jennifer L. Morace. 1997. *Nitrogen and Phosphorus Loading from Drained Wetlands Adjacent to Upper Klamath and Agency Lakes, Oregon*. U.S. Department of the Interior, U.S. Geological Survey : Denver, Company : Branch of Information Services.

- Sòria-Perpinyà, Xavier, Eduardo Vicente, Patricia Urrego, Marcela Pereira-Sandoval, Carolina Tenjo, Antonio Ruíz-Verdú, Jesús Delegido, Juan Miguel Soria, Ramón Peña, and José Moreno. 2021. "Validation of Water Quality Monitoring Algorithms for Sentinel-2 and Sentinel-3 in Mediterranean Inland Waters with In Situ Reflectance Data." *WATER* 13 (5): 686.
- Stanfield, Kevin. 2009. "Developing Methods to Differentiate Species and Estimate Coverage of Benthic Autotrophs in the Potomac Using Digital Imaging." Edited by Drew Ferrier. Master of Science, Hood College. <https://mdsoar.org/handle/11603/8764>.
- Stauffer, Beth A., Holly A. Bowers, Earle Buckley, Timothy W. Davis, Thomas H. Johengen, Raphael Kudela, Margaret A. McManus, et al. 2019. "Considerations in Harmful Algal Bloom Research and Monitoring: Perspectives From a Consensus-Building Workshop and Technology Testing." *Frontiers in Marine Science* 6. <https://doi.org/10.3389/fmars.2019.00399>.
- Stevenson, R. Jan, R. Jan Stevenson, Brian J. Bennett, Donielle N. Jordan, and Ron D. French. 2012. "Phosphorus Regulates Stream Injury by Filamentous Green Algae, DO, and pH with Thresholds in Responses." *Hydrobiologia*. <https://doi.org/10.1007/s10750-012-1118-9>.
- Stillwater Sciences. 2020. "Environmental Impact Report for the Lower Klamath Project License Surrender Volume III." State Clearinghouse No. 2016122047. Prepared for State Water Resources Control Board, Division of Water Rights, Sacramento, CA.
- Strobl, Robert O., and Paul D. Robillard. 2008. "Network Design for Water Quality Monitoring of Surface Freshwaters: A Review." *Journal of Environmental Management* 87 (4): 639–48.
- Strong, Alan E. 1974. "Remote Sensing of Algal Blooms by Aircraft and Satellite in Lake Erie and Utah Lake." *Remote Sensing of Environment* 3 (2): 99–107.
- Stuart, Venetia, Shubha Sathyendranath, Trevor Platt, Heidi Maass, and Brian D. Irwin. 1998. "Pigments and Species Composition of Natural Phytoplankton Populations: Effect on the Absorption Spectra." *Journal of Plankton Research* 20 (2): 187–217.
- Stumpf, Richard P., and Michelle C. Tomlinson. 2007. "Remote Sensing of Harmful Algal Blooms." In *Remote Sensing of Coastal Aquatic Environments*, 277–96. Springer.
- Stumpf, R. P., M. E. Culver, P. A. Tester, M. Tomlinson, G. J. Kirkpatrick, B. A. Pederson, E. Truby, V. Ransibrahmanakul, and M. Soracco. 2003. "Monitoring *Karenia Brevis* Blooms in the Gulf of Mexico Using Satellite Ocean Color Imagery and Other Data." *Harmful Algae* 2 (2): 147–60.
- Suplee, Michael W., Vicki Watson, Mark Teply, and Heather McKee. 2009. "How Green Is Too Green? Public Opinion of What Constitutes Undesirable Algae Levels in Streams." *JAWRA Journal of the American Water Resources Association*. <https://doi.org/10.1111/j.1752-1688.2008.00265.x>.
- Su, Tung-Ching, and Hung-Ta Chou. 2015. "Application of Multispectral Sensors Carried on Unmanned Aerial Vehicle (UAV) to Trophic State Mapping of Small Reservoirs: A Case Study of Tain-Pu Reservoir in Kinmen, Taiwan." *Remote Sensing* 7 (8): 10078–97.
- Taddia, Yuri, Paolo Russo, Stefano Lovo, and Alberto Pellegrinelli. 2019. "Multispectral UAV Monitoring of Submerged Seaweed in Shallow Water." *Applied Geomatics*, May. <https://doi.org/10.1007/s12518-019-00270-x>.
- Tait, Leigh, Jochen Bind, Hannah Charan-Dixon, Ian Hawes, John Pirker, and David Schiel. 2019. "Unmanned Aerial Vehicles (UAVs) for Monitoring Macroalgal Biodiversity: Comparison of RGB and Multispectral Imaging Sensors for Biodiversity Assessments." *Remote Sensing* 11 (19): 2332.

- Tamondong, A., T. Nakamura, Y. Kobayashi, M. Garcia, and K. Nadaoka. 2020. "Investigating the Effects of River Discharges on Submerged Aquatic Vegetation Using Uav Images and GIS Techniques." *ISPRS Annals of the Photogrammetry, Remote Sensing and Spatial Information Sciences* 5: 93–99.
- Tang, G., and P. M. Suter. 2011. "Vitamin A, Nutrition, and Health Values of Algae: Spirulina, Chlorella, and Dunaliella." *Journal of Pharmacy and Nutrition Sciences* 1 (2): 111–18.
- Tehrani, Nadia Abbaszadeh, Milad Janalipour, and Hadiseh Babaei. 2021. "Estimating Water Surface Chlorophyll-a Concentration by Big Remote Sensing Data in the Persian Gulf, Bushehr." *Remote Sensing in Earth Systems Sciences* 4 (1): 87–95.
- Teta, Roberta, Gerardo Della Sala, Alfonso Mangoni, Massimiliano Lega, and Valeria Costantino. 2016. "Tracing Cyanobacterial Blooms to Assess the Impact of Wastewaters Discharges on Coastal Areas and Lakes." *International Journal of Sustainable Development and Planning*. <https://doi.org/10.2495/sdp-v11-n5-804-811>.
- Teta, Roberta, Gerardo Della Sala, Germana Esposito, Mariano Stornaiuolo, Silvia Scarpato, Marco Casazza, Aniello Anastasio, Massimiliano Lega, and Valeria Costantino. 2021. "Monitoring Cyanobacterial Blooms during the COVID-19 Pandemic in Campania, Italy: The Case of Lake Avernus." *Toxins* 13 (7). <https://doi.org/10.3390/toxins13070471>.
- Thomsen, Mads S., Luca Mondardini, Tommaso Alestra, Shawn Gerrity, Leigh Tait, Paul M. South, Stacie A. Lilley, and David R. Schiel. 2019. "Local Extinction of Bull Kelp (*Durvillaea* Spp.) Due to a Marine Heatwave." *Frontiers in Marine Science* 6: 84.
- Toming, Kaire, Tiit Kutser, Alo Laas, Margot Sepp, Birgot Paavel, and Tiina Nõges. 2016. "First Experiences in Mapping Lake Water Quality Parameters with Sentinel-2 MSI Imagery." *Remote Sensing* 8 (8): 640.
- Torn, K., and G. Martin. 2012. "Response of Submerged Aquatic Vegetation to Eutrophication-Related Environment Descriptors in Coastal Waters of the NE Baltic Sea." *Estonian Journal of Ecology*. <https://doi.org/10.3176/eco.2012.2.03>.
- United States Environmental Protection Agency. 2019. "Recommended Human Health Recreational Ambient Water Quality Criteria or Swimming Advisories for Microcystins and Cylindrospermopsin." EPA 822-R-19-001. U.S. Environmental Protection Agency, Office of Water Health and Ecological Criteria Division, Washington, DC.
- . 2021. "Ambient Water Quality Criteria to Address Nutrient Pollution in Lakes and Reservoirs." EPA-822-R-21-005. Office of Science and Technology, Office of Water, U.S. Environmental Protection Agency, Washington, DC.
- {U.S. Department of the Interior, and U.S. Department of Commerce, National Marine Fisheries Service}. 2013. "Klamath Dam Removal Overview - Report for the Secretary of the Interior: An Assessment of Science and Technical Information." 1.1.
- Vadeboncoeur, Yvonne, and Mary E. Power. 2017. "Attached Algae: The Cryptic Base of Inverted Trophic Pyramids in Freshwaters." *Annual Review of Ecology, Evolution, and Systematics* 48 (1): 255–79.
- Vaičiūtė, Diana, Martynas Bučas, Mariano Bresciani, Toma Dabulevičienė, Jonas Gintauskas, Jovita Mėžinė, Edvinas Tiškus, et al. 2021. "Hot Moments and Hotspots of Cyanobacteria Hyperblooms in the Curonian Lagoon (SE Baltic Sea) Revealed via Remote Sensing-Based Retrospective Analysis." *The Science of the Total Environment* 769 (May): 145053.
- Van der Merwe, Deon, and Kevin P. Price. 2015. "Harmful Algal Bloom Characterization at Ultra-High Spatial and Temporal Resolution Using Small Unmanned Aircraft Systems." *Toxins* 7 (4): 1065–78.

- Vander Woude, Andrea, Steve Ruberg, Thomas Johengen, Russ Miller, and Dack Stuart. 2019. "Spatial and Temporal Scales of Variability of Cyanobacteria Harmful Algal Blooms from NOAA GLERL Airborne Hyperspectral Imagery." *Journal of Great Lakes Research* 45 (3): 536–46.
- Van Kirk, Robert W., and Seth W. Naman. 2008. "Relative Effects of Climate and Water Use on Base-Flow Trends in the Lower Klamath Basin 1." *JAWRA Journal of the American Water Resources Association* 44 (4): 1035–52.
- Ventura, Daniele, Andrea Bonifazi, Maria Flavia Gravina, Andrea Belluscio, and Giandomenico Ardizzone. 2018. "Mapping and Classification of Ecologically Sensitive Marine Habitats Using Unmanned Aerial Vehicle (UAV) Imagery and Object-Based Image Analysis (OBIA)." *Remote Sensing* 10 (9): 1331.
- Vincent, Warwick F., and Clive Howard-Williams. 1986. "Antarctic Stream Ecosystems: Physiological Ecology of a Blue-Green Algal Epilithon." *Freshwater Biology* 16 (2): 219–33.
- Virtanen, Pauli, Ralf Gommers, Travis E. Oliphant, Matt Haberland, Tyler Reddy, David Cournapeau, Evgeni Burovski, et al. 2020. "SciPy 1.0: Fundamental Algorithms for Scientific Computing in Python." *Nature Methods* 17 (3): 261–72.
- Viso-Vázquez, Manuel, Carolina Acuña-Alonso, Juan Luis Rodríguez, and Xana Álvarez. 2021. "Remote Detection of Cyanobacterial Blooms and Chlorophyll-a Analysis in a Eutrophic Reservoir Using Sentinel-2." *Sustainability: Science Practice and Policy* 13 (15): 8570.
- Visser, Fleur, Kerst Buis, Veerle Verschoren, and Patrick Meire. 2015. "Depth Estimation of Submerged Aquatic Vegetation in Clear Water Streams Using Low-Altitude Optical Remote Sensing." *Sensors* 15 (10): 25287–312.
- Visser, Fleur, Caroline Wallis, and Anne M. Sinnott. 2013. "Optical Remote Sensing of Submerged Aquatic Vegetation: Opportunities for Shallow Clearwater Streams." *Limnologica*. <https://doi.org/10.1016/j.limno.2013.05.005>.
- Walker, W.W., J. D. Walker, and J. Kann. 2012. "Evaluation of Water and Nutrient Balances for the Upper Klamath Lake Basin in Water Years 1992-2010." Technical Report to the Klamath Tribes Natural Resources Department, Chiloquin, OR.
- Wang, Lei, Min Xu, Yang Liu, Hongxing Liu, Richard Beck, Molly Reif, Erich Emery, Jade Young, and Qiusheng Wu. 2020. "Mapping Freshwater Chlorophyll-a Concentrations at a Regional Scale Integrating Multi-Sensor Satellite Observations with Google Earth Engine." *Remote Sensing* 12 (20): 3278.
- Wang, Qunming, Wenzhong Shi, Zhongbin Li, and Peter M. Atkinson. 2016. "Fusion of Sentinel-2 Images." *Remote Sensing of Environment* 187 (December): 241–52.
- Wang, Xiao-Long, L. U. Yong-long, H. E. Gui-zhen, H. A. N. Jing-yi, and Tie-Yu Wang. 2007. "Exploration of Relationships between Phytoplankton Biomass and Related Environmental Variables Using Multivariate Statistic Analysis in a Eutrophic Shallow Lake: A 5-Year Study." *Journal of Environmental Sciences*. [https://doi.org/10.1016/s1001-0742\(07\)60152-1](https://doi.org/10.1016/s1001-0742(07)60152-1).
- Watanabe, Fernanda, Enner Alcântara, Thanan Rodrigues, Luiz Rotta, Nariane Bernardo, and Nilton Imai. 2018. "Remote Sensing of the Chlorophyll-a Based on OLI/Landsat-8 and MSI/Sentinel-2A (Barra Bonita Reservoir, Brazil)." *Anais Da Academia Brasileira de Ciências* 90 (2 suppl 1): 1987–2000.
- Watercourse Engineering, Inc. 2020. "Klamath River Baseline Water Quality Sampling - 2019 Annual Report." Prepared for the KHSA Water Quality Monitoring Group.

- Watson, Susan B., Arthur Zastepa, Gregory L. Boyer, and Eric Matthews. 2017. "Algal Bloom Response and Risk Management: On-Site Response Tools." *Toxicon: Official Journal of the International Society on Toxinology* 129 (April): 144–52.
- Weber, Cornelius I. 1986. *A Review of Methods for the Analysis of Chlorophyll in Periphyton and Plankton of Marine and Freshwater Systems*. NOAA, Office of Sea Grant.
- Weber, Samuel J., Deepak R. Mishra, Susan B. Wilde, and Elizabeth Kramer. 2020. "Risks for Cyanobacterial Harmful Algal Blooms due to Land Management and Climate Interactions." *The Science of the Total Environment* 703 (February): 134608.
- Wehr, John D. 1981. "Analysis of Seasonal Succession of Attached Algae in a Mountain Stream, the North Alouette River, British Columbia." *Canadian Journal of Botany*.
<https://doi.org/10.1139/b81-200>.
- Weirich, Chelsea A., and Todd R. Miller. 2014. "Freshwater Harmful Algal Blooms: Toxins and Children's Health." *Current Problems in Pediatric and Adolescent Health Care* 44 (1): 2–24.
- Weiss, Francis Joseph. 1952. "The Useful Algae." *Scientific American* 187 (6): 15–17.
- Welch, E. B., J. M. Jacoby, R. R. Horner, and M. R. Seeley. 1988. "Nuisance Biomass Levels of Periphytic Algae in Streams." *Hydrobiologia* 157 (2): 161–68.
- Westrick, Judy A., David C. Szlag, Benjamin J. Southwell, and James Sinclair. 2010. "A Review of Cyanobacteria and Cyanotoxins Removal/inactivation in Drinking Water Treatment." *Analytical and Bioanalytical Chemistry* 397 (5): 1705–14.
- Wetzel, Robert G. 1964. "A Comparative Study of the Primary Production of Higher Aquatic Plants, Periphyton, and Phytoplankton in a Large, Shallow Lake." *Internationale Revue Der Gesamten Hydrobiologie Und Hydrographie*, Publication N, 49 (1): 1–61.
- Whipple, George Chandler. 1914. *The Microscopy of Drinking Water*. Wiley.
- Wickham, Hadley. 2016. *ggplot2: Elegant Graphics for Data Analysis*. Springer.
- Wolny, Jennifer L., Michelle C. Tomlinson, Stephanie Schollaert Uz, Todd A. Egerton, John R. McKay, Andrew Meredith, Kimberly S. Reece, Gail P. Scott, and Richard P. Stumpf. 2020. "Current and Future Remote Sensing of Harmful Algal Blooms in the Chesapeake Bay to Support the Shellfish Industry." *Frontiers in Marine Science* 7.
<https://doi.org/10.3389/fmars.2020.00337>.
- Wood, Roslyn. 2016. "Acute Animal and Human Poisonings from Cyanotoxin Exposure - A Review of the Literature." *Environment International* 91 (May): 276–82.
- Wynne, Timothy T., and Richard P. Stumpf. 2015. "Spatial and Temporal Patterns in the Seasonal Distribution of Toxic Cyanobacteria in Western Lake Erie from 2002–2014." *Toxins* 7 (5): 1649–63.
- Wynne, Timothy T., Richard P. Stumpf, Michelle C. Tomlinson, and Julianne Dyble. 2010. "Characterizing a Cyanobacterial Bloom in Western Lake Erie Using Satellite Imagery and Meteorological Data." *Limnology and Oceanography* 55 (5): 2025–36.
- Wynne, Timothy T., Richard P. Stumpf, Michelle C. Tomlinson, Gary L. Fahnenstiel, Julianne Dyble, David J. Schwab, and Sonia Joseph Joshi. 2013. "Evolution of a Cyanobacterial Bloom Forecast System in Western Lake Erie: Development and Initial Evaluation." *Journal of Great Lakes Research* 39 (January): 90–99.
- Wynne, T. T., R. P. Stumpf, M. C. Tomlinson, R. A. Warner, P. A. Tester, J. Dyble, and G. L. Fahnenstiel. 2008. "Relating Spectral Shape to Cyanobacterial Blooms in the Laurentian Great Lakes." *International Journal of Remote Sensing* 29 (12): 3665–72.
- Xu, Fuxiang, Zhiqiang Gao, Xiaopeng Jiang, Weitao Shang, Jicai Ning, Debin Song, and Jinquan

- Ai. 2018. "A UAV and S2A Data-Based Estimation of the Initial Biomass of Green Algae in the South Yellow Sea." *Marine Pollution Bulletin* 128 (March): 408–14.
- Xu, Min, Hongxing Liu, Richard Beck, John Lekki, Bo Yang, Song Shu, Emily L. Kang, et al. 2019. "A Spectral Space Partition Guided Ensemble Method for Retrieving Chlorophyll-a Concentration in Inland Waters from Sentinel-2A Satellite Imagery." *Journal of Great Lakes Research* 45 (3): 454–65.
- Yadav, Shweta, Minoru Yoneda, Junichi Susaki, Masayuki Tamura, Kanako Ishikawa, and Yosuke Yamashiki. 2017. "A Satellite-Based Assessment of the Distribution and Biomass of Submerged Aquatic Vegetation in the Optically Shallow Basin of Lake Biwa." *Remote Sensing* 9 (9): 966.
- Yang, Bo, Timothy L. Hawthorne, Hannah Torres, and Michael Feinman. 2019. "Using Object-Oriented Classification for Coastal Management in the East Central Coast of Florida: A Quantitative Comparison between UAV, Satellite, and Aerial Data." *Drones* 3 (3): 60.
- Yang, Chengrun, Yuji Akimoto, Dae Won Kim, and Madeleine Udell. 2019. "OBOE: Collaborative Filtering for AutoML Model Selection." In *Proceedings of the 25th ACM SIGKDD International Conference on Knowledge Discovery & Data Mining*, 1173–83. KDD '19. New York, NY, USA: Association for Computing Machinery.
- Yang, Jun, Hong Lv, Jun Yang, Lemian Liu, Xiaoqing Yu, and Huihuang Chen. 2016. "Decline in Water Level Boosts Cyanobacteria Dominance in Subtropical Reservoirs." *The Science of the Total Environment* 557-558 (July): 445–52.
- Yan, Guangjian, Linyuan Li, André Coy, Xihan Mu, Shengbo Chen, Donghui Xie, Wuming Zhang, Qingfeng Shen, and Hongmin Zhou. 2019. "Improving the Estimation of Fractional Vegetation Cover from UAV RGB Imagery by Colour Unmixing." *ISPRS Journal of Photogrammetry and Remote Sensing: Official Publication of the International Society for Photogrammetry and Remote Sensing* 158 (December): 23–34.
- Yin, Feng, Philip E. Lewis, Jose Gomez-Dans, and Qingling Wu. 2019. "A Sensor-Invariant Atmospheric Correction Method: Application to Sentinel-2/MSI and Landsat 8/OLI." <https://eartharxiv.org/repository/view/1034/>.
- Yu, Songyan, Zongxue Xu, Wei Wu, and Depeng Zuo. 2016. "Effect of Land Use Types on Stream Water Quality under Seasonal Variation and Topographic Characteristics in the Wei River Basin, China." *Ecological Indicators* 60 (January): 202–12.
- Zeng, Chuiqing, and Caren Binding. 2019. "The Effect of Mineral Sediments on Satellite Chlorophyll-a Retrievals from Line-Height Algorithms Using Red and Near-Infrared Bands." *Remote Sensing* 11 (19): 2306.
- Zhang, Zhongheng. 2016. "Variable Selection with Stepwise and Best Subset Approaches." *Annals of Translational Medicine* 4 (7): 136.
- Zinke, Peggy, and Claude Flener. 2013. "Experiences from the Use of Unmanned Aerial Vehicles (UAV) for River Bathymetry Modelling in Norway." *Vann* 48: 351–60.
- Zong, Jia-Min, Xin-Xin Wang, Qiao-Yan Zhong, Xiang-Ming Xiao, Jun Ma, and Bin Zhao. 2019. "Increasing Outbreak of Cyanobacterial Blooms in Large Lakes and Reservoirs under Pressures from Climate Change and Anthropogenic Interferences in the Middle--Lower Yangtze River Basin." *Remote Sensing* 11 (15): 1754.
- Zuur, A. F., I. D. Tuck, and N. Bailey. 2003. "Dynamic Factor Analysis to Estimate Common Trends in Fisheries Time Series." *Canadian Journal of Fisheries and Aquatic Sciences. Journal Canadien Des Sciences Halieutiques et Aquatiques* 60 (5): 542–52.

